Universitat de Girona

APPLICATIONS OF COMPUTED TOMOGRAPHY IN DRY-CURED MEAT PRODUCTS

Eva SANTOS GARCÉS

Dipòsit legal: Gl. 1246-2012
http://hdl.handle.net/10803/83672

Philosophiae Doctor (PhD) Thesis

Applications of Computed Tomography in Dry-Cured Meat Products

Eva Santos Garcés

2012

Philosophiae Doctor (PhD) Thesis

Applications of Computed Tomography in Dry-Cured Meat Products

Eva Santos Garcés

2012

PhD degree in Technology

Itinerary of Food Technology

Thesis supervisors:

Dr. Elena Fulladosa i Tomàs and Dr. Pere Gou i Botó

Dissertation presented to compete for the Philosophiae Doctor degree for the University of Girona

Dr. **ELENA FULLADOSA i TOMÀS** researcher affiliated to "Institut de Recerca i Tecnologia Agroalimentàries (IRTA)" Monells (Girona, Spain), and

Dr. **PERE GOU i BOTÓ** researcher affiliated to "Institut de Recerca i Tecnologia Agroalimentàries (IRTA)" Monells (Girona, Spain), and associated professor of the "Departament d'Enginyeria Química Agrària i Tecnologia Agroalimentària (EQATA)" from the University of Girona (UdG) (Girona, Spain)

CERTIFY:

That this work, entitled "*Applications of Computerized Tomography in Dry-Cured Meat Products*", presented by **EVA SANTOS GARCÉS** to obtain the title of doctor, has been carried out under the direction of Dr. **ELENA FULLADOSA i TOMÀS** and Dr. **PERE GOU i BOTÓ**, and meets the requirements to qualify for the European Mention.

Dr. **ELENA FULLADOSA i TOMÀS**

Supervisor

Dr. **PERE GOU i BOTÓ**

Supervisor

This work has been carried out at the Food Technology Programme at the research centre IRTA-Monells (Institut de Recerca i Tecnologies Agroalimentàries) within the framework of the following research projects:

- TRUEFOOD - "Traditional United Europe Food" - European Commission Integrated Project within the 6th RTD Framework Programme (Contract No.: FOOD-CT-2006-016264).

- Q-PorkChains - 6th European Union Framework Integrated Project Q-PorkChains (Contract No.: FOOD-CT-2007-036245).

- INIA (Contract No.: Proyecto PET-2007-08-C11-08 del Plan Específico de Investigación de Teruel).

- AGAUR - Agència de Gestió d'Ajuts Universitaris i de Recerca (Generalitat de Catalunya, Departament d'Economia i Coneixement). Research stage (from 6th April to 5th October, 2011) carried out at the Department of Food Science at the University of Foggia (Italy) (Contract No.: 2010 BE1 00151).

- XaRTA - Xarxa de Referència en Tecnologia dels Aliments de la Generalitat de Catalunya (Contract No.: EvalXaRTA-2011-306260).

Trust in time,

which usually gives sweet solutions

to many bitter difficulties

(Miguel de Cervantes Saavedra – Spanish writer)

Acknowledgments

I am sincerely grateful to my supervisors, especially Dr. Elena Fulladosa and Dr. Pere Gou. Elena I wish to thank you not only for your patience, for your constantly available help and time (inside and outside the office), but also for introducing me to the critical word of scientific thought. Pere I wish to thank you for your fruitful discussions, statistical lessons, help with numbers, and for teaching me that it is always best to be observant and to work quietly.

I would also like to thank Dr. Jacint Arnau, as a head of the Operative Programme of Food Processing and Engineering (Unit 0403), for his serious but friendly advice, critical reading and continuous encouragement.

I also want to thank to Dr. Joan Tibau as director of IRTA-Monells centre and Dr. Josep Maria Monfort, first as director of IRTA-Monells centre, and now as a CEO of IRTA, for giving me the opportunity to carry out my PhD at the IRTA research centre.

I would like also to express my gratitude to co-authors of published papers and all the co-workers who took part in this study. In particular, I would like to thank Dr. Israel Muñoz at IRTA-Monells for his skilful technical assistance and continuous support with the Matlab programme. The assistance of Quim Arbonés, Bernardo Guerra, Alex Morente, Jordi Garcia, Cristina Canals, Pedro Ramos-Diniz, Pep Cabot, Gustavo Rodriguez, and many others, is also appreciated. Dolors Parés from the University of Girona is also thanked.

Dr. Nuria Garcia-Gil and present and former colleagues at IRTA-Monells are greatly acknowledged for contributing to an extraordinarily pleasant working environment, including pleasant coffee breaks and lunches, conversations and scientific discussions, and for the excellent travelling companions. Special thanks to my good friends, Silvia Cofan and Carles Collell, for sharing frustrations and joy.

The University of Foggia is also thanked, especially my supervisor Dr. Janine Laverse for all her help, encouragement and unconditional enthusiasm, and also Dr. Matteo Alessandro Del Nobile, as a head of the research group, for giving me the opportunity to work with them. But also to Foggia,city and friends.

My brother Jose and my friends are also lovingly thanked for their invaluable patience and support in the good moments but mainly in the chaotic moments, and also for the “water-breaks” and the “lost coffees”.

Finally, my deepest gratitude goes to Javi, for giving me an exceptionally personal computer support (usually long distance) and under any circumstance! Patient friend and partner during these last 4 years... It hasn’t been that long, has it?

I would not forget all those animals (especially pigs) without which the realization of this thesis would not have been possible.

I apologize to all those that are not mentioned in these lines, who have helped me at some point in the realization of this project.

This thesis is dedicated with love and sincere appreciation to my parents,

José Manuel and Rosa María,

to who I give my warmest thanks for encouraging me

to start this Adventure.

Esta tesis está dedicada con amor y sincero aprecio a mis padres,

José Manuel y Rosa María,

a los que quiero agradecer el animarme

a comenzar esta Aventura.

Aquesta tesi està dedicada amb amor i sincera estima als meus pares,

José Manuel i Rosa María,

als quals els hi vull agrair el animar-me

a començar aquesta Aventura.

List of Papers

This thesis is based on the following papers, referred to in Roman numerals:

Paper I Fulladosa, E., **Santos-Garcés, E.**, Picouet, P., & Gou, P. (2010). Prediction of salt and water content in dry-cured hams by computed tomography. *Journal of Food Engineering*, 96 (1), 80-85.

Paper II **Santos-Garcés, E.**, Gou, P., Garcia-Gil, N., Arnau, J., & Fulladosa, E. (2010). Non-destructive analysis of a_w, salt and water in dry-cured hams during drying process by means of computed tomography. *Journal of Food Engineering*, 101 (2), 187-192.

Paper III **Santos-Garcés, E.**, Muñoz, I., Gou, P., Garcia-Gil, N., & Fulladosa, E. (2012). Intramuscular fat content estimated by image analysis improves computed tomography based models for estimating salt, water and a_w in dry-cured hams. *Food Chemistry*, (submitted).

Paper IV **Santos-Garcés, E.**, Muñoz, I., Gou, P., Sala, X., & Fulladosa, E. (2012). Tools for studying dry-cured ham processing by using computed tomography. *Journal of Agricultural and Food Chemistry*, 60 (1), 241-249.

Paper V Garcia-Gil, N., **Santos-Garcés, E.**, Muñoz, I., Fulladosa, E., Arnau, J., & Gou, P. (2012). Salting, drying and sensory quality of dry-cured hams subjected to different pre-salting treatments: Skin trimming and pressing. *Meat Science*, 90 (2), 389-392.

Paper VI Picouet, P., Gou, P., Fulladosa, E., **Santos-Garcés, E.**, & Arnau, J. (2012). Estimation of salt diffusivity by Computed Tomography in the *Semimembranosus* muscle during salting of fresh and frozen/thawed hams. *LWT - Food Science and Technology*, (submitted).

Paper VII **Santos-Garcés, E.**, Laverse, J., Gou, P., Fulladosa, E., Frisullo, P., & Del Nobile, M. A. (2012). Addition of different types of fat to non-acid lean fermented sausages: X-ray microcomputed tomography and instrumental texture analyses. *Meat Science*, (submitted).

Table of Contents

List of Figures

Figure 9. Examples of images acquired by µCT from a non-acid pork lean ham fermented sausage sample. The obtained images are maps of spatial distribution of the X-ray attenuations. Grey-scale cross-sectional image (dark pixels representing fat) (A), binary tomographic section (white pixels representing fat) (B) and three-dimensional reconstruction (representing fat 3D distribution) (C).

List of Figures in Papers

Paper I

Paper II

Paper III

Paper IV

Paper V

Paper VI

Paper VII

List of Tables

List of Tables in Papers

Paper I

Paper II

Paper III

Paper IV

Paper V

Paper VII

Paper VII

Abstract

The use of non-destructive technologies in food research and industry is increasing. X-ray based technologies, such as Computed Tomography (CT) and Microcomputed Tomography (μCT), are important as potential tools for the optimization of food industry processes. CT allows the non-destructive control of a product during the whole elaboration process, while μCT permits an accurate study of the internal microstructure of a product.

The objectives of the present study were (1) to assess the usefulness of CT for monitoring and optimizing dry-cured ham elaboration processes, by developing several prediction models as well as CT analytical tools for the non-destructive analysis of salt content, water content and water activity (a_w), and its application in 3 case studies, and (2) using μCT to characterize, evaluate and correlate changes in the microstructure and texture of non-acid pork lean fermented sausages.

Several studies were performed and published in journals included in the Science Citation Index (*Papers*). In Paper I, CT based prediction models for salt content and for the first time water content, at the initial stages of the dry-cured ham elaboration process were developed, using the combination of different tube voltages (80, 120 and 140 kV). In Paper II, because the drying level of the hams was found to affect the predictions significantly, prediction models for salt content and water content, and for

the first time a_w, to be applied specifically at the final stages of the dry-cured ham elaboration process were developed. Specific prediction models for different areas of interest (individual muscles) within the ham were also developed. In Paper III, due to the fact that the intramuscular fat content (IMF) was also observed to increase prediction errors significantly (mainly in water content and a_w), a non-destructive estimation of IMF in dry-cured ham was developed by image analysis of CT tomograms. Prediction models for estimating salt content, water content and a_w, with and without including IMF estimate, were developed for the whole elaboration process. In Paper IV, several CT analytical tools were developed for extracting relevant information from CT tomograms during ham processing and to evaluate salt content, water content and a_w and their distribution in dry-cured hams. CT based prediction models and CT analytical tools were applied in three different case studies in order to validate the usefulness of the proposed tools. These tools were used to study different salting procedures such as pile salting and tumble salting (Paper IV), and different pre-salting treatments such as skin trimming and pressing (Paper V), showing differences in the salt absorption and distribution between processes. Apart from this, salt content and water content predictions combined with a unidirectional diffusion model were used to estimate salt diffusivity in the *Semimebranosus* (SM) muscle during the salting process (Paper VI).

Additionally in Paper VII, µCT was used to study the microstructure and texture of non-acid pork lean fermented sausages supplemented with different types of fat. µCT was used for the microstructure analysis of visible fat in finely minced dry-cured meat products. The relationship between microstructure parameters and instrumental texture (hardness) was also evaluated.

It can be concluded that on the one hand, CT is a useful tool for monitoring salt content, water content, and a_w during the dry-cured ham elaboration process, and that CT can be considered as suitable technology for the characterization and optimization of dry-cured ham elaboration processes. On the other hand, some µCT geometrical parameters can be correlated with instrumental texture of non-acid pork lean fermented sausages, although µCT was found to be not accurate enough to distinguish between pork lean and fat when these constituents were emulsified.

Resumen

La aplicación de tecnologías no destructivas ha aumentado de manera significativa tanto en el campo de la investigación como en el de la industria alimentaria. Las tecnologías basadas en rayos X, como la Tomografía Computarizada (TC) y la Microtomografía Computarizada (μTC), presentan un gran potencial como herramientas para la optimización de los procesos alimentarios. La TC permite un control no destructivo del producto durante todo el proceso de elaboración, mientras que la μTC permite un estudio preciso de la microestructura interna del producto.

Los objetivos planteados en el presente estudio fueron (1) evaluar la utilidad de la TC para el seguimiento y la optimización del proceso de elaboración del jamón curado mediante el desarrollo de varios modelos de predicción, así como herramientas analíticas derivadas de la TC, para el análisis no destructivo del contenido de sal, el contenido de agua y la actividad de agua (a_w), y su aplicación en 3 casos de estudio, y (2) la utilización de la μTC para caracterizar, evaluar y correlacionar los cambios en la microestructura y la textura en embutidos crudos curados elaborados con un contenido de grasa reducido.

Para alcanzar los objetivos previamente mencionados, se realizaron diferentes estudios, los cuales se han publicado en de revistas científicas incluidas en el *Science Citation Index (Papers)*. En el Paper I, se desarrollaron modelos de predicción para

determinar el contenido de sal y, por primera vez, el contenido de agua, en las fases iniciales del proceso de elaboración del jamón curado, utilizando diferentes combinaciones de voltajes (80 kV, 120 kV y 140 kV). Dado que se observó un efecto significativo del nivel de secado de los jamones afectaba significativamente a las predicciones, en el Paper II, se desarrollaron nuevos modelos de predicción para determinar el contenido de sal y el contenido de agua, pero también por primera vez la a_w, en las etapas finales del proceso de elaboración del jamón curado. También se desarrollaron modelos de predicción específicos para diferentes áreas de interés (músculos específicos) en el jamón. En el transcurso de los trabajos efectuados, se observó como el contenido de grasa intramuscular (IMF) contribuía a aumentar el error de predicción (principalmente para el contenido de agua y la a_w). Como consecuencia, en el Paper III, se desarrolló una estimación no destructiva del IMF en jamón curado mediante el análisis de las imágenes de TC. Se desarrollaron modelos de predicción para determinar el contenido de sal, el contenido de agua y la a_w, con y sin incluir el IMF estimado, para todo el proceso de elaboración. En el Paper IV, se desarrollaron varias herramientas analíticas derivadas de la TC a partir de los modelos de predicción, para la evaluación no destructiva del contenido de sal, el contenido de agua y la a_w y su distribución en los jamones curados, y también para extraer información relevante a partir de las imágenes de TC durante el procesado del jamón. Los modelos de predicción y las herramientas analíticas derivadas de la TC desarrollados se aplicaron en tres casos de estudio diferentes, con el objetivo de validar la utilidad de las herramientas propuestas. Estas herramientas se usaron en el estudio de diferentes procesos de salado como el salado en pila y el salado en bombo (Paper IV), y también en el estudio de diferentes tratamientos de presalado como el recorte y el prensado (Paper V), observándose diferencias en cuanto a la absorción y distribución de la sal entre los procesos. Asimismo, las predicciones del contenido de sal y del contenido de agua combinadas con un modelo de difusión unidireccional se utilizaron para calcular la difusión de la sal en el músculo *Semimebranosus* (SM) durante el proceso de salado (Paper VI).

En el Paper VII, se utilizó la µTC para estudiar la microestructura y la textura en embutidos crudos curados reducidos en grasa suplementados con diferentes tipos de

grasa. La µTC se utilizó para el análisis de la microestructura de la grasa visible en embutidos curados elaborados con carne picada a pequeños diámetros. También se evaluó la relación entre los parámetros de microestructura y la textura instrumental (dureza).

De los resultados obtenidos, se puede concluir, por un lado, que la TC es una herramienta útil para monitorizar el contenido de sal, el contenido de agua y la a_w durante el proceso de elaboración del jamón curado. La TC puede ser considerada también como una tecnología adecuada para la caracterización y optimización de los procesos de elaboración del jamón curado. Por otro lado, algunos parámetros geométricos de µTC se pueden correlacionar con la textura instrumental en embutidos crudos curados con un contenido de grasa reducido, aunque se observó que la µTC no permitía distinguir de forma precisa entre el magro de cerdo y la grasa cuando estos componentes forman parte de una emulsión.

Resum

L'aplicació de tecnologies no destructives ha augmentat de manera significativa tant en el camp de la investigació com en el de la indústria alimentària. Les tecnologies basades en raigs X, com ara la Tomografia Computeritzada (TC) i la Microtomografia Computeritzada (μTC), tenen un potencial important com a eines per a l'optimització dels processos alimentaris. La TC permet un control no destructiu del producte durant tot el procés d'elaboració, mentre que la μTC permet un estudi precís de la microestructura interna del producte.

Els objectius plantejats en aquest estudi varen ser (1) avaluar la utilitat de la TC per al seguiment i l'optimització del procés d'elaboració de pernil curat mitjançant el desenvolupament de diversos models de predicció, així com eines analítiques derivades de la TC, per a l'anàlisi no destructiu del contingut de sal, el contingut d'aigua i l'activitat d'aigua (a_w), i la seva aplicació a 3 casos d'estudi, i (2) la utilització de la μTC per caracteritzar, avaluar i correlacionar els canvis en la microestructura i la textura en embotits crus curats elaborats amb un contingut en greix reduït.

Per assolir els objectius prèviament esmentats, es varen realitzar diferents estudis, els quals s'han publicat en revistes científiques incloses en el *Science Citation Index (Papers)*. En el Paper I, es van desenvolupar models de predicció per a TC per determinar el contingut de sal i, per primera vegada, el contingut d'aigua, en les fases

inicials del procés d'elaboració del pernil curat, utilitzant diferents combinacions de voltatges (80 kV, 120 kV i 140 kV). Donat que es va observar un efecte significatiu del nivell d'assecat dels pernils en les prediccions, en el Paper II, es van desenvolupar nous models de predicció per determinar el contingut de sal i el contingut d'aigua, però també per primera vegada l'a_w, en les etapes finals del procés d'elaboració del pernil curat. També es van desenvolupar models de predicció específics per a diferents àrees d'interès (músculs específics) en el pernil. En el decurs dels treballs efectuats, es va observar com el contingut de greix intramuscular (IMF) contribuïa a augmentar l'error de predicció (principalment pel contingut d'aigua i l'a_w). Com a conseqüència, en el Paper III, es va desenvolupar una estimació no destructiva de l'IMF en pernil curat mitjançant l'anàlisi de les imatges de TC. Es van desenvolupar models de predicció per determinar el contingut de sal, el contingut d'aigua i l'a_w, amb i sense incloure l'IMF estimat, per a tot el procés d'elaboració. En el Paper IV, es van desenvolupar diverses eines analítiques derivades de la TC a partir dels models de predicció per a l'avaluació no destructiva del contingut de sal, el contingut d'aigua i l'a_w i la seva distribució en els pernils curats, i també per extreure informació rellevant a partir de les imatges de TC durant el processat del pernil. Els models de predicció i les eines analítiques derivades de la TC desenvolupats es van aplicar a tres casos d'estudi diferents, amb l'objectiu de validar la seva utilitat. Aquestes eines es van utilitzar per a l'estudi de diferents processos de salat com el salat en pila i el salat en bombo (Paper IV), i també per a l'estudi de diferents tractaments de presalat com ara el retallat i el premsat (Paper V), observant-se diferències quant a l'absorció i distribució de la sal entre els processos. Així mateix, les prediccions del contingut de sal i del contingut d'aigua combinades amb un model de difusió unidireccional es van utilitzar per calcular la difusió de la sal en el múscul *Semimebranosus* (SM) durant el procés de salat (Paper VI).

En el Paper VII, es va utilitzar la µTC per estudiar la microestructura i la textura en embotits crus curats complementats amb diferents tipus de greix. La µTC es va utilitzar per a l'anàlisi de la microestructura del greix visible en embotits curats elaborats amb carn picada a petits diàmetres. També es va avaluar la relació entre els paràmetres de microestructura i la textura instrumental (duresa).

Dels resultats obtinguts, es pot concloure, d'una banda, que la TC és una eina útil pel seguiment del contingut de sal, el contingut d'aigua i l'a_w, durant el procés d'elaboració del pernil curat. La TC pot ser considerada també com una tecnologia apropiada per a la caracterització i l'optimització dels processos d'elaboració del pernil curat. D'altra banda, alguns paràmetres geomètrics de μTC es poden correlacionar amb la textura instrumental en embotits crus curats amb un contingut reduït de greix, encara que es va observar que la μTC no permetia distingir de forma precisa entre el magre de porc i el greix quan aquests components es trobaven en una emulsió.

Keywords

Computed tomography; prediction models; salt content; water content; water activity; intramuscular fat content; CT analytical tools; dry-cured ham; dry-cured ham elaboration process; microcomputed tomography; non-acid pork lean fermented sausages; dry-cured meat products

1. INTRODUCTION

1.1. Justification of the study

Dry-cured meat products are widely consumed in the European Union. These are products elaborated with entire muscles or mixtures of lean and fat, where salt is an essential additive. Salt is the main hurdle for the preservation of the product because it reduces its water activity (a_w) (Leistner, 1985), and has also been related to the final characteristics of the product such as colour, texture and flavour. Product fermentation (commonly used in certain types of dry-cured meat products), drying and ripening, complete the elaboration processes. Organoleptic and sensorial characteristics of dry-cured meat products vary enormously depending not only on the raw material and the additives used in the formulation, but also on the different elaboration procedures used in each country and region, which depend on traditions and regulations (Toldrá, 2002; Trichopoulou *et al.,* 2007; Guerrero *et al.,* 2009). Several types of these products, such as dry-cured ham or dry fermented sausages, are produced in Spain.

Dry-cured ham is economically one of the major traditional Spanish meat products, Spain being the largest producer in the world (Jiménez-Colmenero *et al.,* 2010). The elaboration of Spanish dry-cured ham follows traditional systems which have been used for years. Selected green hams (unsalted) are thoroughly rubbed with a mixture containing sodium chloride and additives such as nitrite, nitrate (Honikel, 2008), ascorbate (Toldrá *et al.,* 1997) and sugar (Flores, 1997), the hams are then covered with salt (usually 1 day/kg of raw meat) to achieve the target salt uptake. After this process, hams are washed in cold water and hung in a drying room at 3 - 4ºC for a

resting period at a relative humidity of 75 - 80% until the salt content has been homogenized through the whole ham (Toldrá, 2002), in order to avoid microbiological hazards (especially in the internal parts of the product). Finally, during the drying process, the temperature is progressively increased (from 10 to 20°C) while the water content decreases until hams achieve a weight loss of approximately 33% (Guerrero *et al.,* 1999) and the characteristic texture and aroma of dry-cured ham are obtained (Arnau *et al.,* 1987).

Dry fermented sausages are another important traditional Mediterranean product. The first step of the process involves the grinding of lean and fat, mixing with salt, spices and other ingredients and additives (Fontana *et al.,* 2005; Lebert *et al.,* 2007). The meat paste is then stuffed into either natural or artificial casings of varying diameters. Once stuffed, the sausages are fermented to the desired pH to stabilize the product. Fermentation process results in the desired flavour and texture characteristics. Finally, during the drying process the relative air humidity is gradually reduced to achieve the target water content (Arnau *et al.,* 2007) and final sensory characteristics.

Both the above mentioned products have relatively high salt and fat contents. In the case of Spanish dry-cured ham (‘‘Jamón Serrano”), salt content on dry matter basis (dm) generally ranges from 8% to 15% (Official Journal EC C 371, 1.12.1998), while the Iberian dry-cured ham is characterised by high intramuscular fat content and high a percentage of oleic acid (Cava *et al.,* 2003). In the case of dry fermented sausages, the final salt content can range from 3% to 4.5% depending on the initial salting and fat content generally ranges from 40% to 50% (Wirth, 1988). An excessive intake of salt and fat on the daily diet is strongly linked to health problems, such as cardiovascular and cerebrovascular diseases. International health agencies, such as the World Health Organization (WHO, 2004) by means of the Global Strategy on Diet, Physical Activity and Health, and national health agencies, such as the Spanish Ministry of Health and Consumer Affairs by means of the Spanish Strategy for Nutrition, Physical Activity and Prevention of Obesity (NAOS, 2005), are encouraging the food industry to reduce the salt and fat contents in their products in order to improve the public’s health through a healthy well-balanced diet.

The reduction of these components in meat products without reducing product safety and quality is not straightforward. Salt reduction produces an increase of a_w values, which implies a lower microbiological stability (Leistner, 1985). Proteolysis activity in dry-cured ham is also affected by salt reduction (Arnau *et al.,* 1998), causing texture defects such as excessive softness (Parolari *et al.,* 1994; Virgili *et al.,* 1995) and pastiness (García-Garrido *et al.,* 2000), but also affecting the flavour of the final product (García *et al.,* 1991; Toldrá and Flores, 1998; Ruiz *et al.,* 2002). Reduction of fat content in meat products has been found to reduce consumers' acceptability, cause technological problems and decrease the sensory quality of the products (Wirth, 1988; Claus and Hunt, 1991; Giese, 1996; Miles, 1996; Jiménez-Colmenero, 1996, 2000; Wood *et al.,* 2003).

Traditional processes for the elaboration of dry-cured meat products are empirical and time-consuming. In addition, some of the quality evaluations of these products, at given points of the process, are still performed by experts, which results in subjective determinations (Toldrà, 2002; Arnau *et al.,* 2007). In the food industry, the idea of replacing these traditional systems for more optimized innovative ones is growing. For this reason, understanding product development from quality, safety and sensory points of view, in the case of salt or fat reduced products, but also in the case of standard products, is of special interest. Until now, destructive analytical methods have been used to measure the variation of the physicochemical properties of the product during the elaboration processes. Therefore, the implementation of non-destructive technologies for monitoring a product during the whole elaboration process, and to provide objective information on specific parameters is of major interest.

Non-destructive analyses are based on the high resolution of equipment sensors combined with the mathematical capabilities of current computers software. Nevertheless, these methods must be previously calibrated for each type of component and product. These calibrations could facilitate a fast non-destructive analysis of the studied product as well as the simultaneous determination of multiple components (i.e. salt content, water content, and a_w).

A variety of non-destructive technologies have been used in the meat industry for different purposes. Some examples are total body electrical conductivity (TOBEC) (Berg *et al.,* 1994), electromagnetic induction (Ham Grading-System) (Serra and Fulladosa, 2011), bioelectrical impedance (BIA) (Swantek *et al.,* 1992; Daza *et al.,* 2006), video image analysis (VIA) (Branscheid *et al.,* 1995; Jia *et al.,* 2010), ultrasounds (Wilson, 1992; Niñoles *et al.,* 2011), nuclear magnetic resonance (NMR) (Beauvallet and Renou, 1992; Ruiz-Cabrera *et al.,* 2004; Straadt *et al.,* 2012), Magnetic Resonance Imaging (MRI) (Fantazzini *et al.,* 2005; Antequera *et al.,* 2007; Pérez-Palacios *et al.,* 2010) or X-ray based technologies (Skjervold *et al.,* 1981; Sørheim and Berg, 1987a; Mitchell *et al.,* 1998; Brienne *et al.,* 2001; Håseth *et al.,* 2008, 2012; Frisullo *et al.,* 2010). The implementation of these technologies, correctly calibrated, could lead to a better understanding and control of raw materials and elaboration processes, and could also be interesting in the food research field in order to improve current elaboration technologies. Nevertheless, their implementation in on-line systems is not straightforward.

1.2. X-ray based technologies

1.2.1. Principles of X-ray based technologies

X-rays (or Röntgen rays) are a type of electromagnetic radiation first described by Wilhelm Conrad Röntgen in 1895. X-rays have a wavelength range of 0.01 to 10 nanometres, which covers the area of the electromagnetic spectrum between gamma and ultraviolet radiation (Figure 1).

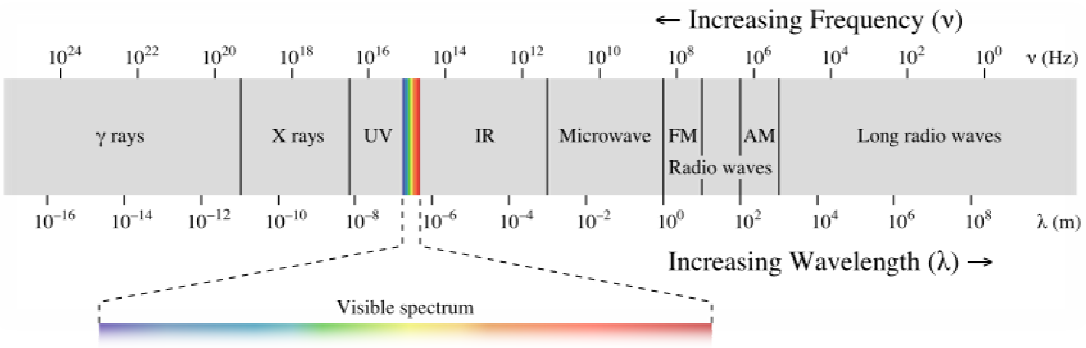

Figure 1. Electromagnetic spectrum.

Basic operating principles of X-ray technologies include the generation of X-rays by an X-ray source and the capture of them by a specific detector (i.e. a film sensitive to X-ray or a digital detector) after passing through the scanned object. X-ray images are obtained without a sample preparation or chemical fixation of the scanned object, and no radiation remains in the object after the irradiation.

The application of these technologies in meat research is based on the different X-ray attenuations that tissues of different densities produce (Seeram, 2009), which allow distinguishing between biological structures (Skejervold *et al.,* 1981). X-rays emitted by this type of equipment lose part of their energy when they interact with the product tissues, to different degrees depending on the tissue density, as expressed by Beer's law:

$$I = I_0 \exp(-\mu x)$$

where I is the intensity of the transmitted X-ray (the radiation exiting from the tissue), I_0 is the intensity of the incident radiation (the radiation entering to the tissue), μ is the linear attenuation coefficient of the tissue, and x is the sample thickness (the distance travelled by the radiation through the tissue). The attenuation coefficient μ is determined by the atomic number and electron density of the tissue components; the higher the atomic number and electron density, the higher the attenuation coefficient. In addition, attenuation coefficient (μ) is also dependent on the incident X-ray energy (tube voltage) (Vinegar *et al.,* 1987).

X-ray radiography, X-ray inspectors, Dual energy X-ray absorptiometry (DXA), Computed tomography (CT) or Microcomputed tomography (μCT) are devices based on this principle. These devices can have different configurations, combine the use of one or more tube voltages and obtain information from one or more angles (depending on the detector type). X-ray technologies have mainly been used for medical diagnoses (i.e. for diagnoses of diseases, to measure bone mineral density and body composition, etc.), but in recent years their use has been extended to other areas such as industrial control or food technology (Gonzalez and Woods, 2001).

1.2.2. X-ray radiography

X-ray radiography is one of the earliest developed X-ray technologies, and uses ionizing radiation for imaging internal structures (Goldman, 2007a). In X-ray radiography, an X-ray beam (originating from one X-ray voltage) is directed (in a one angle direction) to the middle of the section under examination (Figure 2A). An X-ray detector consists on a film sensitive to X-rays, placed under the radiated sample. X-ray radiography is a projection of a large amount of information on one single plane, which results in a two dimensional (2D) representation where all the internal structures were superimposed onto each other (radiograph). This type of X-ray technology is useful in the detection of bone tissues, but is less useful in the imaging of soft tissues (Cartz, 1995; Maire *et al.,* 2001; Goldman, 2007b).

1.2.3. X-ray inspectors

X-ray inspectors are based on the same principle as X-ray radiography, but the detector is digital (Figure 2B). In this case, the object is transported on a conveyor belt through the machine and several consecutive images of the object are acquired during the scanning procedure. Like X-ray radiography, this technology is also based on a two compartmental model (only bone and soft tissues can be distinguished). The amount of radiation used in this type of scanning is extremely low (less than one-tenth the dose of standard X-ray radiography) (Haff and Toyofuko, 2008).

1.2.4. Dual energy X-ray absorptiometry (DXA or DEXA)

Dual energy X-ray absorptiometry (DXA) is an enhanced device from X-ray imaging technology. The DXA procedure involves the acquisition of 2D images combining two different X-ray energy levels (Figure 2C), which are directed in a one angle direction. Image processing is carried out by using algorithms (mathematical procedures) in order to integrate the information obtained from the two X-ray voltages. DXA measurements are based on a three compartmental model (rather than two compartments). Therefore, bone mineral and soft tissues can be distinguished from

the acquired images, but also lean and fat tissues can be differentiated from soft tissue (Kohrt, 1997; Speakman *et al.,* 2001; Binkley and Adle, 2010).

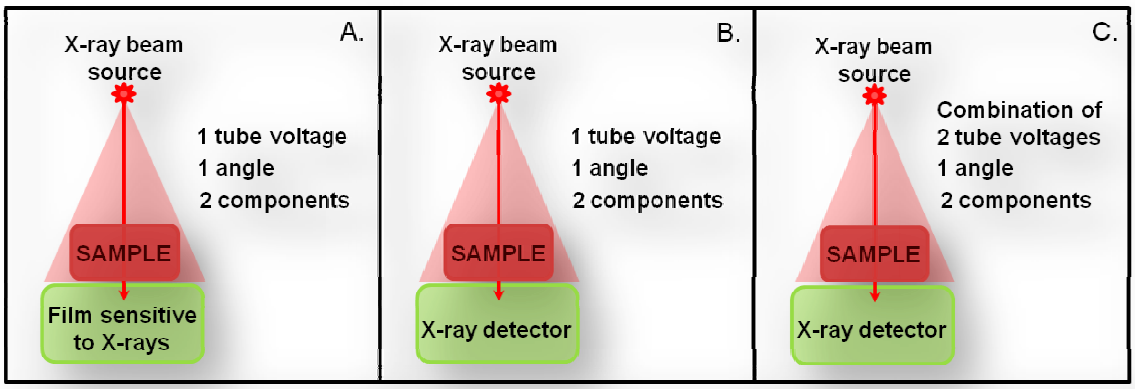

Figure 2. Detail of X-ray technologies operation principles: X-ray radiography (A), X-ray inspectors (B), and Dual energy X-ray absorptiometry (DXA) (C).

1.2.5. Computed Tomography (CT)

The first X-ray Computed tomography (CT) scanner was developed in 1972 by Godfrey Hounsfield and was considered to be one of the most important inventions of the twentieth century (Nobel Prize 1979). Ever since, this technology has been modified and greatly improved. The CT scanner significantly increases acquired information when compared to other X-ray devices because the information of many contiguous radiographs (of a certain finite thickness) that come from different angle views is combined. High-quality images are obtained. In addition, a 3D representation of an object can be carried out digitally by stacking several tomograms of the scanned object.

X-ray CT scanners basically consist of a gantry where X-rays are generated and detectors are oppositely placed, an electric generator, and a work station in which taken measurements are reconstructed into images (or tomograms). The basic principles of X-ray CT technology include three main processes: data acquisition, data processing and image display.

During the data acquisition stage, images are acquired by means of a rapid rotation of the X-ray beam sources (one tube voltage) and the detectors around the object (360°) (Figure 3).

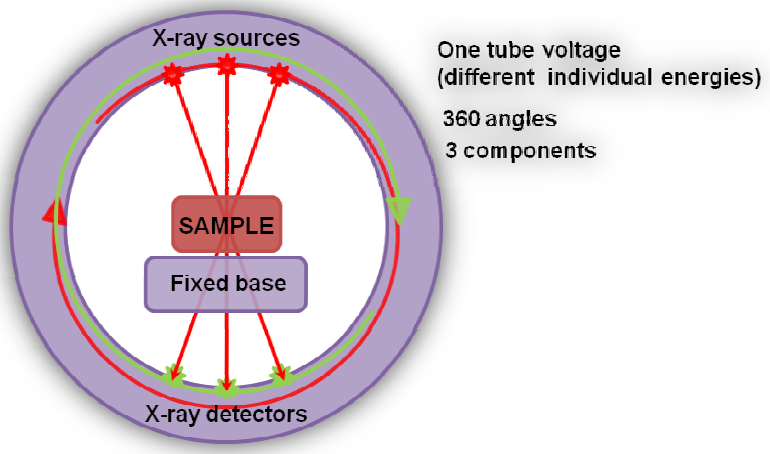

Figure 3. Computed tomography (CT) operation principle.

Radiations transmitted by the object, represented as measurements of the attenuation reduction inside the three-dimensional object, are recorded by the detectors (which are aligned with the X-ray emission source). CT attenuation values (expressed as Hounsfield units (HU)) are calculated from the intensity transmitted from the object (*I*), and are defined as the difference of attenuation coefficients (μ) between a given matter (*i*) relative to water (*w*) (Kalender, 2005):

$$\text{CT value (HU)} = \frac{\mu_i - \mu_w}{\mu_w} \times 1000$$

X-ray CT scanners are able to work with different energies, and various filters can be applied, which provide different attenuation values.

During the data processing (or image reconstruction) stage, a matrix of CT attenuation values is obtained from the acquired data. The final image (or tomogram) is generated from these matrixes of HU values. Each pixel in the tomograms (defined as a square element of an image) corresponds to one CT attenuation value and has a given grey value. Brighter tones symbolize regions with higher density and where X-ray attenuations are higher (i.e. lean tissue) whereas regions with lower absorption coefficients are presented as dark tones (i.e. fat tissue). CT reconstructed images (2D) are made up of pixels, whereas CT acquired images (3D) are made up of voxels (3D pixel) (Du and Sun, 2004; Seeram, 2009). Finally, acquired data can be displayed on a digital monitor or digitally stored for later analysis.

1.2.6. Microcomputed Tomography (µCT)

X-ray microcomputed tomography (µCT) allows the improvement the spatial resolution order of CT scanners from mm to µm. The first µCT machine was created by Jim Elliot around 1980. This technology also allows a detailed 3D reconstruction of the internal microstructure of the scanned object by combining X-ray microscopy and tomographical algorithms (Kerckhofs *et al.,* 2008; Mizutani and Suzuki, 2012). In addition, several morphological parameters can be obtained from the reconstructed 3D images.

µCT equipment consists of an X-ray beam source, a digital X-ray detector (usually a digital X-ray sensitive CCD-camera), a rotatable sample stage, an electric generator, and a controlling computer. The basic principles of µCT include the same processes as described before for CT (data acquisition, data processing, and image display), but in this case the X-ray source and the detectors are fixed, while the sample base rotates (180 or 360°). In µCT the conical X-ray beam traverses the object from different viewing angles and is recorded by an X-ray sensitive camera (CCD) where an enlarged radiograph of the object is produced (Figure 4). The magnification is determined by the ratio of the distances from the tube to the detector and to the object. The spatial resolution of the equipment is limited by the focus of the tube. The resolution of measurement depends on the object size and the magnification used. For µCT 3D reconstruction, all 2D cross-sectional images (tomograms) of the object are consecutively stacked using an appropriate algorithm (i.e. Feldkamp). Finally, acquired images can be processed and analysed by the µCT software (Lim and Berigou, 2004).

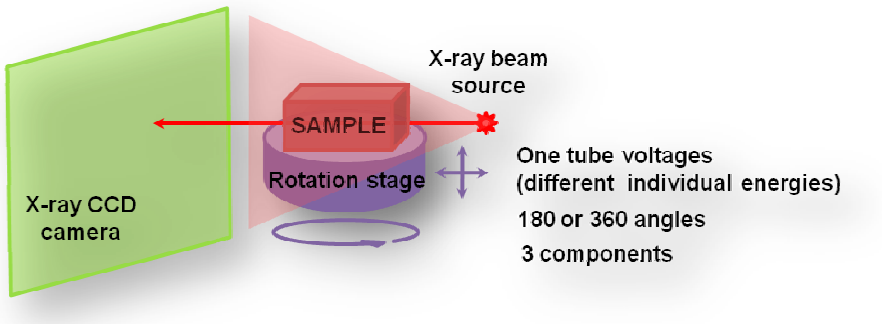

Figure 4. Microcomputed tomography (µCT) operation principle.

µCT can be considered as a non-destructive technology when it is applied to the study of small objects such as bones of small animals (i.e. mouse) (Verdelis *et al.,* 2011), insect organs (Mizutani *et al.,* 2007; van de Kamp *et al.,* 2011), or human teeth (Zou *et al.,* 2011). Nevertheless, in the study of larger sized products (i.e. fermented sausages) the µCT analysis needs a sampling step first, which implies the destruction of the product.

1.3. Application of X-rays in food technology (Background)

Non-destructive X-ray based technologies, such as X-rays inspector, Dual Energy X-rays Absorptiometry (DXA), Computed tomography (CT), or Microcomputed tomography (µCT) have become an active resource in scientific research and product development in the food industry for different purposes.

Technology of X-ray inspectors has been commonly used in the food industry, generally in packaged foods, for the detection of metal, plastic or glass foreign bodies (Haff and Toyofuko, 2008). Recently, this technology has also been used in the food industry for the non-invasive monitoring of eye formation in cheese during ripening, providing promising results (Kraggerud *et al.,* 2009). Its introduction into the meat industry is also in progress.

DXA has been used in meat science to determine the composition (fat, lean and bone) of live pigs (Mitchell *et al.,* 1996; Pomar and Rivest, 1996) and sheep (Pearce *et al.,* 2009; Hunter *et al.,* 2011), as well as carcasses (Mitchell *et al.,* 1998; Hunter *et al.,* 2011) and carcass dissected tissues of pigs (Marcoux *et al.,* 2003) and lambs (Mercier *et al.,* 2006). Furthermore, Brienne *et al.,* (2001) reported the potential of DXA technology to determine fat content in different types of boned fresh meat. More recently, Kröger *et al.* (2006) suggested DXA scanning also as a promising tool for meat tenderness evaluation.

CT has been demonstrated to be useful in the study of a wide range of foods. CT technology has been used in the evaluation of food quality in fruits (i.e. peaches)

(Barcelon *et al.,* 1999) and in the study of the eye formation in Jarlsberg cheese (Strand, 1985, Abrahamsen *et al.,* 2006; Kraggerud *et al.,* 2009). It has also been used for the prediction of fat content in fatty fish species, such as Atlantic salmon (*Salmo salar*) (Rye, 1991; Kolstad *et al.,* 2004; Folkestad *et al.,* 2008) and Atlantic cod (*Gadus morhua*) (Kolstad *et al.,* 2008). In meat research, CT has been used to estimate body composition in animals (i.e. pigs and lambs) (Skjervold *et al.,* 1981; Luiting *et al.,* 1995; Toldi *et al.,* 2007), but also it has been successfully used for measuring lean meat percentage in pig carcasses (Allen, 2003; Font i Furnols *et al.,* 2009; Font i Furnols and Gispert, 2009; Picouet *et al.,* 2010). Due to the accuracy of CT measurements, it has been included in the EU legislation as a suitable reference method for carcass classification (Commission Regulation (EC) 1249/2008).

The strong correlation found between salt content and CT attenuation values (Sørheim and Berg, 1987a), together with the feasibility of CT scanning to distinguish between tissues with different attenuation values (Frøystein *et al.,* 1989), highlighted the use of CT as a useful tool for studying salting and curing processes in fish (i.e. cod or salmon) (Håseth *et al.,* 2009; Segtnan *et al.,* 2009) and meat products (i.e. dry-cured ham).

Sørheim and Berg (1987a, b) and Frøystein *et al.* (1989) were the first to quantify and describe the salt distribution in dry-cured hams using CT. Sørheim and Berg (1987a, b) reported that CT offered a picture of salt diffusion in dry-cured ham after resting (Figure 5).

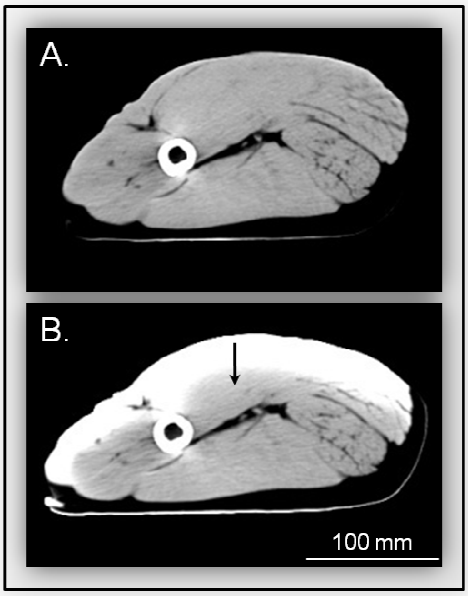

Figure 5. CT cross-sectional images of a dry-cured ham before salting (A), and after salting (B). High attenuation values result in bright pixels (i.e. lean tissue) and low attenuation values result in dark pixels (i.e. fat tissue). The femoral bone is represented in white. Salt diffusion is illustrated by the increase of the bright area (white) and marked with an arrow. Added salt markedly changes the density (or attenuation) of the product tissues (mainly lean and fat tissues due to salt ions (Na^+: sodium, and Cl^-: chloride) have higher densities than the main meat constituents (C: carbon, H: hydrogen, O: oxygen, and N: nitrogen).

No similar studies were presented until 2004 when Vestergaard *et al.* used a meat model system (pork loin) to estimate salt penetration in pork loin. Subsequently, Vestergaard *et al.* (2005) studied salt distribution in dry-cured hams by using CT and image analysis. Results showed that the chemical salt content of an entire dry-cured ham at the end of the elaboration process correlated well to the CT values obtained from a 10 mm slice taken during the process. In this study, the potential utility of line profiles as a promising tool for the analysis of salt distribution and dehydration within a ham was proposed.

More recently, the first mathematical calibration models based on CT attenuation values for salt content in ground pork and in dry-cured ham were presented by Håseth *et al.* (2007). Nevertheless, major errors were found in the models, due to the disturbance of various chemical compositions (mainly due to water and intramuscular fat contents) and to the limitation that the use of only a one tube voltage (130 kV) implies. In a later study, Håseth *et al.* (2008) enhanced the precision of the previously developed calibration models by combining the information obtained using different tube voltages (80, 110 and 130 kV). In a very recently study, Håseth *et al.* (2012) also studied salt diffusion and predicted the ultimate salt content in Norwegian dry-cured ham using CT.

Nevertheless, the negative effect of the drying level and the intramuscular fat content on the precision of the prediction (Vestergaard *et al.,* 2004; Håseth *et al.,* 2007, 2008) was not solved. Besides, CT has not been calibrated to predict other important parameters such as water content neither a_w in dry-cured ham.

μCT is another X-ray based technique that has been successfully used in food industry for the study of cellular microstructure of a wide range of food products, such as cereals and derivates (Van Dalen *et al.,* 2003; Lim and Barigou, 2004; Bellido *et al.,* 2006; Chaunier *et al.,* 2007), bread (Falcone *et al.,* 2004; Falcone *et al.,* 2005; Babin *et al.,* 2005; Babin *et al.,* 2006), cookies (Pareyt *et al.,* 2009), dairy products (Van Dalen *et al.,* 2003; Lim and Barigou, 2004), chocolate (Lim and Barigou, 2004; Haedelt *et al.,* 2005), fruits (Lammertyn *et al.,* 2002; 2003; Mendoza *et al.,* 2007; Léonard *et al.,* 2008) and vegetables (Kuroki *et al.,* 2004).

µCT has been recently introduced in meat science. Frisullo *et al.* (2009) evaluated the usefulness of µCT to study the fat microstructure and distribution of a coarsely minced fatty processed meat product, such as Italian salami, obtaining promising results. Later, Frisullo *et al.* (2010) quantified intramuscular fat content in a raw product (beef muscles) by using µCT. In this study, detailed information about intramuscular fat microstructure and distribution were also obtained.

Nevertheless, no µCT studies have been found dealing with minced dry-cured meat products elaborated with reduced fat content or fat substitutes or neither when the mixture of pork lean and fat is finely minced. To understand the relationship between microstructure and texture analysis when a same minced meat product is elaborated following different formulations might be also interesting.

2. OBJECTIVES

The main objective of this thesis was to develop X-rays based methods, specifically Computed Tomography (CT) and Microcomputed Tomography (μCT), for the non-destructive analysis of dry-cured meat products and asses their usefulness. The following specific objectives were carried out within the framework of the main objective:

I. To develop CT based prediction models for the local determination of salt content, as well as water content and water activity (a_w) in dry-cured ham throughout the elaboration process by using the combination of various tube voltage settings (80, 120, and 140 kV). To achieve this objective, several steps were performed:

- The development of specific models suitable for different elaboration times and for different areas of interest within the ham (individual muscles).
- The evaluation of the effect of drying level and intramuscular fat content (IMF) on the salt content, water content and a_w predictions.

II. To estimate non-destructively the IMF in specific regions of the ham by image analysis of CT tomograms, and to improve the models for predicting salt content, water content, and a_w through the inclusion of IMF estimate into the prediction models.

III. To develop several CT analytical tools (distribution diagrams, line profiles and regions of interest (ROIs)) for the non-destructive study of the composition and distribution of local salt content, water content, and a_w, in dry-cured hams during the elaboration process.

IV. To apply the developed methods (predictive models and CT analytical tools) to different case studies:

- The study of the effect of different pre-salting treatments (skin trimming and pressing) on salt absorption and distribution.
- The study of different salting procedures (pile salting and tumble salting).
- The estimation of salt diffusivity in the *Semimebranosus* muscle (SM) during the salting process, by combining developed CT based models and a unidirectional diffusion model.

V. To study the microstructure of non-acid pork lean fermented sausages elaborated with the addition of different types of fat (backfat, sunflower oil, DAGs) or without added fat. To achieve this objective, several steps were performed:

- The evaluation of microstructural changes produced by the addition to the sausage formulations of different types of fat (backfat, sunflower oil, DAGs), by using µCT.
- The evaluation of the relationship between instrumental texture (hardness) and µCT geometrical parameters.

3. METHODOLOGY

To achieve the objectives, several studies were performed. The studies have been published or submitted to international scientific journals included in the Science Citation Index.

In Paper I, CT based prediction models for salt content and water content at the initial stages of the dry-cured ham elaboration process were developed, using the combination of different tube voltages (80, 120 and 140 kV).

In Paper II, CT based prediction models for salt content, water content and a_w at the final stages of the dry-cured ham elaboration process were developed, using also the combination of different tube voltages (80, 120 and 140 kV). Specific prediction models for different muscles or groups of muscles within the ham (*Semimembranosus* (SM), *Biceps femoris* (BF), and *Semitendinosus* (ST) muscles) were developed too.

In Paper III, a non-destructive estimation of IMF in dry-cured ham was developed by image analysis of CT tomograms. Prediction models for estimating salt content, water content and a_w, with and without including the IMF estimate, were developed for the whole elaboration process. Specific prediction models for different muscles or groups of muscles within the ham (*Biceps femoris* (BF) and *Semitendinosus* (ST) muscles) were developed too.

In Paper IV (Part 1), several CT analytical tools (distribution diagrams, line profiles, and regions of interest (ROIs)) were developed from the CT based prediction models for the non-destructive evaluation of salt content, water content and a_w and their distribution in dry-cured hams.

In Paper IV (Part 2), developed CT based prediction models and CT analytical tools were applied to study salt absorption and distribution in hams which had undergone different salting procedures (pile salting and tumble salting).

In Paper V, developed CT based prediction models and CT analytical tools were applied to study salt absorption and distribution in hams which had undergone different pre-salting treatments (skin trimming and pressing).

In Paper VI, CT based prediction models for salt content and water content combined with a unidirectional diffusion model were used to estimate salt diffusivity in the SM muscle during the salting process.

In Paper VII, µCT was used to study and correlate microstructure and texture of non-acid pork lean fermented sausages supplemented with different types of fat.

3.1. Scanning conditions

3.1.1. Computed Tomography (CT) scanning

CT scanning of hams was carried out using a CT scanner model HiSpeed Zx/I from General Electric Healthcare (GE Healthcare, Barcelona, Spain) located at IRTA-CENTA (Monells, Girona, Spain) (see Figure 6).

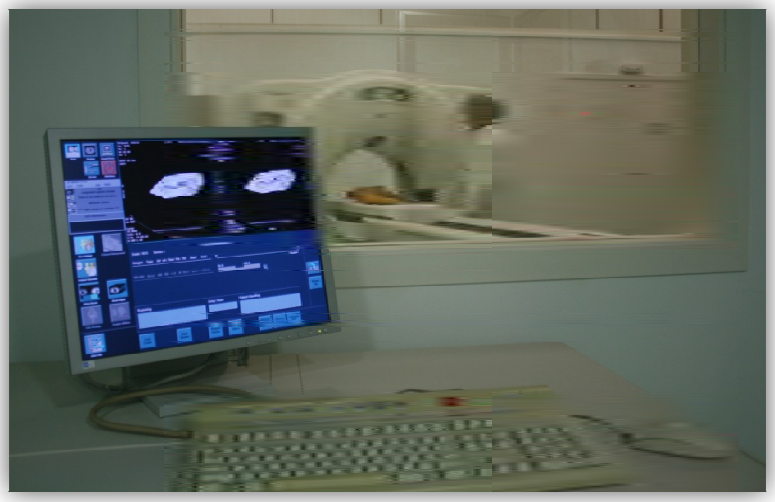

Figure 6. CT equipment General Electric HiSpeed Zx/i.

The hams scanning protocol is displayed in Figure 7. 10 mm thick tomograms were obtained from all the hams at 10 cm from the aitch bone in the distal direction (at the widest part of the ham). In order to scan the hams which were always in the same position, two metallic benchmarks (2 mm diameter) were placed inside the ham bones as a reference.

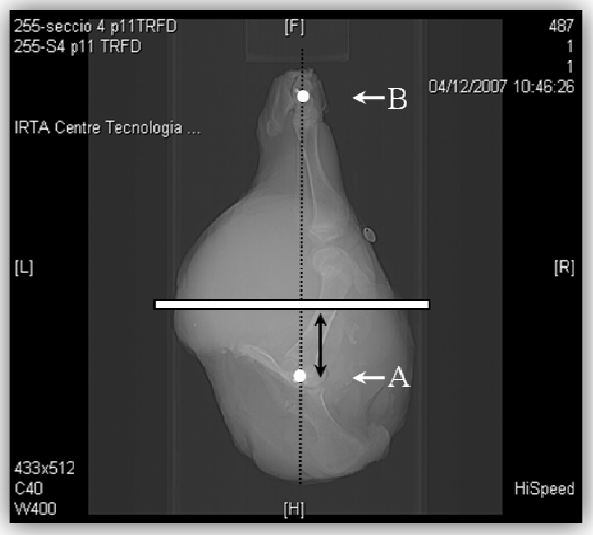

Figure 7. Orthogonal image taken using X-rays showing the anatomy of a dry-cured ham. Hams were aligned in the scanner to a centreline (dashed line) defined by 2 benchmarks, one screwed onto the aitch bone (A) and the other onto the end of the ischial bone (B). CT scans were always taken at 10 cm (↔) from the aitch bone in the distal direction.

Operation settings consisted of using three independent tube voltages (80, 120 and 140 kV), a constant current of 250 mA, and a scan rotation time of 2 seconds, to further combine the information obtained from each tube voltage. Image size was 512 x 512 pixels and Displayed Field of View (DFOV) was 461 x 461 mm^2 with a spatial resolution of 1.1 pixels/mm. The algorithm STD+ from General Electric was used to reconstruct the images because it gives a high contrast spatial resolution in samples containing soft tissue (lean and fat) and mineral phases (mainly salt). Each voxel had a volume of 8.1 mm^3 and had an average CT attenuation value expressed in HU obtained at 80, 120, and 140 kV (HU_{80}, HU_{120} and HU_{140}, respectively). Matrixes of HU values or tomograms of 10 mm thick (Figure 7) were acquired, saved and then retrieved for further automated analysis using the CT work station software (Centricity Radiology RA600 v.7.0, GE Medical Systems, Barcelona, Spain) in Paper I and Paper II, or with Matlab software (MATLAB, Ver. 7.7.0, The Mathworks Inc., Natick, MA, USA) in Papers III, IV, V and VI.

3.1.2. Microcomputed Tomography (µCT) scanning

µCT scanning of non-acid pork lean fermented sausages was carried out using a high-resolution desktop X-ray µCT scanner model Skyscan 1172 (Skyscan 2005, Skyscan N.V., Vluchtenburgstraat, Aartselaar, Belgium) located at the University of Foggia (Foggia, Italy) (see Figure 8).

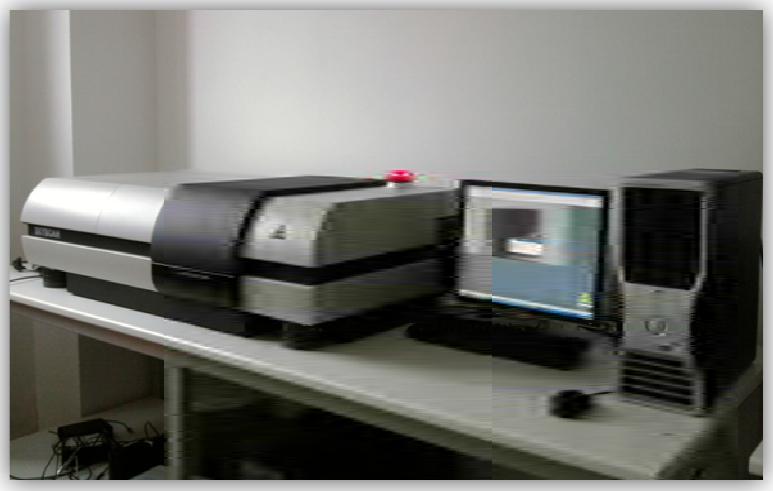

Figure 8. µCT equipment Skyscan 1172.

Before the µCT analysis a sampling step was carried out. From each non-acid pork lean fermented sausage, four 15 mm thick slices were cut by a slicing machine. From each slice, a specimen was accurately carved with a scalpel into cubes of 15 x 15 x 15 mm^3. The specimens, which were wrapped in parafilm to avoid moisture loss (parafilm does not interfere with the X-rays), were used in the µCT analysis.

Power settings of the cone beam source were operated at a voltage of 100 kV and a constant current of 100 µA. The X-rays detector was a 2D medium 16-bit X-ray CCD camera with 2000 x 1048 pixels, and a filter of Al 0.5 (aluminium) was applied to cut out the low-energy X-ray radiation to reduce the non-linear X-ray absorption in dense materials (beam hardening). The distance source–object–camera was adjusted to produce images with a pixel size of 17.13 µm (spatial resolution) (68.52 μm^3).

For image acquisition, the scan protocol included a rotation which covered an area of 180° at a rotation step of 0.60°, and an exposure time of 1.475 second per frame. Four-frame averaging was used to improve the signal to noise ratio. Each µCT scan

time was approximately 37 minutes, producing 244 serial cross-sectional projections (500 x 500 pixels per image).

For the 3D reconstruction and image processing a total of 146 image slices with a slice spacing of 0.069 mm were selected as volume of interest (VOI), and a 10 x 10 mm^2 region of interest (ROI) was chosen from the centre of the scanned slice in view and was then copied to all the slices in the selected VOI. Thereafter, µCT grey-scale tomograms (2D) acquired for each sample (Figure 9A) were converted by binarisation to a set of flat cross-sectional images (2D) (Figure 9B), which were also reconstructed to a 3D image from the collective sum of all contiguous set of 146 cross-sectional image slices (Figure 9C). From these 3D images several internal morphological parameters were calculated. µCT geometric parameters measured in the present study are summarized in Table 1.

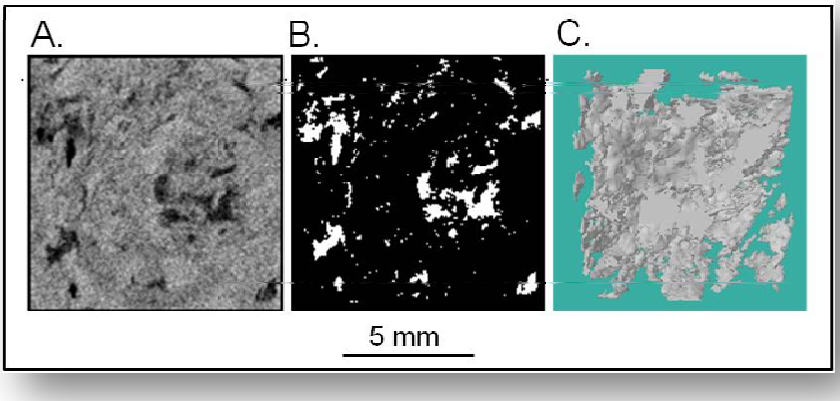

Figure 9. Examples of images acquired by µCT from a non-acid pork lean fermented sausage sample. The obtained images are maps of spatial distribution of the X-ray attenuations. Grey-scale cross-sectional image (dark pixels representing fat) (A), binary tomographic section (white pixels representing fat) (B), and three-dimensional reconstruction (representing fat 3D distribution) (C).

Table 1
Summary of the 3D µCT geometrical parameters used in this study.

Parameter name	Parameter symbol	Unit	Description
Percent object volume	POV	%	Proportion of the VOI occupied by binarised solid objects
Object surface/Volume ratio	OSVR	mm^{-1}	The ratio of solid surface to volume measured in 3D within the VOI
Fragmentation index	FI	mm^{-1}	Inverse index of connectivity
Structure thickness	ST	mm	Local thickness for a point in a solid
Structure separation	SS	mm	Thickness of the spaces as defined by binarisation within the VOI
Degree of anisotropy	DA	none	Measure of the preferential alignment of a considered constituent
Number of objects	NO	none	Total number of discreet binarised objects within the VOI

3.2. Working plan

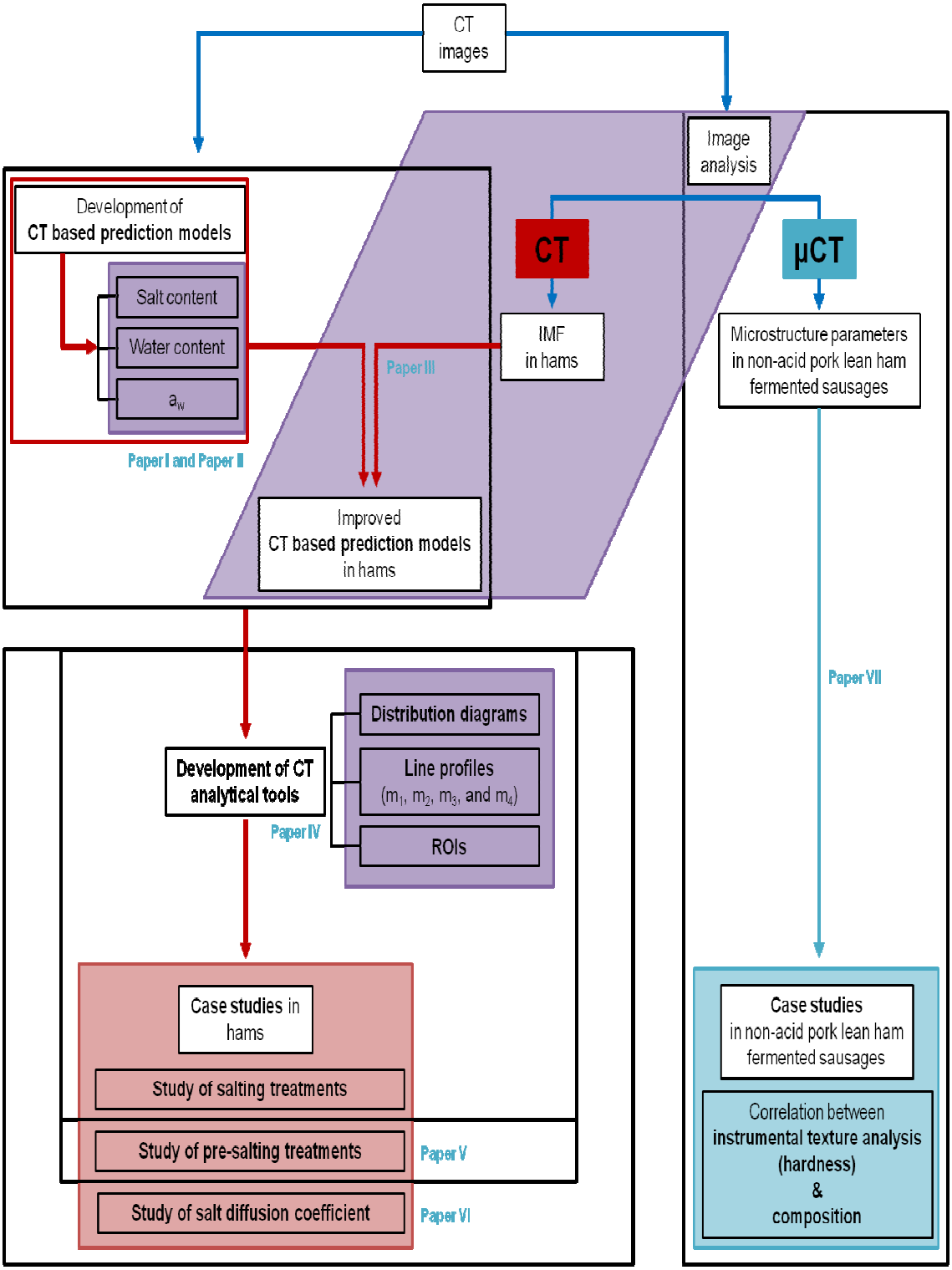

4. RESULTS

Paper I

Fulladosa, E., **Santos-Garcés, E.**, Picouet, P., & Gou, P. (2010). Prediction of salt and water content in dry-cured hams by computed tomography. *Journal of Food Engineering*, 96 (1), 80-85.

Fulladosa, E., Santos-Garcés, E., Picouet, P., Gou, P. “Prediction of salt and water content in dry-cured hams by computed tomography”. *Journal of food engineering*. Vol. 96, issue 1 (January 2010) : p. 80-85

http://www.sciencedirect.com/science/article/pii/S026087740900346X

DOI: http://dx.doi.org/10.1016/j.jfoodeng.2009.06.044

Cited by in Scopus (8)

Received 16 January 2009. Revised 10 June 2009. Accepted 24 June 2009. Available online 30 June 2009.

Abstract

Application of computed tomography (CT) in meat science is based on the different X-ray attenuations that tissues of different density produce. Processed data generate images (tomograms) where different biological structures may be distinguished. CT is of special interest for the study of the meat curing processes since a high density of salt ions produce a marked increase of CT attenuation values. Therefore, salt diffusion and distribution can be easily followed throughout the process. In this study, prediction models for salt and water content in dry-cured ham have been developed, obtaining errors of prediction of 0.3% NaCl and 1.5% water. Fat content and drying level significantly affect the precision of salt and water content predictions. A certain underestimation of salt content in fatty samples was observed. CT and the developed predictive models may be useful in the meat industry as a tool for characterizing and optimizing salting processes.

Keywords

- Computed tomography;
- Dry-cured ham;
- NaCl;
- Water;
- Fat;
- Prediction models

Paper II

Santos-Garcés, E., Gou, P., Garcia-Gil, N., Arnau, J., & Fulladosa, E. (2010). Non-destructive analysis of aw, salt and water in dry-cured hams during drying process by means of computed tomography. *Journal of Food Engineering*, 101 (2), 187-192.

Eva Santos-Garcés, Pere Gou, Núria Garcia-Gil, Jacint Arnau, Elena Fulladosa. “Non-destructive analysis of a_w, salt and water in dry-cured hams during drying process by means of computed tomography”. *Journal of food engineering*. Vol. 101, issue 2 (November 2010) : p. 187-192

http://www.sciencedirect.com/science/article/pii/S0260877410003286

http://dx.doi.org/10.1016/j.jfoodeng.2010.06.027

Cited by in Scopus (4)

Received 15 March 2010. Revised 28 June 2010. Accepted 30 June 2010. Available online 6 July 2010.

Abstract

Computed tomography (CT) has been previously used as a non-destructive technology to accurately determine salt and water content in dry-cured ham at the initial stages of the elaboration process. However, since the accuracy of predictive models has been affected by the dry level of the sample, in this study, prediction models for salt and water contents and also for a_w to be applied during drying process were developed. Results showed that the number of independent variables needed to obtain regression models with a similar accuracy to the models previously developed is higher in drier samples. Furthermore, an important effect of fat content is also observed since prediction of a_w, salt content and water content were significantly improved when the fattiest samples were removed from the calibration or when fat content was included in the predictive models. Because of the different physicochemical characteristics of muscles, models developed specifically for *Semimembranosus* (SM), *Biceps femoris* (BF) or *Semitendinosus* (ST) muscles were more accurate. It can be concluded that models for prediction during the drying process were accurate enough to consider CT as a useful tool applicable for controlling and optimizing the dry-cured ham elaboration processes.

Keywords

- Computed tomography;
- Dry-cured ham;
- Fat;
- Prediction models;
- a_w;
- Salt;
- Water

Paper III

Santos-Garcés, E., Muñoz, I., Gou, P., Garcia-Gil, N., & Fulladosa, E. (2012). Intramuscular fat content estimated by image analysis improves computed tomography based models for estimating salt, water and aw in dry-cured hams. *Food Chemistry*, (submitted).

Food Chemistry
(submitted)

Intramuscular fat content estimated by image analysis improves computed tomography based models for estimating salt, water and a_w in dry-cured hams

Eva Santos-Garcés [a], Israel Muñoz [a], Pere Gou [a], Núria Garcia-Gil [a], Elena Fulladosa [a, *]

[a] IRTA. XaRTA. Food Technology. Finca Camps i Armet, E-17121 Monells, Spain

[*] Corresponding author: Tel: +34972630052, fax: +34972630373, e-mail: elena.fulladosa@irta.cat

Abstract

Computed tomography (CT) has been proposed as a method for the non-destructive prediction of salt content, water content and water activity (a_w) in dry-cured ham. However, intramuscular fat content (IMF) produces an important disturbance in the predictions, mainly in water content and a_w predictions. In this study, IMF was estimated in *Biceps femoris* (BF) and *Semitendinosus* (ST) muscles of dry-cured ham by image analysis of CT tomograms. New CT based models for salt content, water content, and a_w predictions were obtained including the IMF estimate into the model. An independent data set was used to validate and compare the prediction models with and without including IMF estimate. When including the IMF estimate into the models, errors of prediction were reduced from 0.266 to 0.191% for salt content, from 4.58 to 2.24% for water content, and from 0.0100 to 0.0059 for a_w. The non-destructive determination of IMF by image analysis of CT tomograms in dry-cured ham can be used to improve the CT based models for estimating salt content, water content and a_w.

Keywords: *Computed tomography, image analysis, dry-cured ham, intramuscular fat content*

1. Introduction

In recent years, computed tomography (CT) has been successfully introduced into the meat industry as a non-destructive tool for a wide range of applications. CT is now included in the EU legislation as a suitable reference method for carcass classification (Commission Regulation (EC) 1249/2008) because it provides extremely accurate measurements of carcass composition, in terms of lean, fat and bone tissues (Allen, 2003; Font i Furnols, Teran, & Gispert, 2009; Font i Furnols, & Gispert, 2009; Vester-Christensen *et al.,* 2009; Picouet, Teran, Gispert & Font i Furnols, 2010). The use of CT to correctly distinguish salt in cured meat products was also described by Sørheim and Berg (1987a, b) and Frøystein, Sørheim, Berg, & Dalen (1989) in dry-cured ham. CT later was calibrated and mathematical models were proposed to determine salt content (Vestergaard, Risum, & Adler-Nissen, 2005; Håseth, Høy, Kongsro, Kohler, Sørheim, & Egelandsdal, 2008; Fulladosa, Santos-Garcés, Picouet, & Gou 2010; Santos-Garcés, Gou, Garcia-Gil, Arnau, & Fulladosa, 2010; Santos-Garcés, Muñoz, Gou, Sala, & Fulladosa, 2012), water content (Fulladosa *et al.,* 2010; Santos-Garcés *et al.,* 2010; Santos-Garcés, Gou, Garcia-Gil, Muñoz, Arnau, Fulladosa, 2010; Santos-Garcés *et al.,* 2012) and water activity (a_w) (Santos-Garcés *et al.,* 2010a,b; Santos-Garcés *et al.,* 2012) under different conditions and at different stages of the dry-cured ham elaboration process. CT analytical tools, in combination with the prediction models mentioned above, have provided quantitative information on local salt content, water content, and a_w, and their distribution within the ham throughout the process (Vestergaard *et al.,* 2005; Santos-Garcés *et al.,* 2012). These CT analytical tools have been applied to monitor and compare different salting processes (Santos-Garcés *et al.,* 2012), to evaluate hams that have undergone different pre-salting treatments, such as skin trimming or pressing (Garcia-Gil, Santos-Garcés, Muñoz, Fulladosa, Arnau, & Gou 2012), and to estimate NaCl diffusivity in the *Semimembranosus* (SM) muscle during salting process of hams (Picouet, Gou, Fulladosa, Santos-Garcés, & Arnau, 2012).

The main drawback of CT based models is the disturbance that fat produces in the predictions, which has been widely described (Vestergaard, Erbou, Thauland, Adler-Nissen, & Berg, 2004; Håseth, Egelandsdal, Bjerke, & Sørheim, 2007; Håseth *et al.,* 2008; Fulladosa *et al.,* 2010; Santos-Garcés *et al.,* 2010a, b; Santos-Garcés *et al.,* 2012). Intramuscular fat content (IMF) produces an increase of prediction errors, mainly in water content and a_w predictions. Several studies have reported that the errors of prediction significantly decreased when fatty samples were left out of the models (Håseth *et al.,* 2007; Fulladosa *et al.,* 2010) or when information on analytical IMF was included into the models Håseth *et al.,* 2007; Santos-Garcés *et al.,* 2010a, b). Nevertheless, although Brun, Gispert, Valero, & Font i Furnols (2011) described CT as a promising tool for the determination of IMF in raw hams by means of image analysis, estimation of IMF in samples that have undergone a salting process is not straightforward. Since salted fat presents higher attenuation values than non-salted fat (due to the higher density of Na^+ and Cl^- ions), it might be recognized as false lean. In dry-cured ham, only the subcutaneous and the intermuscular fat have been successfully segmented from CT tomograms using image analysis (Santos-Garcés *et al.,* 2012).

The aims of this study were (1) the non-destructive estimation of IMF in dry-cured ham muscles by image analysis of CT tomograms, and (2) the improvement of CT based models for predicting salt content, water content, and a_w through the inclusion of IMF estimate into the models.

2. Material and Methods

2.1. Hams

Sixty-three commercial hams were selected at different stages of the dry-curing elaboration process: resting (n = 15), drying (n = 15), and end of process (n = 33). The hams came from seven different producers in order to obtain a representative sample of the industrial market in terms of salt, water and fat contents.

2.2. Scanning conditions and sample preparation

CT scanning of hams was performed

using a scanner model HiSpeed Zx/i from General Electric Healthcare (GE Healthcare, Barcelona, Spain). An axial protocol was used with settings of 80, 120 and 140 kV, 250 mA and rotation time of 2 seconds. Image size was 512 x 512 pixels and Displayed Field of View (DFOV) was 461 x 461 mm^2. The algorithm STD+ from General Electric was used to reconstruct the images because it gives a high contrast spatial resolution in samples containing soft tissue (lean and fat) and mineral phases (mainly NaCl). Each pixel had a squared area of 0.81 mm^2 and had three CT values expressed in Hounsfield Units (HU) obtained at 80, 120, and 140 kV (HU_{80}, HU_{120} and HU_{140}, respectively). Matrixes of HU values were saved and retrieved with Matlab software (MATLAB, Ver. 7.7.0, The Mathworks Inc., Natick, MA, USA) for further automated analysis.

In order to obtain a sufficient quantity of the sample for chemical analysis, two consecutive 10 mm thick tomograms were obtained at 10 cm from the aitch bone in the distal direction (at the widest part of the ham) (Figure 1A). From each tomogram, three different Regions of Interest (ROIs) were selected from different zones of the slice to achieve a wide range of compositions, in terms of salt, water, and fat contents. ROI 1 contained the *Biceps femoris* (BF) muscle, ROI 2 contained the *Semitendinosus* (ST) muscle, and ROI 3 contained the *Semimembranosus* (SM) muscle (Figure 1B). The average CT values of the two consecutive tomograms were performed, obtaining for each ROI, a HU_{80}, HU_{120} and HU_{140} values.

To develop and validate the models for estimating IMF, salt content, water content, and a_w, hams were divided into two sets; a calibration data set (n = 42) for modelling and a validation data set (n = 21). To define both sets, hams were arranged according to the analytical IMF of the ST muscle, and

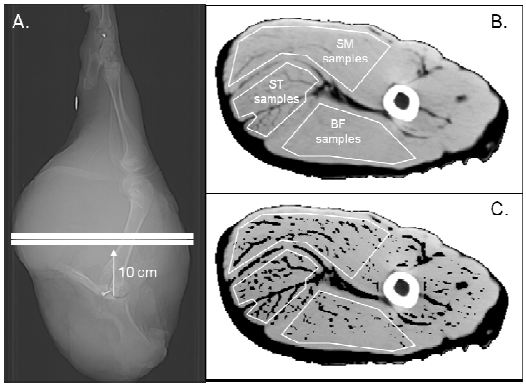

Figure 1. CT scans location (A). Cross-sectional CT image (tomogram) obtained at 80 kV, in which sampled ROIs from *Semimembranosus* (SM), *Biceps femoris* (BF) and *Semitendinosus* (ST) muscles are indicated (B). CT image after segmentation, where intramuscular fat is illustrated by the black area within each ROI (C).

subsequently distributed alternatively, one ham for validation and two hams for calibration. In this way, both sets of samples covered the whole range of IMF values.

Sampling of the ROIs was performed as described by Fulladosa *et al.* (2010). For the calibration data set, 126 ROI samples were obtained (42 SM, 42 BF and 42 ST samples). The validation data set contained 63 further ROI samples (21 SM, 21 BF and 21 ST samples). The ROIs were cut out of the ham slices and immediately vacuum packed in plastic bags. Each sample was minced, homogenized and analyzed for salt, water and fat contents, and a_w.

2.3. Chemical analysis

All analyses were performed in triplicate. Water activity was measured using Aqualab (AquaLab Series 3TE, Decagon Devices, Inc., Pullman, Washington, USA); the analytical standard deviation was 0.001%. Chloride content was determined according to ISO 1841-2 (1996) using a potentiometric titrator 785 DMP Titrino (Metrohm AG, Herisau, Switzerland); the analytical standard deviation was 0.03%. Water content was analysed by drying at 103 ± 2 ºC until reaching a constant weight (AOAC, 1990); the analytical standard deviation was 0.19%. The total fat content was measured by Soxtec extraction (SoxCap 2047 and Soxtec 2055) according to ISO 1443 (1973); the analytical standard deviation was 0.37%.

2.4. IMF estimate by image analysis of CT tomograms

Matlab scripts written in-house were developed to analyze specific ROIs of the matrixes of values obtained from the tomograms. Composition of the hams varied greatly in terms of salt, water and fat contents, therefore the segmentation had to be robust so that the extraction of data features was consistent. For each ROI, IMF was segmented at 80 kV matrix by filtering the image using the fast Fourier transform (FFT) and applying a Gaussian high pass filter. After filtering, the images were converted back to the spatial domain and pixels with HU values equal to or below -5 were labelled as IMF by a threshold operation. The area of the matrix (number of pixels) considered as IMF

was expressed as percentage of IMF area (IMF area (%)) which was calculated as the ratio IMF area/total area.

The relationship between the analytical IMF and the IMF area (%) was evaluated. A Weibull cumulative distribution function was selected for estimating IMF through the IMF area (%) obtained by image analysis of CT tomograms. The non-linear least square method was used to determine the model parameters by means of Matlab software. The coefficient of determination (R^2) and the Root Mean Square Error of Prediction or Calibration (RMSEC) were calculated as was described in Santos-Garcés *et al.* (2010). The IMF prediction model was validated with the validation data set and the R^2 and the Root Mean Square Error of Validation (RMSEV) were also calculated.

2.5. Development of prediction models

CT based prediction models for salt content, water content, and a_w were fitted with the BF and ST samples from the calibration data set (n = 84) using the regression procedure (REG procedure) from SAS package (SAS Institute Inc., Cary, NC, USA, 2001). Model independent variables (HU_{80}, HU_{120} and HU_{140}) were selected by Stepwise method. Models also including IMF estimate were fitted. Significant levels to enter and keep the dependent variables in the model were p = 0.25 and p = 0.10, respectively.

Regression models (salt content, water content, and a_w) obtained Santos-Garcés *et al.* (2010), which did not include IMF estimate in the model, were validated with the BF and ST samples from the calibration data set (n = 84). In addition, the new prediction models developed in the present study (with and without including IMF estimate) were also validated with the BF and ST samples from the validation data set (n = 42). The R^2, the RMSEC, and the RMSEV were calculated as was described above.

3. Results and Discussion

3.1. IMF estimation

Analytical IMF of the samples used in this study ranged from 0.7 to 16.4% for the calibration data set, and from 0.6 to

13.8% for the validation data set. Although SM, BF and ST muscles were initially considered to develop the IMF prediction model, samples from the SM muscle were finally removed from the model. The image analysis employed was not accurate enough to properly distinguish IMF present in SM muscle, due to the high gradient of salt achieved in the external muscles during the post-salting stages. It must be highlighted that IMF can be estimated during the entire dry-cured ham elaboration process only in internal muscles, which present a more homogeneous salt distribution than external ones.

Figure 2 shows the relationship between the IMF area (%) segmented by image analysis of CT tomograms and the analytical IMF. IMF estimate can be calculated with the following equation:

IMF estimate (%) =

$$21.2 - 20.39 \times \exp\left(-\left(\text{IMF area (\%)} / 36.79\right)^{4.466}\right)$$

This model had an RMSEC of 0.75% and an R^2 of 0.967. Figure 3 shows the relationship between the analytical IMF and the IMF estimate in the external validation set (n = 42). The global RMSEV was 1.48%, but it was lower in leaner samples (RMSEC = 0.67% for IMF ≤ 4%) than in the fatter samples (RMSEC = 1.30% for IMF ≥ 4%). Although these errors were high in comparison to analytical errors, IMF estimate may improve the CT based models, which is demonstrated in the next section.

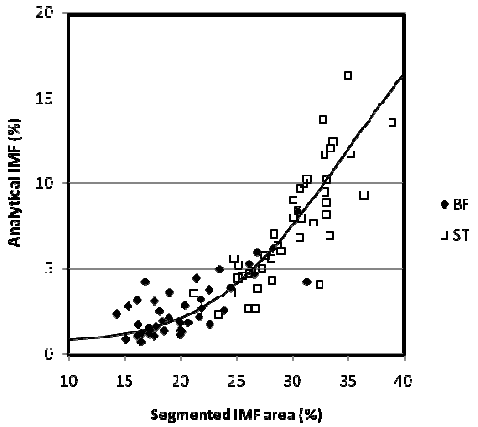

Figure 2. Analytical intramuscular fat content (IMF) versus segmented IMF area (IMF area (%)) by image analysis of CT tomograms for the calibration data set (n = 84). BF: *Biceps femoris*; ST: *Semitendinosus*. The line represents the IMF estimate [*IMF estimate (%) = 21.2 – 20.39 x exp (- (IMF area (%) / 36.79)* $^{4.466}$*)].*

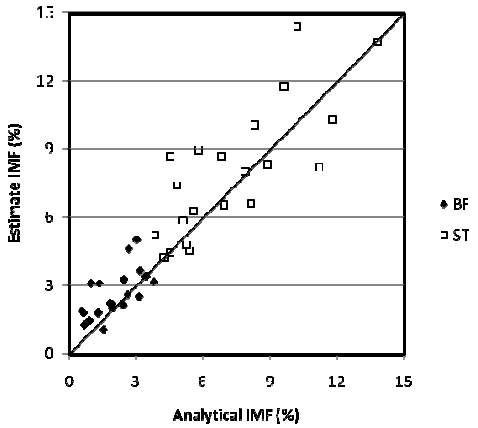

Figure 3. Relationship between the estimate and the analytical intramuscular fat content (IMF) for the validation data set (n = 42). BF: *Biceps femoris* muscle; ST: *Semitendinosus* muscle. The line represents the perfect 1:1 relationship between *x* and *y*.

3.2 Prediction models including non-destructive IMF estimation

Figure 4 shows the relationship between the analytical IMF and the errors (measured - predicted) for salt content, water content, and a_w when the models previously developed by Santos-Garcés *et al.* (2010) were applied on the calibration data set (n = 84). RMSEV values obtained in the present study for water content and a_w (5.33% and 0.0127, respectively) were higher than those found by Santos-Garcés *et al.* (2010) (3.53% and 0.0099, respectively). This fact could be explained by the differences in IMF between the samples of the calibration data set of the present study (IMF = 5.12% and SD_{BF} = 3.56) and the samples used by Santos-Garcés *et al.* (2010) (IMF = 3.66% and SD = 3.28). Moreover, for the studied parameters, an error dependency on IMF was observed in both BF and ST muscles, mainly in water content and a_w predictions. Salt content was underestimated in the fattiest samples (Figure 4A), while water content and a_w were overestimated (Figures 4B and 4C, respectively). Similar results were obtained by Fulladosa *et al.* (2010) and Santos-Garcés *et al.* (2010). IMF produced a decrease of attenuation values which in turn produced an underestimation of salt content, water

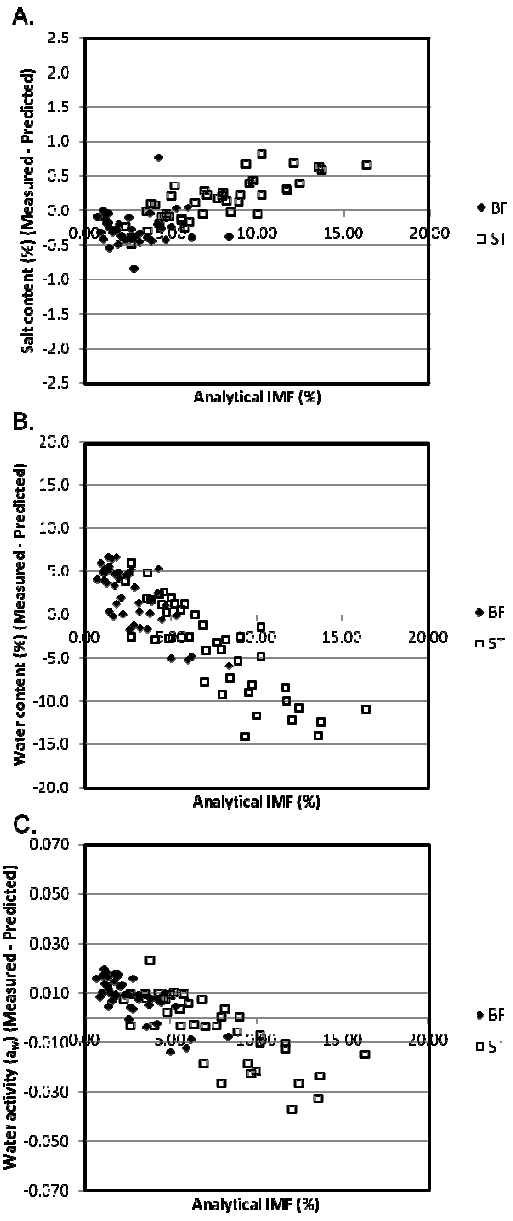

Figure 4. Prediction errors as a function of intramuscular fat content (IMF) for salt content (A), water content (B) and a_w (C), obtained using prediction models* obtained by Santos-Garcés *et al.* (2010) on samples from calibration data set (n = 84). BF: *Biceps femoris* muscle; ST: *Semitendinosus* muscle.

* Models: Salt (%) = $0.91 + 0.2222 \cdot HU_{80} - 0.2631 \cdot HU_{120} + 0.0389 \cdot HU_{140}$

Water (%) = $80.2 + 0.425 \cdot HU_{80} - 0.616 \cdot HU_{120}$

$a_w = 1.0207 - 0.00145 \cdot HU_{80} + 0.00164 \cdot HU_{120} - 0.00064 \cdot HU_{140}$

content and a_w predictions. The effect of fat on CT attenuation values was also reported by Vestergaard *et al.* (2004), who remarked that minor differences in IMF (i.e. between muscles) can produce significant differences on attenuation values.

To take into account the differences in analytical IMF between samples from the current study and those obtained by Santos-Garcés *et al.* (2010), new prediction models were calculated for the calibration data set (n = 84). The new models were developed with and without including IMF estimate (Table 1, Table 2 and Table 3). Moreover, since characteristics of different muscles can influence the predictions (Fulladosa *et al.*, 2010; Santos-Garcés *et al.*, 2010), specific models for each single muscle (BF and ST) were developed. The performance of the new prediction models (with and without including IMF estimate) was tested with the external validation data set (n = 42). RMSEC and RMSEV were similar in all cases. Water content prediction models including IMF estimate reduced both, RMSEC and RMSEV errors (Table 1, Table 2 and Table 3). Even though the accuracy of the salt predictability was also improved by including IMF estimate into the models, this parameter was

Table 1
Prediction models for salt content, with and without including intramuscular fat content (IMF) estimate. HU_{80}, HU_{120} and HU_{140} are the CT values expressed in Hounsfield units (HU) obtained at 80, 120 and 140 kV, respectively. RMSEC: Root Mean Square Error of Prediction or Calibration; R^2: Coefficient of determination; RMSEV: Root Mean Square Error of Validation; BF: *Biceps femoris* muscle; ST: *Semitendinosus* muscle.

Muscles in data set	Prediction models	RMSEC	R^2	RMSEV
Without including IMF estimate				
BF + ST	Salt (%) = $1.88 + 0.2297 \cdot HU_{80} - 0.1856 \cdot HU_{120} - 0.0607 \cdot HU_{140}$	0.266	0.965	0.327
BF	Salt (%) = $1.13 + 0.2113 \cdot HU_{80} - 0.2174 \cdot HU_{120}$	0.199	0.983	0.238
ST	Salt (%) = $1.42 + 0.2074 \cdot HU_{80} - 0.1793 \cdot HU_{120} - 0.0355 \cdot HU_{140}$	0.254	0.966	0.246
Including IMF estimate				
BF + ST	Salt (%) = $1.26 + 0.2379 \cdot HU_{80} - 0.2499 \cdot HU_{120} + 0.0625 \cdot IMF$	0.191	0.982	0.265
BF	Salt (%) = $1.45 + 0.2437 \cdot HU_{80} - 0.2577 \cdot HU_{120} + 0.0487 \cdot IMF$	0.188	0.985	0.228
ST	Salt (%) = $1.10 + 0.2314 \cdot HU_{80} - 0.2413 \cdot HU_{120} + 0.0627 \cdot IMF$	0.201	0.979	0.260

Table 2
Prediction models for water content, with and without including intramuscular fat content (IMF) estimate. HU_{80}, HU_{120} and HU_{140} are the CT values expressed in Hounsfield units (HU) obtained at 80, 120 and 140 kV, respectively. RMSEC: Root Mean Square Error of Prediction or Calibration; R^2: Coefficient of determination; RMSEV: Root Mean Square Error of Validation; BF: *Biceps femoris* muscle; ST: *Semitendinosus* muscle.

Muscles in data set	Prediction models	RMSEC	R^2	RMSEV
Without including IMF estimate				
BF + ST	Water (%) = 86.0 + 0.8580·HU_{80} - 2.4040·HU_{120} + 1.3259·HU_{140}	4.58	0.543	5.17
BF	Water (%) = 102.4 + 1.1617·HU_{80} - 1.6016·HU_{120}	2.78	0.749	2.01
ST	Water (%) = 90.6 + 1.2345·HU_{80} - 2.6677·HU_{120} + 1.0881·HU_{140}	3.90	0.716	5.17
Including IMF estimate				
BF + ST	Water (%) = 96.0 + 0.5870·HU_{80} - 1.2437·HU_{120} + 0.3933·HU_{140} - 1.2630·IMF	2.24	0.892	1.77
BF	Water (%) = 89.4 - 0.1543·HU_{120} - 1.2710· IMF	2.30	0.829	1.84
ST	Water (%) = 95.4 + 0.6617·HU_{80} - 1.4291·HU_{120} + 0.5051·HU_{140} - 1.2802·IMF	2.12	0.918	1.91

Table 3
Prediction models for a_w, with and without including intramuscular fat content (IMF) estimate. HU_{80}, HU_{120} and HU_{140} are the CT values expressed in Hounsfield units (HU) obtained at 80, 120 and 140 kV, respectively. RMSEC: Root Mean Square Error of Prediction or Calibration; R^2: Coefficient of determination; RMSEV: Root Mean Square Error of Validation; BF: *Biceps femoris* muscle; ST: *Semitendinosus* muscle.

Muscles in data set	Prediction models	RMSEC	R^2	RMSEV
Without including IMF estimate				
BF + ST	a_w = 1.0606 + 0.00158·HU_{80} - 0.00509·HU_{120} + 0.00254·HU_{140}	0.0100	0.855	0.0133
BF	a_w = 1.0936 + 0.00239·HU_{80} - 0.00382·HU_{120}	0.0062	0.946	0.0065
ST	a_w = 1.0828 + 0.00277·HU_{80} - 0.00630·HU_{120} + 0.00215·HU_{140}	0.0074	0.926	0.0153
Including IMF estimate				
BF + ST	a_w = 1.0859 + 0.00121·HU_{80} - 0.00237·HU_{120} - 0.00271·IMF	0.0059	0.949	0.0065
BF	a_w = 1.0809 + 0.00109·HU_{80} - 0.00221·HU_{120} - 0.00195·IMF	0.0055	0.959	0.0054
ST	a_w = 1.0879 + 0.00187·HU_{80} - 0.00418·HU_{120} + 0.00106·HU_{140} - 0.00189·IMF	0.0058	0.954	0.0098

the least affected (Figure 4 and Figure 5). In general, specific models developed for the BF muscle were more accurate than models that included both BF and ST samples (Santos-Garcés *et al.,* 2010), and the errors dependency on IMF nearly disappeared. These results are of special interest since the BF muscle is the most problematic one.

Figure 5 and Figure 6 show the relationship between the analytical IMF and the errors (measured - predicted) for salt content, water content, and a_w values for water content and a_w were higher than those found by (Santos-Garcés *et al.,* 2010). This fact can be explained because the hams in this study were obtained from seven different producers and at different stages of the elaboration processes.

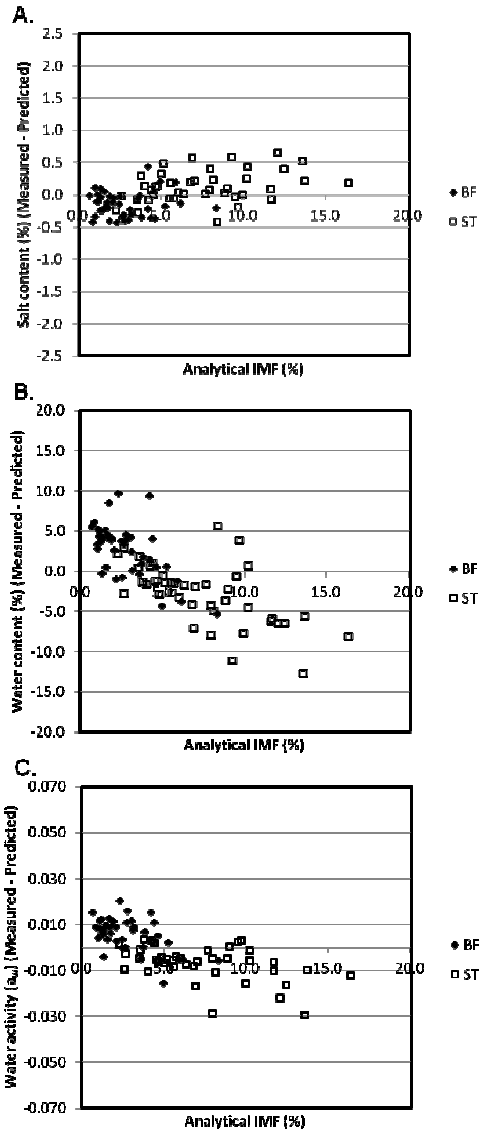

Figure 5. Deviation errors as a function of intramuscular fat content (IMF) for salt content (A), water content (B) and a_w (C) in calibration data set (n = 84), obtained with new prediction models without including IMF estimate into the prediction models. BF: *Biceps femoris* muscle; ST: *Semitendinosus* muscle.

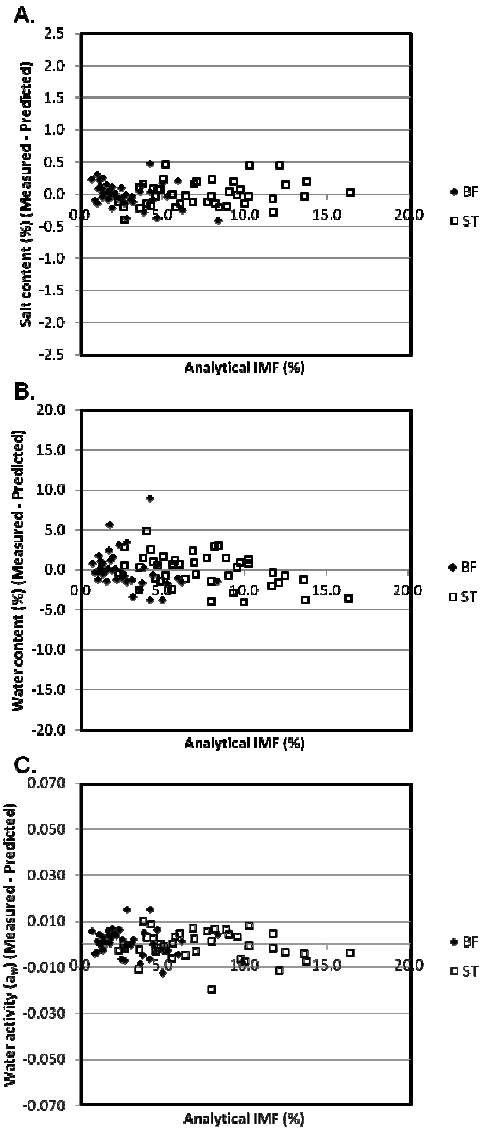

Figure 6. Deviation errors as a function of intramuscular fat content (IMF) for salt content (A), water content (B) and a_w (C) in calibration data set (n = 84), obtained with new prediction models including IMF estimate into the prediction models. BF: *Biceps femoris* muscle; ST: *Semitendinosus* muscle.

This sampling procedure resulted in a wider range of variability (in terms of salt, water and fat contents) in comparison to the hams used in previous studies (Fulladosa *et al.,* 2010; Santos-Garcés *et al.,* 2010a; Santos-Garcés *et al.,* 2012), which may explain the higher RMSEC, but it may also increase the robustness of the new prediction models when they are applied to commercial dry-cured hams.

In Figure 5, the same errors dependency on IMF as in the models developed by Santos-Garcés *et al.* (2010) was observed. However, this errors dependency disappeared when IMF estimate was included into the prediction models (Figure 6).

The combination of two (80 and 120 kV) or three voltages (80, 120 and 140 kV) and the IMF estimate in most cases gave the lowest prediction errors. The use of one voltage (120 kV) and the IMF estimate is also feasible for water content prediction in the case of the BF muscle. However, since IMF was estimated from the 80 kV matrixes, a minimum of two energies (80 and 120 kV) were needed to obtain an optimal estimation. Therefore, the incorporation of the non-destructive IMF estimate can reduce to two (80 and 120 kV) the number of CT voltages needed, representing a reduction of the cost of the analysis of prediction using CT in dry-cured ham. Although IMF estimate was slightly underestimated in the fattiest samples, a high improvement in the predictions when IMF estimate was included into the models was found in the ST muscle (Table 1, Table 2 and Table 3), which is the fattiest one.

The addition of IMF estimate can provide a major improvement in a wide range of CT applications. For instance, the higher accuracy of a_w predictions may establish CT as a suitable method for the determination of microbiological stability in dry-cured ham.

4. Conclusions

Non-destructive estimate of IMF in dry-cured ham samples can be achieved by image analysis of CT tomograms, apart from on external muscles during the post-salting stages. The inclusion of IMF estimate into the models significantly improves the prediction by reducing the errors of prediction in the models from 0.266 to 0.191% for salt content, from 4.58 to 2.24% for water content, and from 0.0100 to 0.0059 for a_w in BF and ST muscles. Moreover, the number of CT energies needed when IMF estimate is included in the prediction models decreases from three to two, which means a reduction in cost of CT analysis.

Acknowledgements

This work was supported by the 6th EU framework Integrated Project Q-Porkchains (Contract No. FOOD-CT-2007-036245), and the XaRTA - Reference Network on Food Technology from the Government of Catalonia (Contract No. EvalXaRTA-2011-306260). The information in this document reflects only the authors' views and the Community is not liable for any use that may be made of the information contained therein. We thank Gustavo Rodriguez Artero for technical assistance.

References

Allen, P. (2003). WP3 Summary. EUPIGCLASS Final Workshop, 6-7 October 20013. Roskilde, Denmark. URL (http://www.eupigclass.net/Work3/04_Paul_WP%203Summary-filer/frame.htm).

AOAC. (1990). Official method 950.46, moisture in meat, B. air drying. In: Helrich K. (Ed.), Official Methods of Analysis of the Association of Official Analytical Chemists, 15th ed., vol. II. Association of Official Analytical Chemists, Inc., Arlington, p. 931.

Brun, A., Gispert, M., Valero, A., & Font i Furnols, M. (2011). Determinación del porcentaje de grasa intramuscular en lomo de cerdo mediante métodos químicos y métodos no invasivos. *EUROCARNE*, 199, 70-77.

Commission Regulation (EC) (1249/2008) of 10 December 2008 laying down detailed rules on the implementation of the Community scales for the classification of beef, pig and sheep carcasses and the reporting of prices thereof.

Font i Furnols, M., & Gispert, M. (2009). Comparison of different devices for predicting the lean meat percentage of pig carcasses. *Meat Science*, 83 (3), 443–446.

Font i Furnols, M., Teran, F., & Gispert, M. (2009). Estimation of lean meat content in pig carcasses using x-ray computed tomography images and PLS regression. *Chemometrics and Intelligent Laboratory Systems*, 98 (1), 31–37.

Frøystein, T., Sørheim, O., Berg, S.A., & Dalen, K. (1989). Salt distribution in cured hams, studied by computer X-ray tomography. *Fleischwirtschaft,* 69 (2), 220–222.

Fulladosa, E., Santos-Garcés, E., Picouet, P., & Gou, P. (2010). Salt and water content prediction by computed tomography in dry-cured hams. *Journal of Food Engineering*, 96 (1), 80–85.

Garcia-Gil, N., Santos-Garcés, E., Muñoz, I., Fulladosa, E., Arnau, J., & Gou, P. (2011). Salting, drying and sensory quality of dry-cured hams subjected to different pre-salting treatments: Skin trimming and pressing. *Meat Science,* 90 (2), 386–392.

Håseth, T., Egelandsdal, B., Bjerke, F., & Sørheim, O. (2007). Computed tomography for quantitative determination of sodium chloride in ground pork and dry-cured hams*. Journal of Food Science*, 72 (8), 420–427.

Håseth, T., Høy, M., Kongsro, J., Kohler, A., Sørheim, O., & Egelandsdal, B. (2008). Determination of sodium chloride in pork meat by computed tomography at different voltages. *Journal of Food Science*, 73 (7), 333–339.

ISO 1443. (1973). Determination of total fat content. International Organization for Standardization, Geneva.

ISO 1841–2. (1996). Determination of Chloride Content – Part 2: Potentiometric Method. International Organization for Standardization, Geneva.

Picouet, P., Teran, F., Gispert, M., & Font i Furnols, M. (2010). Lean content prediction in pig carcasses, loin and ham by computerized tomography (CT) using a density model. *Meat Science*, 86 (3), 616–622.

Picouet, P., Gou, P., Fulladosa, E., Santos-Garcés, E., & Arnau, J. (2012). Estimation of salt diffusivity by Computed Tomography in the *semimembranosus* muscle during dry curing of hams. *LWT – Food Science and Technology, (submitted)*.

Santos-Garcés, E., Gou, P., Garcia-Gil, N., Arnau, J., & Fulladosa, E. (2010a). Non-destructive analysis of a_w, salt and water in dry-cured hams during drying process by means of computed tomography. *Journal of Food Engineering*, 101 (2), 187–192.

Santos-Garcés, E., Gou, P., Garcia-Gil, N., Muñoz, I., Arnau, J., & Fulladosa, E. (2010b). Non-destructive prediction of water activity, water and fat contents in dry-cured ham by computed tomography. *Proceedings of the 6th International conference on Water in Food*, Reims, France, March 21–23.

Santos-Garcés, E., Muñoz, I., Gou, P., Sala, X., & Fulladosa, E. (2012). Tools for studying dry-cured ham processing by using computed tomography. *Journal of Agricultural and Food Chemistry,* 60 (1), 241–249.

Sørheim, O., & Berg, S. A. (1987a). Computed X-ray tomography (CT) as a non-destructive method to study salt distribution in meat. In W. Baltes, P. Baardseth, P. Czedik-Eysenberg, J. Davidek, A. Davies, P. Dirinck, C. Genty, S. A. Jensen, R. Linko, P. Mattson, C. Mercier, W. Pfannhauser, E. Pungor, & N. Skovgaard (Eds.), *Rapid analysis in food processing and food control* (pp 196–200). MATFORSK: Ås, Norway.

Sørheim, O., & Berg, S. A. (1987b). Dry cured hams produced from frozen/thawed raw materials. *Proceedings of the 33rd International Congress of Meat Science and Technology*, Helsinki, Finland, pp 327–329.

Vester-Christensen, M., Erbou, S. G. H., Hansen, M. F., Olsen, E. V., Christensen, L. B., Hviid, M., Ersbøll, B. K., & Larsen, R. (2009). Virtual dissection of pig carcasses. *Meat Science*, 81 (4), 699–704.

Vestergaard, C., Erbou, S. G., Thauland, T., Adler-Nissen, J., & Berg, P. (2005). Salt distribution in dry-cured ham measured by computed tomography and image analysis. *Meat Science*, 69 (1), 9–15.

Vestergaard, C., Risum, J., & Adler-Nissen, J. (2004). Quantification of salt concentrations in cured pork by computed tomography. *Meat Science*, 68 (1), 107–113.

Paper IV

Santos-Garcés, E., Muñoz, I., Gou, P., Sala, X., & Fulladosa, E. (2012). Tools for studying dry-cured ham processing by using computed tomography. *Journal of Agricultural and Food Chemistry,* 60 (1), 241-249.

Eva Santos-Garcés, Israel Muñoz, Pere Gou, Xavier Sala, and Elena Fulladosa. "Tools for Studying Dry-Cured Ham Processing by Using Computed Tomography". *Journal of agricultural and food chemistry*. Vol. 60, issue 1 (January 11 2012): p. 241-249

http://pubs.acs.org/doi/abs/10.1021/jf203213q

DOI: http://dx.doi.org/10.1021/jf203213q

Publication Date (Web): December 5, 2011

Abstract

An accurate knowledge and optimization of dry-cured ham elaboration processes could help to reduce operating costs and maximize product quality. The development of nondestructive tools to characterize chemical parameters such as salt and water contents and a_w during processing is of special interest. In this paper, predictive models for salt content (R^2 = 0.960 and RMSECV = 0.393), water content (R^2 = 0.912 and RMSECV = 1.751), and a_w (R^2 = 0.906 and RMSECV = 0.008), which comprise the whole elaboration process, were developed. These predictive models were used to develop analytical tools such as distribution diagrams, line profiles, and regions of interest (ROIs) from the acquired computed tomography (CT) scans. These CT analytical tools provided quantitative information on salt, water, and a_w in terms of content but also distribution throughout the process. The information obtained was applied to two industrial case studies. The main drawback of the predictive models and CT analytical tools is the disturbance that fat produces in water content and a_w predictions.

Keywords:
Computed tomography; dry-cured ham; predictive models; salt; water; a_w; CT analytical tools

Paper V

Garcia-Gil, N., **Santos-Garcés, E.**, Muñoz, I., Fulladosa, E., Arnau, J., & Gou, P. (2012). Salting, drying and sensory quality of dry-cured hams subjected to different pre-salting treatments: Skin trimming and pressing. *Meat Science*, 90 (2), 389-392.

N. Garcia-Gil, E. Santos-Garcés, I. Muñoz, E. Fulladosa, J. Arnau,P. Gou. “Salting, drying and sensory quality of dry-cured hams subjected to different pre-salting treatments: Skin trimming and pressing”. *Meat science.* Volume 90, Issue 2, February 2012, Pages 386–392

Received 18 May 2011. Revised 3 August 2011. Accepted 5 August 2011. Available online 12 August 2011

http://www.sciencedirect.com/science/article/pii/S0309174011002865

http://dx.doi.org/10.1016/j.meatsci.2011.08.003

Cited by in Scopus (1)

Abstract

The effects of skinning in a V-shape and pressing of hams on salting, drying and sensory characteristics of dry-cured hams were assessed. Salt and water contents and a_w were determined in the central part of the ham during processing by computed tomography. Overall salt and water contents were also chemically analysed. Sensory analyses were performed on the final product. Partial skinning or pressing increased both salt uptake and final weight loss, but did not reduce the intra-batch variability in salt uptake. Moreover, trimmed hams exhibited a higher salt content in the inner areas of the hams after resting. Trimmed dry-cured hams showed less metallic flavour, higher saltiness and more mature flavour in the *biceps femoris* muscle, and lower pastiness and adhesiveness as well as higher crumbliness and aged flavour in both the *biceps femoris* and the *semimembranosus* muscles. Pressing treatment caused less metallic flavour only in *biceps femoris* muscle and higher saltiness.

Highlights

► Skin trimming or pressing before salting increased the average salt absorption. ► Neither skin trimming nor pressing reduced the variability in the salt absorption. ► Trimming in a V shape accelerated the weight loss of the hams. ► With skin trimming salt reached faster the innermost part of the ham.

Keywords

- Dry-cured ham;
- Skin trimming;
- Pressing;
- Sensory analysis

Paper VI

Picouet, P., Gou, P., Fulladosa, E., **Santos-Garcés, E.**, & Arnau, J. (2012). Estimation of salt diffusivity by Computed Tomography in the *Semimembranosus* muscle during salting of fresh and frozen/thawed hams. *LWT - Food Science and Technology*, (submitted).

LWT - Food Science and Technology
(submitted)

Estimation of salt diffusivity by Computed Tomography in the *Semimembranosus* muscle during salting of fresh and frozen/thawed hams

Pierre A. Picouet [a, *], Pere Gou [a], Elena Fulladosa [a], Eva Santos-Garcés [a], Jacint Arnau [a]

[a] IRTA. XaRTA. Food Technology. Finca Camps i Armet, E-17121 Monells, Spain

[*] Corresponding author: Tel.: +34 972630052; fax: +34 972630373; e-mail: pierre.picouet@irta.es

Abstract

In the elaboration of dry-cured hams, the understanding of salt diffusion is an important step to optimise salt uptake. Calibrated computed tomography (CT) gives non-destructive measurements of salt and water contents. The aim of this study is to develop a simplified methodology based on an unidirectional diffusion model and CT measurements for assessing salt diffusion in *Semimembranous* muscle during dry curing of ham. To test the methodology, five pairs of hams were selected. One ham from each pair was subjected to a freezing/thawing treatment before salting period. CT images of a central section were taken during the 16 days of the salting period. From each voxel, salt and water contents were determined and introduced in the diffusion model. Thus, NaCl diffusion coefficients were calculated for each ham. Resulting diffusion coefficients are in the same order of magnitude than values given by literature. As expected, higher diffusion coefficients were found for frozen/thawed hams samples. Combination of calibrated CT measurements with a simple diffusion model can be used to obtain a non-destructive estimation NaCl diffusivity during dry curing of ham.

Keywords: *Diffusion, NaCl, CT, tomography, salt, salting, ham, modelling, non-destructive*

Nomenclature:

$[W]_i$	Water content (kg/kg) of voxel i	η	Boltzmann's space time variable express as $\xi/\sqrt{t}$
$[S]_i$	Salt content (kg/kg) of voxel i	Δx	Distance (m) between the centres of two contiguous voxels
$[F]_i$	Fat content (kg/kg) of voxel i	t	processing time (s)
$[P]_i$	Protein content (kg/kg) of voxel i	x	abscissa (m) in the direction from surface to centre
S^0_m	Average volumetric Salt content kg/m^3 at day 0	D_s	Apparent diffusivity coefficient of salt
S_i	Volumetric Salt content in kg/m^3 in voxel i	ρ_i	density (kg/m^3) of voxel i
S_0	Volumetric Salt content in kg/m^3 at the surface		

1. Introduction

In dry-cured ham elaboration, the salting process is an important step to be understood for optimisation of salt uptake. During salting, Spanish hams are covered with salt (NaCl) and relative humidity of the salting chamber is maintained at a certain level (above 75%). It can be assumed that there is a continuous source of NaCl and modelling the diffusion of salt can be a useful tool to understand salt intake in such products. Some works have focused on the diffusion of salt in meat products, measuring the local salt content with standard chemical methods, for instance the research done by Palmia, Mazoyer, Diaferia, Baldini, & Poreta (1992) in Italian ham or by Graiver, Pinotti, Califano, & Zaritzky (2006) in pork tissues. Moreover, salt diffusion in meat products has been studied with non-invasive methods such as ^{22}Na-radioisotope method (Vestergaard, Lohmann-Andersen, & Adler-Nissen, 2007) or with ^{1}H-NMR and ^{23}Na-NMR methods (Bertram, Holdsworth, Whittaker, & Andersen, 2005; Hansen, Van der Berg, Ringgaard, Stodkilde-Jorgensen, & Karlsson, 2008). More recently Costa-Corredor, Pakowski, Lenczewski & Gou (2010) have evaluated the simulation of simultaneous water and salt diffusion in dry fermented sausages.

In recent years, food scientists have been looking for new non invasive

technologies to monitor the evolution of salt during the dry-curing process of hams. Computed tomography (CT) is a non destructive 3 dimension (3D) imaging technique that gives a density mapping of the entire scanned region. In food science, CT has been used to predict carcass composition (Romvári, Szabó, Kárpáti, Jovács, Bázár, & Horn, 2006; Font i Furnols, Teran, & Gispert, 2009; Picouet, Teran, Gispert, & Font i Furnols, 2010) but also for NaCl content determination. Frøystein, Sørheim, Berg, & Dalen, (1989) found that X-ray density from CT images correlated closely with salt concentration in cured meat and that can be a useful non-destructive tool to monitor dynamic changes. Vestergaard, Risum & Adler-Nissen (2004) used a CT equipment to determine NaCl content in pork loin muscle and later established a segmentation of CT images to follow salt distribution (Vestergaard et al., 2009). NaCl content was also determined in ground pork samples and small samples of dry-cured hams by CT (Håseth, Høy, Kongsro, Kohler, Sørheim, & Egelandsdal, 2008). More recently, calibration models for NaCl content, moisture content and water activity in pork hams during the salting and the resting periods (Fulladosa, Santos-Garcés, Picouet, & Gou, 2010) and during the resting period (Santos-Garcés, Gou, Garcia-Gil, Arnau, & Fulladosa, 2010; Santos-Garcés, Muñoz, Gou, Sala, & Fulladosa, 2012) were created using CT. At the same time, different articles (Arnau 1998; Barat, Grau, Ibáñez, & Fito, 2005; Grau, Albarracin, Toldrá, Antequera, & Barat, 2008) have shown the interest of freezing the ham before salting, to have more homogeneous batch, easier to transport from production place to the transformer. Frozen/thawed hams have also shown a more rapid salt intake (Sørheim, & Berg, 1987; Bañón, Cayuel, Granados, & Garrido, 1999; Barat, Grau, Ibáñez, & Fito, 2005; Serra, Fulladosa, Gou, Arnau, 2010).

The objective of this work is to develop a simplified, non-destructive methodology based on common diffusion equations and CT measurements for assessing the apparent salt diffusion (D_s) in *Semimembranosus* muscle during salting of fresh and frozen/thawed hams without interfering with the process at study.

2. Material and Methods

2.1. Salt diffusion modelling

2.1.1 Principle of the Salt Diffusion Model

To simplify the problematic, different conditions were established:

- The model was applied on a one dimension direction, from surface to the centre in the *Semimembranosus* (SM) muscle of ham.
- The model was based on the 2nd Fick's law considering a continuous source and a semi-infinite media.
- Shrinkage due to water loss was not considered in the model.

The classical diffusion unidirectional equation for a continuous source and a semi-finite media can be established as (Crank, 1979):

$$\frac{\partial S}{\partial t} = \frac{\partial}{\partial x} D_S \left(\frac{\partial S}{\partial x}\right) \quad \text{EQ 1}$$

Where S is the volumetric salt content (kg/m^3) for a defined voxel volume, D_s (m^2/s) the apparent salt diffusivity, x the distance in the unidirectional X axis (m) and t time in seconds.

The following boundaries conditions were established:

- S = 0 when t=0 for x>0,
- S = S_0 when x=0 for all time,
- S = 0 when x infinite for all time.

2.1.2 Determination of density

The density ρ_i for each voxel i was calculated using a modified equation presented by Buffler (1993):

$$\rho_i = 1740x[S]_i + 1290x[P]_i + 920x[F]_i + 1000x[W]_i \quad \text{EQ2}$$

Where, $[S]_i$, $[P]_i$, $[F]_i$ and $[W]_i$ are respectively salt, protein, fat and water content (kg/kg) of voxel i.

2.1.3 Resolution of diffusivity equation

Following the same procedure as Ruiz-Cabrera, Foucat, Bonny, Renou, & Daudin (2005), with a Boltzmann transformation to combine in a single variable space and time, considering a constant temperature and the conditions established in 2.1.1, the numerical solution of EQ 1 is presented in the next equation:

$$D_s = -\frac{1}{2}\left(\frac{\partial}{\partial S}\right)_{S_0} \times \int_{S_0}^{0^+} \partial S \quad \text{EQ 3}$$

where $\eta = x / \sqrt{t}$ in m/s$^{1/2}$.

The relationship between the volumetric salt content for each voxel S_i and the variable η was fitted to the following exponential equation:

$$S = S_0 \times e^{(b\times)} \quad \text{EQ 4}$$

Which can be converted in EQ 4.1.

$$\eta = \frac{1}{b} \times \text{Ln}\left(\frac{S}{S_0}\right) \quad \text{EQ 4.1}$$

EQ 4.1 permits to have a numerical solution of EQ 3 where all parameters can be described with experimental data and fitting parameters (b and S_0). The following equation gives the apparent salt diffusivity from the surface to the centre.

$$D_s = \frac{1}{2b^2} \quad \text{EQ 5}$$

2.2.1 Raw ham processing and salting

Hams from 5 pork carcass with an average pH of 5.8±0.1 and an average initial weight of 12.7±0.5 kg were purchased in a local slaughterhouse. Hams were vacuum-packed in PA/PE bags and one ham from each carcass ($H_{1\text{-}1}$, $H_{2\text{-}1}$, $H_{3\text{-}1}$, $H_{4\text{-}1}$ and $H_{5\text{-}1}$) was stored at refrigerated temperature (2 ºC ± 1 ºC) for 8 days. Whereas the other ham from each carcass ($H_{1\text{-}2}$, $H_{2\text{-}2}$, $H_{3\text{-}2}$, $H_{4\text{-}2}$ and $H_{5\text{-}2}$) were frozen at -18 ºC ± 1 ºC. The freezing process was monitored with a data logger Testo 177 (Testo AG, Germany) and a thermocouple T probe inserted in the centre of the ham. Frozen hams were kept at -18 ºC during 2 days and then defrosted in a cooling room at 3°C ± 2°C until reaching an internal temperature of 2°C ± 1°C. The overall freezing and defrosting process took 7 days. Hams were manually rubbed with a salting mixture containing: 10 g NaCl, 1.0 g dextrose, 0.50 g sodium ascorbate, 0.15 g KNO_3 and 0.15 g $NaNO_2$ per kg of raw ham. Next, hams were covered with salt and stored at 3°C ± 2°C. A permanent plastic marker was inserted in all the hams to facilitate the CT-scanning of the same slice throughout the salting period. Approximately 10 min before CT scanning, hams were removed from the salting box, brushed to remove the salt of the surface and weighted. After CT-scanning, hams were covered again with salt. The total time for the operation was less than 30 min. This operation was repeated at day 4, day 7 or 8, day 11 or 12, and day 16 of the salting process.

2.2.2 Computed Tomography (CT) measurements

CT scanning was performed, using a CT model HiSpeed Zx/i from General Electric Healthcare (GE Healthcare – Spain). An axial protocol was used with setting 80, 120 and 140 kV, 250 mA and a rotation time of 2s. Image size was 512 x 512 voxels, displayed field of view (DFOV) was 460 mm and slice depth was 10 mm thus giving a voxel´s volume of 0.9 x 0.9 x 10 = 8.1 mm^3. A single slice (Figure 1) was scanned at 10 cm from the aitch bone towards distal part of the ham (i.e., approx the widest part of the ham) and the scanned volume always contained the *Semimembranosus* (SM) muscle. As in all CT equipment, X-ray attenuation was expressed in Hounsfield Units (HU) DICOM (Digital Imaging and Communications in Medicine) images which mainly measures the bulk density in the voxel. The acquired were imported and analyzed using the software Matlab R2008b (The MathWorks Inc, Natick, Massachusetts, USA).

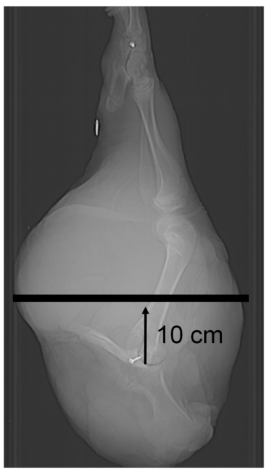

Figure 1. 2D image of a fresh ham indicating the position, at 10 cm of the aitch bone, where the single CT slice was taken for all samples.

2.2.3 Meat Composition

The salt (NaCl) and moisture contents were determined from X-ray attenuation values (i.e. DICOM images in Hounsfield Unit HU) using the salt and water prediction models reported by Fulladosa, Santos-Garcés, Picouet & Gou (2010). As shown in Figure 2, in order to adapt experimental data to the unidirectional model developed in paragraph 2.1, only a small proportion of the voxels (60 x 9 voxels) representing *Semimembranosus* muscle was considered in this study. To reduce the effect of beam hardening, a filter (density below -100 HU) was introduced and 2 voxels of the interlayer between air and ham were eliminated. The maximum volume V_{sm} used in this work was 4.4 cm^3 and all $[S]_i$ and $[W]_i$ values were averaged on the unidirectional axe X giving a 60 x 1 voxels line. A constant ratio [P]/[F] =

8.78 for *Semimembranosus* muscle, was considered (Armero, Navarro, Nadal, Baselga & Toldrá, 2002). During the salting procedure, for each voxel "i", fat and protein were recalculated using experimental data of water and salt (see EQ 6.1 and 6.2).

$$[F]_i = \frac{1 - [W]_i - [S]_i}{9.78} \qquad \text{EQ 6.1}$$

$$[P]_i = \frac{1 - [W]_i - [S]_i}{1 + 1/8.78} \qquad \text{EQ 6.2}$$

2.2.4 Mathematical Fitting

The fitting procedure of the exponential equation EQ 4 was made using the IGOR Pro 6.2 software (WaveMetrics Inc, Lake Oswego, USA) and the best values of the fitting parameters are the ones that minimize the value of Chi-square, (ChiSq). Validation of the fitting curves was conducted showing the correlation coefficient R^2 and the root mean square error RMSE as defined by:

$$RMSE = \sqrt{\sum_{j=1}^{N} \frac{1}{N} \times (S_j - S_{pj})^2}$$

Where S_j is the experimental data and S_{pj} the predicted data calculated from EQ 4.

2.3 Statistical analysis

A one-way analysis of variance (ANOVA) was performed with XLSTAT-Pro (Win) 7.5.3 (Addinsoft SARL, Paris, France). The model included the pre-treatment (fresh and frozen) as fixed effect. Comparisons between pre-treatments were evaluated with the Tukey test.

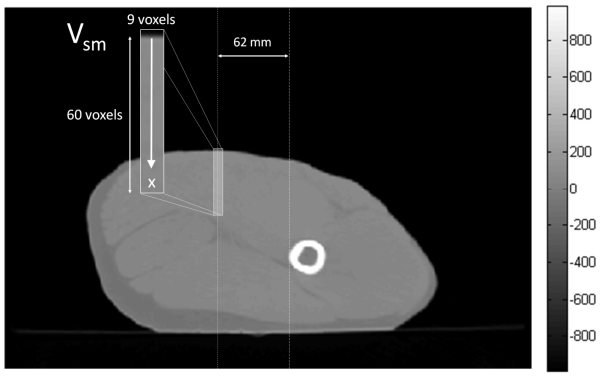

Figure 2. Presentation of a CT image from sample $H_{5\text{-}2}$ taken with a 80 kV voltage on day 0. The image presents the volume V_{sm} of SM muscle considered in this study as well as the unidirectional salt penetration axis.

3. Results and discussion

From table 1 we have the composition, determine by CT scans, of the *Semimembranosus* muscle before salting, with a homogeneous salt (0.5%±0.1 kg/kg) and moisture content (73.3%±0.5 kg/kg) for all hams. There is

no difference (P>0.05) between the fresh and frozen/thawed hams. On the selected volume of SM muscle, the evolution of the salt concentration $[S]_i$ on the unidirectional axis X was determined at different scanning time. Figure 3 presents the scatter plot of the average [S] and [W] content at 25 mm from the surface for a volume of 218 mm^3 before salting, after 4 days salting and at the end of the salting period at day 16. For a same salting day a 95% confidence ellipses have been calculated and plotted. Although the differences between fresh and frozen/thawed hams were not statistically different (P>0.05) at day 4, fresh ham had a slightly higher water content ([W] = 73.5%±1.2 kg/kg) and lower salt content ([S] = 0.9%±0.1kg/kg) than frozen/thawed hams ([W] = 71.7%±0.6 kg/kg; [S] = 1.4%±0.2kg/kg). At day 16, the salt content increases to 3.8%±0.2 kg/kg for fresh hams and to 4.8%±0.2 kg/kg for frozen/thawed hams. For moisture, at day 16, we have a decrease to 67.6%±1.3 kg/kg for fresh samples and to 65.6%±0.8 kg/kg for frozen/thawed samples.

As suggested by different authors (Bañón, Cayuela, Granados, & Garrido, 1999; Barat, Grau, Ibáñez, & Fito, 2005; Serra, Fulladosa, Gou, & Arnau, 2010) a frozen/thawed pre-treatment increases the intake of salt in ham. In an area which includes SM muscle, Bañón, Cayuela, Granados, & Garrido (1999) had a significant difference of 33% in the salt content between fresh samples (4.6% kg/kg) and frozen/thawed samples (6.1 % kg/kg). At the end of the salting period, Serra, Fulladosa, Gou, & Arnau (2010) found an increase of 26% between fresh (12.7% as desalted-dry-matter basis) and frozen/thawed

Table 1
Semimembranous muscles composition before salting.

	$H_{1\text{-}1}$	$H_{2\text{-}1}$	$H_{1\text{-}2}$	$H_{2\text{-}2}$	$H_{3\text{-}1}$	$H_{3\text{-}2}$	$H_{4\text{-}1}$	$H_{4\text{-}2}$	$H_{5\text{-}1}$	$H_{5\text{-}2}$
[W] (kg/kg) (1)	73.8%	73.6%	73.6%	73.5%	73.5%	73.5%	72.8 %	72.3 %	73.0 %	73.1 %
[F] (kg/kg) (2)	2.6%	2.6%	2.7%	2.7%	2.7%	2.7%	2.7%	2.8%	2.7%	2.7%
[P] (kg/kg) (2)	23.1%	23.2%	23.3%	23.4%	23.4%	23.4%	23.9%	24.3 %	23.8 %	23.7 %
[S] (kg/kg) (1)	0.5%	0.6%	0.5%	0.5%	0.4%	0.4%	0.6 %	0.7 %	0.5 %	0.5 %

(1) Values were calculated from CT measurements before salting at day 0.
(2) Values were estimated from [W] and [S] values determined1 by CT and considering [P]/[F] = 8.78 (Armero *et al.,* 2002).

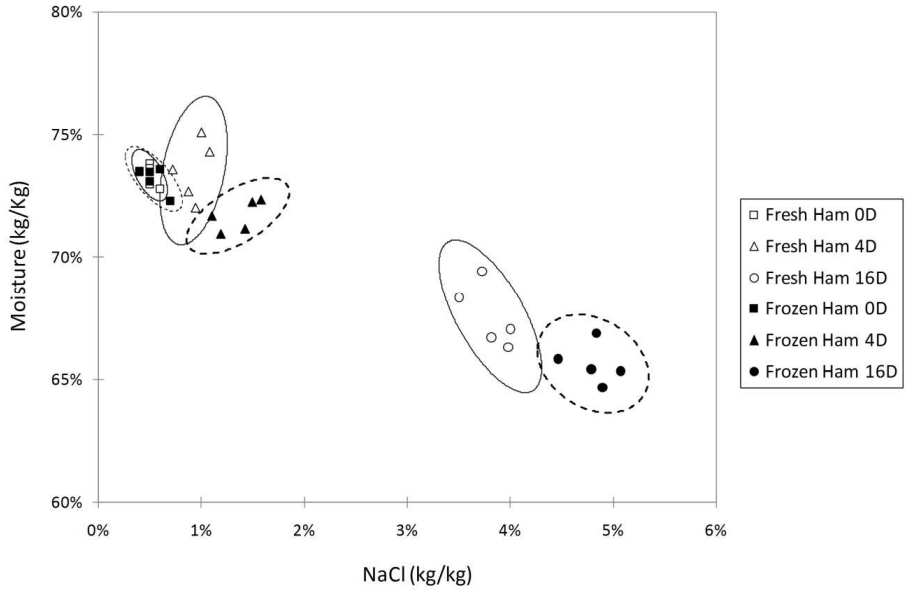

Figure 3. Scatter plot of the average NaCl and moisture content determined by CT at 25 mm from the surface along the axe X, for fresh (empty symbols) and frozen/thawed (plain symbols) hams, before salting (square), on day 4 (triangle) and on day 16 (circle). For each selected salting day a 95% confidence ellipses were plotted.

(16.0% as desalted-dry-matter basis) hams. In this paper, at the end of the salting period, the frozen/thawed samples had 25% more salt than the fresh ones, a similar value to the two examples cited above.

For the determination of volumetric salt content S_i for each voxel i, the following calculation was done: $S_i = ([S]_i \times \rho_i) - S^0_m$ where ρ_i is the density calculated using equation EQ 2, EQ 6.1 and EQ 6.2, S^0_m the average volumetric salt content per voxel at day 0 and $[S]_i$ the salt content in kg/kg. To have a temporal vision of the salt concentration the Boltzmann's space time variable η using the time value was calculated. Thus S_i each voxel i along the x axes was related with the space time variable η. Results of these calculations for sample $H_{5\text{-}2}$ are presented in Figure 4 where the evolution of the volumetric salt content S with the space time variable η is shown for sample $H_{5\text{-}2}$. These experimental data points were fitted with EQ 4 and results of the fitting procedure for the ten samples are presented in Table 2. R^2 ranged from 0.955 and 0.984 indicating that the exponential equation EQ 4 is appropriate for the fitting of the evolution of volumetric salt content with the variable η. The volumetric salt

content at the surface S_0 was also estimated with EQ 4 and gives results from 136.4 kg/m^3 for sample H_{4-1} to 183.4 kg/m^3 for sample H_{3-2}. Average S_0 values are respectively 150.9 ±9.6 kg/m^3 and 157.5±14.5 kg/m^3 for fresh and pre-frozen samples. Calculation with EQ 5 gives the apparent salt diffusivity D_s from the surface to the centre. For fresh samples we have values of 0.72 x10^{-10} m^2/s (sample H_{5-1}) to 1.06 x10^{-10} m^2/s (sample H_{2-1}) for the fresh samples and for frozen/thaw samples values from 0.99 x10^{-10} m^2/s (sample H_{3-2}) to 1.41x10^{-10} m^2/s (sample H_{1-2}). The average apparent salt diffusivity of the frozen/thawed samples (D_S =1.21±0.14 x10^{-10} m^2/s) is 30% higher ($P < 0.05$) than the fresh samples average value (D_S = 0.93±0.12 x10^{-10} m^2/s).

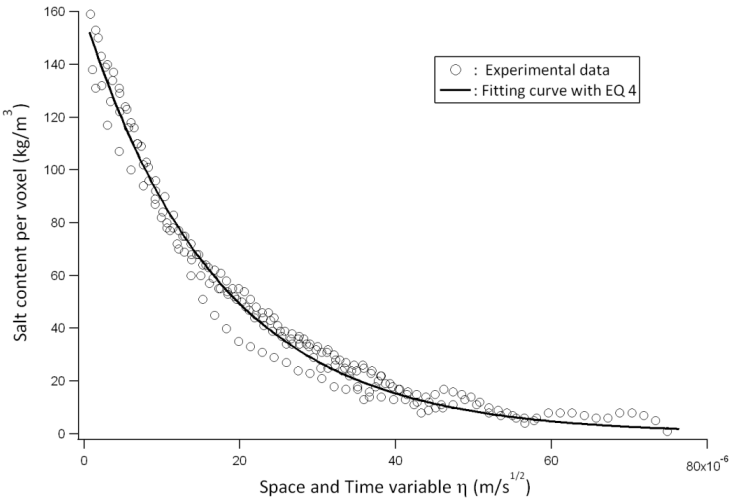

Figure 4. Master curve of sample H_{5-2} showing the evolution of the experimental data (circle) of the volumetric salt content per voxel S_i (kg/m^3), determined by CT with the Boltzmann's space time variable η (m/s$^{1/2}$). Fitting curve (plain line) of the experimental data established with EQ 4.

Table 2
Fitting Parameters of EQ 4 of the 10 hams presented with the *RMSE* values and the correlation factor R^2.

Parameters	H_{1-1}	H_{2-1}	H_{3-1}	H_{4-1}	H_{5-1}	H_{1-2}	H_{2-2}	H_{3-2}	H_{4-2}	H_{5-2}
S_0 (kg/m^3)	145.6 ±2.2	159.5 ±1.9	150.1 ±1.8	136.4 ±1.5	162.9 ±2.0	157.9 ±1.5	147.9 ±2.2	183.4 ±1.8	140.5 ±2.0	157.7 ±1.5
b	69555 ±1402	68781 ±1064	73638 ±71230	73596 ±1130	83303 ±1390	59633 ±799	62345 ±1270	71079 ±958	64716 ±1250	64621 ±842
D_s (m^2/s)	1.03 x10^{-10}	1.06 x10^{-10}	0.92 x10^{-10}	0.92 x10^{-10}	0.72 x10^{-10}	1.41 x10^{-10}	1.29 x10^{-10}	0.99 x10^{-10}	1.19 x10^{-10}	1.20 x10^{-10}
RMSE (kg/m^3)	7.3	11.4	6.0	0.20	0.49	5.7	7.8	5.9	6.5	0.41
R^2	0.958	0.974	0.975	0.983	0.976	0.981	0.958	0.984	0.962	0.983

Diffusion data calculated in this paper are in the same range than the ones presented in literature. Fox (1980) gives an effective diffusion coefficient of 2.2 $x10^{-10}$ m^2/s for the ion chloride in SM pork muscle. In Italian ham, Palmia, Mazoyer, Diaferia, Baldini, & Poreta (1992) obtained a value of 2.6 $x10^{-10}$ m^2/s for the effective diffusion coefficient of chloride in SM muscle. In pork loin immersed in a brine solution at 2ºC, Vestergaard, Risum, & Adler-Nissen (2004) estimated values between 2 and 4 $x10^{-10}$ m^2/s. On pork tissue (*Longinusdorsi* muscle at 4°C), immersed in a 30 g/l NaCl and 100 g/l solutions, Gravier, Pinotti, Califano, & Zaritzky (2009) found respectively diffusion coefficient of NaCl of 0.60 $x10^{-10}$ m^2/s and 1.70 $x10^{-10}$ m^2/s. Using a Medical Resonance Imaging (MRI) equipment, Håseth, Høy, Kongsro, Kohler, Sørheim, & Egelandsdal (2008) found diffusion coefficients with values ranging from 3 to 7 $x10^{-10}$ m^2/s for pork loins immersed in a brine solution. Recently, Costa-Corredor, Muñoz, Arnau, & Gou (2010) reported a salt diffusion coefficient of 3.9 $x10^{-10}$ m^2/s for the SM ham muscle. The lowest diffusion values calculated in this study, with respect to the literature cited above, could have different explanations. Experimental data do not full fit completely boundaries conditions at the surface of the samples ($S = S_0$ when x=0 for all t). The layer of salt could generate a beam hardening phenomena (Håseth, Høy, Kongsro, Kohler, Sørheim, & Egelandsdal, 2008), increasing the difficulty to estimate with CT measurements the salt content values for the point x=0. In our study the evolution of water was taken into account in the calculation of the density for each voxel but the small shrinkage effect due to water loss was not considered and might have an effect on the variable η. While most of the previous works (Vestergaard, Risum, & Adler-Nissen, 2005; Hansen, Van der Berg, Ringgaard, Stodkilde-Jorgensen, & Karlsson, 2008; Graiver, Pinotti, Califano, & Zaritzky, 2009) are based on cylinders or small cubs of muscle immersed in brine, this work presents a quantitative estimation of salt diffusion in the SM muscle of the whole ham during dry curing salting. Nevertheless, the estimates of salt diffusion coefficients are in the same order of magnitude than the above cited literature.

Differences between fresh and frozen/thawed samples are reflected not only in the salt content present at the end of the salting period but also in the apparent diffusion coefficient determined in this study. If data are seen for the five pairs, all frozen/thawed samples have a higher apparent diffusion coefficient then their fresh counterpart. This implies that CT measurements coupled with the proposed diffusion model could be of great interest to evaluate the effect of green ham characteristic and pre-treatment on apparent NaCl diffusivity.

4. Conclusion

NaCl diffusivity in *Semimembranous* muscle of whole hams during salting period could be estimated using a calibrated computed tomography equipment coupled to a unidirectional diffusion model. This simple diffusion model could be a profitable tool to quantify, in a non-destructive way, the effect of treatments such as freezing thawing procedure before salting on the diffusivity of NaCl.

Acknowledgments

The Authors are grateful to Jordi Garcia and Grau Matas for their assistance. This work was partially supported by the Q-Porkchains European commission Integrated Project within the Sixth RTD Framework Programme (Contract No. FOOD-CT-2006-036245) and the INIA (Project RTA2010-00029-CO4-01). The information in this document reflects only the authors' views and the Community is not liable for any use that may be made of the information contained therein.

References

Armero, E., Navarro, J.L., Nadal, M.L., Baselga, M., & Toldra, F. (2002). Lipid Composition of Pork muscle as affected by sire genetic type. *Journal of Food Biochemistry,* 26 (2), 91–102.

Arnau, J. (1998). Tecnología del jamón curado en distintos países. In *El jamón curado. Tecnología y Análisis de Consumo*. *Simposio Especial*. 44th ICoMST, Ed. Estrategias Alimentarias. Barcelona. (pp. 10–21).

Bañón, S., J.M Cayuela, J.M., Granados, M.V., & Garrido M.D. (1999). Pre-cure freezing affects proteolysis in dry-cured hams. *Meat Science*, 51 (1), 11–16.

Barat, J.M., Grau, R., Ibáñez, J.B. & Fito, P., (2005). Post-salting studies in Spanish cured ham manufacturing. Time reduction by using brine thawing/salting. *Meat Science*, 69 (2), 201–208.

Bertram, H.C., Holdsworth, S.J., Whittaker, A.K. & Andersen, H.J. (2005). Salt diffusion and distribution in meat studied by Na-23 nuclear magnetic resonance

imaging and relaxometry. *Journal of Agricultural and Food Chemistry*, 23 (20), 7814–7818.

Buffler, C.H. (1993), "*Dielectric Properties of Foods and Microwave Material*" In Microwave Cooking and Processing, New York USA, Van Nostrand Reinhold.

Costa-Corredor, A., Pakowski, Z., Lenczewski, T., & Gou, P. (2010). Simulation of simultaneous water and salt diffusion in dry fermented sausages by the Stefan–Maxwell equation. *Journal of Food Engineering,* 97 (3), 311–318.

Costa-Corredor, A., Muñoz, I., Arnau, J., & Gou, P. (2010). Ion uptakes and diffusivities in pork meat brine-salted with NaCl and K-lactate. *LWT - Food Science and Technology,* 43 (8), 1226–1233.

Crank. J. (1979). *The Mathematic of Diffusion*. Oxford University Press, ISBN 019 8534116, 520 pages.

Font i Furnols, M, Teran, F., & Gispert, M. (2009). Estimation of lean meat content in pig carcasses using X-ray Computed Tomography and PLS Regression. *Chemometrics and Intelligent Laboratory Systems,* 98 (1), 31–37.

Fox, J.B., (1980). Diffusion of chloride, nitrite and nitrate in beef and pork. *Journal of Food Science,* 45 (6), 1740–1744.

Froystein, T., Sørheim, O., Berg, S.A. & Dalen, K. (1989). Salt distribution in cured hams, studied by computer X-ray tomography. *Fleischwirtschaft*, 69 (2), 220–222

Fulladosa, E., Santos-Garcés, E., Picouet, P.A., & Gou, P. (2010). Prediction of salt and water content in dry-cured hams by computed tomography. *Journal of Food Engineering,* 96 (1), 80-85.

Gou, P., Comaposada, J., & Arnau, J. (2002). Meat pH and meat fibre direction effects on moisture diffusivity in salted ham muscles dried at 5°C. *Meat Science*, 61 (1), 25–31.

Gou, P., Comaposada, J., & Arnau, J. (2004). Moisture diffusivity in the lean tissue of dry-cured ham at different process time. *Meat Science*, 67 (1), 203–209.

Graiver, N., Pinotti, A.,Califano, A., & Zaritzky, N. (2006). Diffusion of sodium chloride in pork tissue. *Journal of Food Engineering*, 77 (4), 910–918.

Graiver, N., Pinotti, A.,Califano, A., & Zaritzky, N. (2009). Mathematical modeling of the uptake of curing salts in pork meat. *Journal of Food Engineering,* 95 (4),533–540.

Grau, R., Albarracin, W., Toldrá, F., Antequera, T., & Barat, J.M., (2008). Study of salting and post-salting stages of fresh and thawed Iberian hams. *Meat Science*, 79 (4), 677–682.

Håseth, T.T., Høy, M., Kongsro, J., Kohler, A., Sørheim, O., & Egelandsdal, B., (2008). Determination of sodium chloride in pork meat by computed tomography at different voltages. *Journal of Food Science,* 73 (7), 333–339.

Hansen, C.L., Van der Berg, F., Ringgaard, S., Stodkilde-Jorgensen, H., & Karlsson, A.H., (2008). Diffusion of NaCl in meat studied by 1H and 23Na magnetic resonance imaging. *Meat Science,* 80 (3), 851–856.

Palmia, F., Mazoyer, C., Diafaria, C., Baldini, P., & Poretta D. (1992). Salt and water distribution in typical Italian hams. *Revista Española de Ciencia y Tecnología de Alimentos*, 32 (1), 71–83.

Picouet, P.A., Terran, F., Gispert, M., & Font i Furnols, M. (2010). Lean Content prediction in pig carcass by computed tomography (CT) using a density model, *Meat Science*, 86 (3), 616–622

Romvári, R., Dobrowolski ,A., Repa, I., Allen, P., Olsen, E. Szabó, A., & Horn, P. (2006). Development of a computed tomographic calibration method for the determination of lean meat content in pig carcasses. *Acta Veterinaria Hungarica,* 54 (1), 1-10.

Ruiz-Cabrera, M.A., Foucat, L., Bonny, J.M., Renou, J.P., & Daudin, J.D. (2005). Assessment of water diffusivity in gelatine gel from moisture profiles II. Data processing adapted to material shrinkage. *Journal of Food Engineering,* 68 (2), 221–231.

Santos-Garcés, E., Gou, P., Garcia-Gil, N., Arnau, J., & Fulladosa, E. (2010). Non-destructive analysis of a_w, salt and water in dry-cured hams during drying process by means of computed tomography.

Journal of Food Engineering, 101 (2), 187–192.

Santos-Garcés, E., Muñoz, I., Gou, P., Sala, X., & Fulladosa, E. (2012). Tools for studying dry-cured ham processing by using computed tomography. *Journal of Agricultural and Food Chemistry,* 60 (1), 241–249.

Serra, X., Fulladosa, E., Gou, P., & Arnau, J. (2010).Models to predict the final salt content of dry-cured hams. *6th FOODSIM, International Conference on Simulation and Modeling in the Food and Bio-Industry*, Braganza (Portugal), Proceedings, 13–16.

Sørheim, O., & Berg, S.A., (1987). Dry cured hams produced from frozen/thawed raw materials. *XXXIII International Congress of Meat Science and Technology*, Helsinki (Finland), Proceedings, 1–7.

Vestergaard, V., Risum, J., & Adler-Nissen, J. (2004). Quantification of salt concentrations in cured pork by computed tomography. *Meat Science,* 68 (1), 107–113.

Vestergaard, C., Erbou, S.G., Thauland, T., Adler-Nissen, J., & Berg P. (2005) Salt distribution in dry-cured ham measured by computed tomography and image analysis. *Meat Science,* 69 (1), 9–15.

Vestergaard, C., Lohmann-Andersen, B., & Adler-Nissen J. (2007). Sodium diffusion in cured pork determined by 22Na radiology. *Meat Science,* 76 (2), 258–265.

Paper VII

Santos-Garcés, E., Laverse, J., Gou, P., Fulladosa, E., Frisullo, P., & Del Nobile, M. A. (2012). Addition of different types of fat to non-acid lean fermented sausages: X-ray microcomputed tomography and instrumental texture analyses. *Meat Science*, (submitted).

Meat Science
(submitted)

Addition of different types of fat to non-acid lean fermented sausages: X-ray microcomputed tomography and instrumental texture analyses

E., Santos-Garcés [a], J., Laverse [b], P., Gou [a], E., Fulladosa [a, *], P., Frisullo [b], M.A. Del Nobile [b, c]

[a] IRTA. XaRTA. Food Technology. Finca Camps i Armet, E-17121 Monells, Spain

[b] Department of Food Science, University of Foggia, Via Napoli 25, 71100 Foggia, Italy

[c] Istituto per la Ricerca e le Applicazioni Biotecnologiche per la Sicurezza e la Valorizzazione dei Prodotti Tipici e di Qualità, Università degli Studi di Foggia, BIOAGROMED – Via Napoli 52, 71100 Foggia, Italy

[*] Corresponding author: Tel.: +34 972630052, fax: +34 972630373, e-mail: elena.fulladosa@irta.cat

Abstract

X-ray microcomputed tomography (μCT) technique was used for microstructure analysis in four different types of non-acid pork lean fermented sausages, three of them supplemented (5%) with different types of fat (pork backfat, sunflower oil or diacylglycerols (DAGs)). Data from μCT analysis were related to instrumental texture (hardness). Although μCT analysis identified fat particles and air holes, the technique was not accurate enough to distinguish between pork lean and fat when these constituents were emulsified. Only μCT geometrical parameters related to the meat matrix (emulsion of pork lean and fat) gave useful information about the product microstructure. Parameters such as percent object volume (POV), object surface/volume ratio (OSVR), degree of anisotropy (DA), structure thickness (ST), and number of objects (NO) were correlated with instrumental hardness.

Keywords: *X-ray microcomputed tomography, non-acid pork lean fermented sausages, low fat, microstructure, texture*

1. Introduction

Health problems such as coronary heart diseases and obesity, which are associated to high fat ingestion (Tabas, 2002; WHO, 2003; Mozaffarian, Aro, & Willett, 2009), have been widely described focussing attention on the fat contributed from meat (Committee on Medical Aspects of Food Policy, 1984, 1994; Department of Health, 1994; British Nutrition Foundation, 1996; Enser, Hallet, Hewitt, Fursey, & Wood, 1996; Higgs, 2000; Fernández-Ginés, Fernández-López, Sayas-Barberá, & Pérez-Alvarez, 2005). Nevertheless, the reduction of fat content in meat products has been found to reduce consumers' acceptability, cause technological problems and decrease sensory quality of the products (Wirth, 1988; Claus, & Hunt, 1991; Giese, 1996; Miles, 1996; Jiménez-Colmenero, 1996, 2000; Wood, Richardson, Nute, Fisher, Campo, Kasapidou, Sherard, & Enser, 2003).

The reduction of fat content and the simultaneous addition of more healthy oil-based fat substitutes have been widely studied in different dry-cured meat products (Muguerza, Ansorena, & Astiasarán, 2004; Severini, De Pilli, & Baiano, 2003; Ansorena & Astiasarán, 2004; Valencia, Ansorena, & Astiasarán, 2006a; Pelser, Linssen, Legger, & Houben, 2007). Olivares, Navarro, Salvador, & Flores (2010) reported that the minimum fat content added in the production of dry fermented sausages for consumers' acceptability was 16%, which approximately correspond to a 50% fat reduction of similar commercialised products. Replacement of pork backfat by an oil substitute in the production of Chorizo de Pamplona yields an acceptable product from a sensory point of view. The use of around 25% of pre-emulsified olive oil (Muguerza, Gimeno, Ansorena, Bloukas, & Astiasarán, 2001) and pre-emulsied soy oil (Muguerza, Ansorena, & Astiasarán, 2003) in Chorizo de Pamplona have been proved to be suitable alternatives. More recently, Mora-Gallego, Serra, Guàrdia, Miklos, Lametsch, & Arnau (2011) reported that sunflower oil is a promising ingredient to reduce the negative effects on the sensory properties caused by the fat reduction in non-acid pork lean fermented sausages. Furthermore, the addition of carbohydrate in nature replacers (Mendoza, García, Casas, & Selgas,

2001; García, Domínguez, Gálvez, Casas, & Selgas, 2002; Osburn & Keeton, 2004; Koutsopoulos, Koutsimanis, & Bloukas, 2008; Salazar, García, & Selgas, 2009) or protein in nature replacers (Bloukas, Paneras, & Fournitzis, 1997; Muguerza *et al*., 2001, 2003; Kayaardi & Gök, 2003; Severini *et al*., 2003; Ansorena & Astiasarán, 2004; Muguerza, Gimeno, Ansorena, & Astiasarán, 2004; Valencia *et al*., 2006a, 2006b; Cáceres, García, & Selgas, 2007; Pelser *et al*., 2007; Kotsopoulos *et al*., 2008; Del Nobile, Conte, Incoronato, Panza, Sevi, & Marino, 2009) have also provided promising fat reduced products from consumers acceptability and health points of view. Recent studies were focused in the use of diacylglycerols (DAGs) as an innovative fat substitute strategy (Miklos, Xu, & Lametsch, 2011; Mora-Gallego *et al.,* 2011).

X-ray microcomputed tomography (μCT) is a technique based on the differences in X-ray attenuation values produced by the differences of constituents' density within a sample. This technique allows an accurate reconstruction of the internal microstructure of the scanned samples (Kerckhofs, Schrooten, Van Cleynenbreugel, Lomov, & Wevers, 2008). μCT has been successfully used in food industry for the study of cellular microstructure of a wide range of food products (Lammertyn, Dressalaers, Van Hecke, Jancsók, Wevers, & Nicolaï, 2002; 2003; Van Dalen, Blonk, Van Aalst & Hendriks, 2003; Kuroki, Oshita, Sotome, Kawagoe, & Seo, 2004; Lim & Barigou, 2004; Falcone, Baiano, Zanini, Mancini, Tromba, Montanari, & Del Nobile, 2004; Falcone, Baiano, Zanini, Mancini, Tromba, Dreossi, Montanari, Scuor, & Del Nobile, 2005; Haedelt, Pyle, Beckett, & Niranjan, 2005; Babin, Della Valle, Chiron, Cloetens, Hoszowska, Pernot, Réguerre, Salvo & Dendievel, 2006; Bellido, Scanlon, Page & Hallgrimsson, 2006; Mendoza, Verboven, Mebatsion, Kerckhofs, Wevers, & Nicolaï, 2007; Léonard, Blancher, Nimmol, & Devahastin, 2008). Nevertheless, there are only few studies that try to relate μCT and texture characteristics. Babin, Della Valle, Dendievel, Lassoued, & Salvo (2005) studied the effect of different compositions of bread and related their effects to microstructure using μCT and texture analysis. Relationship between texture, mechanical properties and

microstructure of cornflakes derived from four corn varieties was also studied by Chaunier, Valle, & Lourdin (2007) using µCT. Recently, Pareyt, Talhaoui, Kerckhofs, Brijs, Goesaert, Wevers, & Delcour (2009) studied the impact of sugar and fat levels on cookie structure and their influence on the macroscopic, microscopic and mechanical properties of this product using the same technology.

The accuracy of µCT to determine fat content and its spatial distribution in minced meat products has been previously demonstrated. Frisullo, Laverse, Marino, & Del Nobile (2009) reported the usefulness of µCT to provide an accurate percentage of fat volume and detailed information on the structure of the fat present in five different types of Italian salami. Nevertheless, no studies focused on the correlation of texture properties and structure changes in meat products have been found. Understanding how the reduction of fat content and the use of different types of fat influence on the final microstructure, as well as the texture properties, could help to improve the formulation of fat reduced minced meat products.

The objectives of this study were to evaluate changes in the microstructure and texture of non-acid pork lean fermented sausages with the addition of 5% of different types of fat, and also to evaluate the relationship between µCT measurements and instrumental texture.

2. Material and methods

2.1. Product formulation and elaboration process

Samples used in this study were obtained from the study done by Mora-Gallego *et al.* (2011). Three batches of non-acid pork lean fermented sausages were manufactured using pork lean ham (95%) and different types of fat (5%) (pork backfat, sunflower oil or DAGs). Another further batch was elaborated using pork lean with no added fat. The pork lean used had an average water content of 70.7 ± 0.1%.

In all cases, pork lean was trimmed of fat and minced at Ø 8 mm. For each batch with added fat, the corresponding back fat or oils (0.6 kg) were mixed in a grinder (Dito-Sama K55, Dito-Sama S.A., Aubusson, France) with 1 kg of meat until forming a paste

that was added to the rest of the meat (10.4 kg). A total of 12 kg of meat paste per batch was obtained. The same procedure was followed for the batch elaborated with no added fat, obtaining a total of 11.4 kg of meat paste. All mixtures (pork lean and 5% of fat or pork lean without added fat) were minced at Ø 3 mm. The following additives per kilogram of pork lean were added to the mixtures: NaCl 20 g, black pepper 1.50 g, lactose 20 g, potassium lactate (78% purity) 20 g, sodium ascorbate 0.5 g, sodium nitrite 0.15 g and potassium nitrate 0.15 g. The meat paste was stuffed into Ø 50 mm Fibran casings, immersed in a water and mould (*Penicillium candidum*) bath and hung to dry for two months with increasing temperature from 3°C to 18°C and decreasing relative humidity from 90% to 70%. Sausages were periodically weighed until reaching an estimated final water content referred to de-fatted dry matter of 55%. This estimated final water content was calculated with the average initial water content of pork lean, percentages of added fat and weight losses. Four sausages per batch were packaged in polyamide-polyethylene bags (Sacoliva, Sabadell, Spain) with modified atmosphere (80% N2 : 20% CO2) and stored at 3°C for one month.

2.2. Sample preparation

From each fermented sausage, four 15 mm thick slices were cut with a slicing machine. From each slice, a specimen was accurately carved with a scalpel into cubes of 15 x 15 x 15 mm^3. Specimens were wrapped in parafilm to avoid moisture loss. The specimens were used in the µCT analysis (the parafilm does not interfere with the X-rays) and instrumental texture analysis. The same specimens were minced, homogenized and used for chemical analysis.

2.3. X-ray microcomputed tomography analysis

All the specimens (n = 64) were imaged under the same conditions (at 20°C ± 2°C), using the Skyscan 1172 high-resolution desktop X-ray microcomputed tomography system (Skyscan 2005, Skyscan N.V., Vluchtenburgstraat, Aartselaar, Belgium). Each specimen was placed on a rotational plate; the source and the

detector were fixed, while the sample was rotated during measurement. Power settings were 100 kVp and 100 µA. A CCD camera with 2000 x 1048 pixels was used to record the transmission of the conical X-ray beam through all samples. The distance source–object–camera was adjusted to produce images with a pixel size of 17.13 µm. Four-frame averaging, a rotation step of 0.60° and an exposure time of 1475 ms were chosen to minimize the noise, covering a view of 180º. Smoothing and beam-hardening correction steps were applied to suppress noise and beam hardening artefacts (nonlinear X-ray absorption) (Goldman, 2007a), respectively. Beam hardening correction was only moderately applied (set to 25% within NRecon) due to the use of an aluminium filter during acquisition. This filter acts to suppress low energy X-rays from the source, thus minimizing-beam-hardening artefacts. Ring artefacts (Figure 1) were also corrected (Goldman, 2007b; Abu Anas, Lee, & Hasan, 2011; Sadi, Lee, & Hasan, 2010). A fast ring artefacts reduction (set to 7 within NRecon) was also applied. Once initial parameters were set, the acquisition step was completely automated and did not require operator assistance. Scan time, on average, required 37 min. A set of 2D flat cross-section images was obtained for each sample after tomographical reconstruction by the Skyscan reconstruction software NRecon. Three-dimensional (3D) reconstructions of specimens were created by effectively stacking all two-dimensional tomographs, a total of 146 slice images with a slice spacing of 0.069 mm.

2.4. Image processing and analysis

For image processing and analysis, the Skyscan software CTAnalyser was used. A 10 x 10 mm^2 region of interest (ROI)

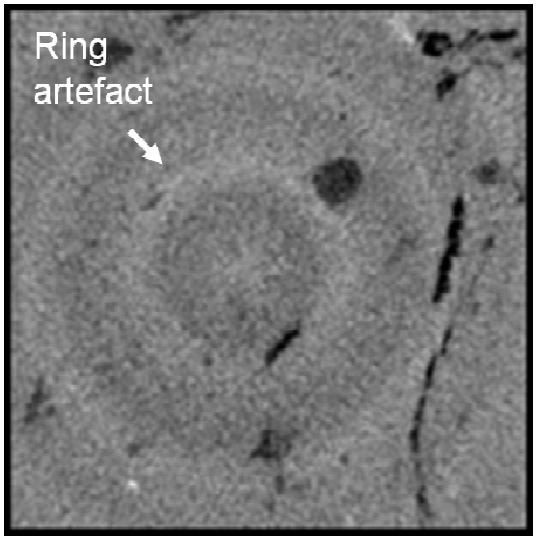

Figure 1. Example of ring artefact caused by an error or drift in the calibration of a detector relative to the other detectors.

was chosen from the centre of the scanned slice in view and was then copied to all the slices in our selected volume of interest (VOI). The original grey-scale cross-sectional images were converted into binary images (black and white) for the subsequent data analysis. This step was carried out by an automatic threshold (Sahoo, Soltani, Wong, & Chen, 1988) which assigns the value 1 to all pixels whose intensity was below a given grey tone value and 0 to all the others. Because non-acid pork lean fermented sausages samples consisted of three constituents (fat, meat matrix and air holes) two different segmentations were carried out. First, air holes were differentiated from the other constituents (fat and meat matrix). Second, fat was differentiated from meat matrix. All binary images obtained (3 images per sample corresponding to the three constituents) were used to calculate the microstructural properties of each constituent.

For data analysis, prior to 3D reconstruction, a component-labelling algorithm, available within CTAnalyser, was used to isolate the largest 3D connected structures. All reconstructions were created using an adaptive rendering (locality 10 and tolerance 0.25) algorithm and saved as P3G surface model (SkyScan model format). P3G models were then imported into the Skyscan visualisation software CTvol.

The following geometric parameters were measured: (i) the percent object volume (POV) is the percentage of a considered constituent (i.e. fat, meat matrix or air holes) present within the VOI of the sample; the value obtained from µCT analysis is the percentage of V_f/V_{tot} where V_f is the volume of a considered constituent and V_{tot} is the total volume; (ii) the object surface/volume ratio (OSVR) which is the basic parameter in order to characterise the complexity of the structure and to estimate the object thickness (i.e. the size and distribution of fat, meat matrix or air holes in each sample); (iii) the fragmentation index (FI), developed and defined by Hahn, Vogel, Pompesius-Kempa, & Delling (1992) as the index of the structural connectivity; it calculates the relative convexity or concavity of the object surface, based on the principle that concavity indicates connectivity and

convexity indicates isolated disconnected structures (Lim & Barigou, 2004); (iv) the degree of anisotropy (DA) which measures the preferential alignment of a considered constituent (i.e. fat, meat matrix or air); (v) the structure thickness (ST), for a point in solid is defined by Hildebrand & Ruegsegger (1997) as the diameter of the largest sphere which fulfils two conditions; the sphere encloses the point (but the point is not necessarily the centre of the sphere) and the sphere is entirely bounded within the solid surfaces; (vi) the structure separation index (SS) which is the thickness of the spaces and it can be calculated either from 2D or 3D images; (vii) the number of objects (NO) which reports the total number of discrete binarised objects within the VOI.

2.5 Instrumental texture

An instrumental texture compression test was carried out in all the specimens (n = 64). A Texture Analyser (Zwick/Roell, testXpert II, V3.2, Copyright © 1996-2010, Zwick GmbH & Co.KG, August-Nagel-Strasse 11, D-8907901m) with a 10 kN load cell and a 60 mm diameter compression plate was used. Specimens from sausages were compressed once to 75% of their total height, at a crosshead speed of 1 mm/s. Textural analyses were performed at ambient temperature (20 ºC ± 2 ºC). Hardness (N), defined as the maximum peak force during the compression (Bourne, 1978), was recorded.

2.6. Chemical analysis

Analyses of all sausages were performed in triplicate. Water content was analyzed by drying at 103°C ± 2°C until a reaching constant weight (AOAC, 1990). The total fat content was measured by Soxtec extraction (SoxCap 2047 and Soxtec 2055) according to ISO 1443 (1973).

2.7. Statistical analysis

Analyses of variance were done with the General Linear Model (GLM) procedure of the statistical SAS package (SAS Institute, 2001). The average of the specimens obtained for each sausage was used for the analyses of variance. The type of added fat was included in the model as a fixed effect. Pearson correlation coefficients

between µCT parameters of the individual specimens and hardness were calculated with CORR procedure of SAS package.

3. Results and discussion

3.1. Microstructural properties

Because air holes appeared during the drying process of non-acid lean fermented sausages, three constituents (fat, meat matrix and air holes) were distinguished in the µCT analysis. The sausages elaborated with no added fat had approximately 5% of fat content at the end of the process, whereas the sausages with 5% of different types of added fat had around a 12% of fat content (Table 1). Sausages with no added fat contained the highest water content, in agreement with their higher initial water content due to the absence of added fat.

Frisullo *et al.* (2009) reported that the percentage of fat volume of a minced meat sample can be determined by the µCT geometric parameter percent object volume (POV). In this study, POV was calculated as the percentage of each constituent present within the sample (POV-fat, POV-meat matrix and POV-holes) (Table 2). The average POV-fat of sausages with no added fat was 4.41%, similar to analytical fat content (4.84%). However, the POV-fat of the other batches were lower than their analytical fat content, especially in DAGs sausages, which had a POV-fat similar to sausages with no added fat. Since µCT has been previously used to satisfactorily determine fat content in fatty minced meat products, such as Italian salami (Frisullo *et al.,* 2009), problems in the fat detection in the case of non-acid pork lean fermented sausages seem to be related to the product characteristics (elaboration settings and reduced fat content).

Table 1
Mean values and standard deviation of the percentage of fat content, water content, weight loss, and de-fatted dry matter measured by chemical analysis.

	No added fat	Back fat	Sunflower oil	DAGs	RMSE
Fat content (%)	4.84^{a} ± 0.72	12.29^{b} ± 0.66	11.19^{b} ± 0.91	12.23^{b} ± 0.71	0.738
Water content (%)	33.15^{a} ± 0.08	30.59^{b} ± 0.69	31.35^{b} ± 0.70	31.15^{b} ± 0.04	0.494
Mean weight loss (%)	59.54^{a} ± 0.37	57.17^{b} ± 0.03	$56.75^{b, c}$ ± 0.27	56.42^{c} ± 0.02	0.231
De-fatted dry matter (%)	0.53 ± 0.87	0.54 ± 0.59	0.55 ± 0.98	0.55 ± 0.35	0.016

$^{a, b}$ Means within a row without a common letter are significantly different (P<0.05).

In this study, the mixture of pork lean and fat minced at Ø 3 mm resulted on an emulsified meat matrix made up of the pork lean and the main part of added fat. When both these constituents are emulsified they might not be distinguish by µCT equipment, as part of the fat might become invisible and therefore not quantified. Therefore, only visible fat (fat objects) and the portion of fat present in a liquid form (i.e. oil) that fills in small holes and fissures might be identified as fat by the equipment.

POV-fat values for sausages elaborated with no added fat were similar to their analytical fat content because they did not contain so much emulsified fat (invisible). Differences on the POV-fat values obtained for sausages elaborated with 5% of added fat depended on the melting point of the added type of fat. Melting point of the three different types of fat used in this study are in the order: sunflower oil (around -17°C) < backfat (30 - 40°C) < DAGs (45°C). The smaller the melting point, the more likely the fat had

Table 2
Mean values and standard deviation of µCT geometric parameters[x] and texture characterization (hardness) for the four batches of non-acid fermented sausages with low fat content. RMSE are also included.

Parameter	No added fat	Back fat	Sunflower oil	DAGs	RMSE
POV					
POV-holes	2.71 ± 5.76	2.77 ± 3.17	5.96 ± 3.50	5.71 ± 6.04	3.156
POV-fat	4.41 ± 1.52^{b}	6.58 ± 2.17^{a}	7.43 ± 2.58^{a}	4.30 ± 1.09^{b}	1.232
POV-meat matrix	92.99 ± 6.72	90.81 ± 4.74	86.76 ± 5.89	90.13 ± 6.98	3.918
Meat Matrix					
OSVR-meat matrix	0.0014^{b} ±0.00036	0.0019$^{a, b}$ ± 0.00045	0.0022^{a} ± 0.00068	0.0016$^{a, b}$ ± 0.00033	0.00040
FI-meat matrix	-0.009 ±0.0022	-0.011 ±0.0020	-0.009 ± 0.0018	-0.011 ± 0.0045	0.00172
ST-meat matrix	1176.1^{a} ± 65.63	976.5^{b} ± 80.41	961.4^{b} ± 88.17	971.6^{b} ± 69.32	76.40
SS-meat matrix	599.6 ± 179.02	549.2 ± 55.67	634.6 ± 130.56	875.9 ± 489.68	270.17
DA-meat matrix	0.37^{a} ± 0.094	0.23^{b} ± 0.085	0.30^{a} ± 0.087	0.31^{a} ± 0.084	0.0403
NO-meat matrix	137.6^{b} ± 31.89	256.7^{a} ± 40.43	224.5^{a} ± 57.97	145.1^{b} ± 34.11	42.36
Texture					
Hardness	2017.8^{a} ± 192.14	1017.0^{b} ± 181.92	937.1^{b} ± 107.96	1090.2^{b} ± 93.33	150.31

$^{a, b}$ Means within a row without a common letter are significantly different (P<0.05).

x µCT geometric parameters: POV, percent object volume (%); OSRV, object surface/volume ratio (mm^{-1}); FI, fragmentation index (mm^{-1}); DA, degree of anisotropy (no units); ST, structure thickness (mm); SS, structure separation index (mm); NO, number of objects (no units); Hardness, maximum force (N).

fissures present in the sausages and therefore becoming visible (Figure 2 and Figure 3). These findings explained the order of magnitude obtained for the POV-fat (sunflower>backfat>DAGs). In the case of DAGs, only the fat present on the pork lean could be detected (POV-fat values no significantly different (P>0.05) to sausages elaborated with no added fat). DAGs were the most emulsified (invisible) type of fat utilized since it was totally spread within the minced pork lean (POV-meat matrix). In contrast to sunflower oil, no oil filling in the meat matrix holes' was found in the case of DAGs since DAGs become liquid at 45°C. Therefore, the use of DAGs as a fat substitute can reduce the visible fat content in non-acid pork lean sausages. These findings show that the µCT equipment can be used to determine fat content present on meat minced products when the mixture of pork lean and fat is minced at big diameters, i.e. Italian salami (Frisullo *et al.,* 2009), but not with small minced diameters or emulsions. Because the same amount of pork lean was used in all the batches, no significantly differences in the POV-meat matrix were found. In addition, although no significant differences were obtained, sausages elaborated with a 5% of different types of added fat contained a higher number of holes.

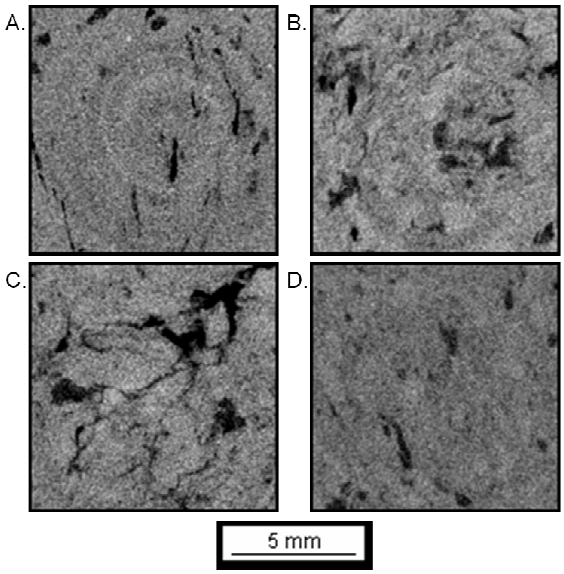

Figure 2. Examples of grey-scale cross-sectional images of non-acid fermented sausages with low fat content manufactured without added fat (A), with 5% pork backfat (B), with 5% sunflower oil (C) and with 5% diacylglycerols (DAGs) (D).

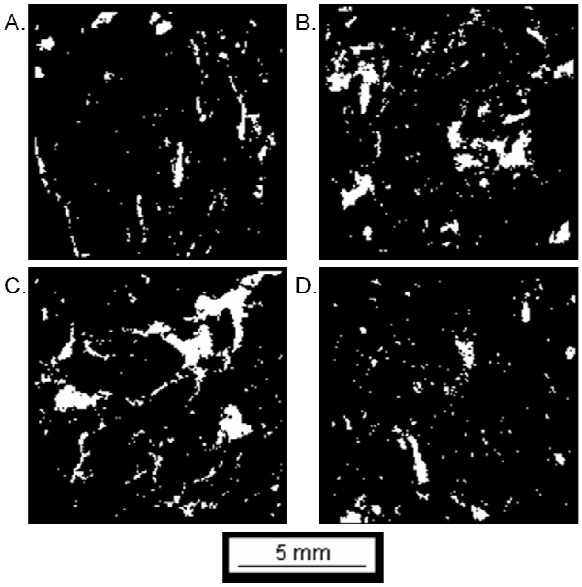

Figure 3. Examples of binary tomographic sections of non-acid fermented sausages with low fat content that illustrate the separation of the fat (in white) and non-fat (in black) phases: without added fat (A), with 5% pork backfat (B), with 5% sunflower oil (C) and with 5% diacylglycerols (DAGs) (D).

Because µCT was not accurate enough to measure the fat geometric parameter when final products result on emulsions, only the µCT geometric parameters obtained for the meat matrix were used to determine microstructural properties on the sausages.

The object surface/volume ratio (OSVR) parameter is related to the constituents' size and its distribution within the sample. The higher the value, the smaller the constituent size and also the more finely distributed it is in the sample. The highest OSVR-meat matrix values were obtained when backfat was added in the formulation, because the addition of fat into the pork mixture during the minced process. Sunflower oil has the lowest melting point of the added types of fat, which facilitated its accumulation in the small holes and fissures presents in the meat matrix.

Fragmentation index (FI-meat matrix) was negative and similar for all the batches ($P>0.05$), suggesting that meat matrixes were made up of a continuous network of objects (Lim & Barigou, 2004). The degree of anisotropy (DA-meat matrix), which is a measure of 3D structural symmetry, indicates the presence or absence of a preferential alignment of meat matrix objects along a particular direction (a value of 0 corresponds to total isotropy whereas a value of 1 corresponds to total anisotropy). All the batches have a low degree of anisotropy, meaning low alignment, connection and orientation of the internal structure of the product, as was expected in a minced meat product. The anisotropy in this product decreases when holes or visible fat objects homogenously break the alignments and connections of internal structure of meat matrix. The anisotropy was slightly decreased by the addition of backfat, but not by the addition of sunflower oil or DAGs. The effect of backfat may be due to the fact that it was homogenously distributed during mixture preparation, and part of it was visible with µCT. The lack of effect of DAGs and sunflower may be due to the facts that, on the one hand, DAGs were not visible with µCT and, on the other hand, sunflower oil was only visible when it was accumulated in holes and fissures, which were not homogenously distributed.

Since size distribution ratio is correlated to the thickness (Frisullo *et al.,* 2010), the smaller the constituent OSVR the bigger is its thickness diameter (ST). ST-meat matrix of sausages with no added fat was higher with respect to sausages with added fat. These findings are also in agreement with OSVR-meat matrix values (ST-meat matrix increases while OSVR-meat matrix decreases). The structure separation (SS-meat matrix) defined as the distance between binary objects, was not significantly different between the four types of sausages ($P>0.05$).

The number of objects (NO-meat matrix), which reports the total number of discrete binarised objects, was affected by the type of added fat and might be related to the POV-fat geometrical parameter. Sausages with higher POV-fat values, with backfat or sunflower oil, showed the highest NO-meat matrix, meaning a more divided meat matrix.

Similar values obtained in all batches for FI-meat matrix, SS-meat matrix and the DA-meat matrix might be probably due to the fact that the size of the objects that divided the meat matrix (visible fat and air holes) was also similar. The differences in OSVR-meat matrix, ST-meat matrix and NO-meat matrix were due to the highest visible fat content (higher POV-fat values).

3.2. Hardness

Dry meat samples with higher water content are expected to be softer (Virgili, Parolari, Schivazappa, Bordini, & Borri, 1995; Serra, Ruiz-Ramirez, Arnau, & Gou, 2005). However, the addition of fat (backfat, sunflower oil or DAGs), although significantly reduced the water content (Table 1), it also reduced the instrumental hardness with respect the sausages without added fat (Table 2). Therefore, fat addition causes a hardness reduction as has been previously reported (Muguerza, Fistab, Ansorenaa, Astiasarana, & Bloukasb, 2002). Although no significant differences were found between types of fat, a slight decrease in the hardness was observed for sunflower oil sausages in comparison to backfat and DAGs. These results are in agreement with several studies focused in the reduction of fat content in different kinds of sausages, where the addition of oil in liquid form

as fat substitute such as olive oil (Bloukas *et al.,* 1997a; Muguerza *et al*., 2001; Del Nobile *et al.,* 2009) or soy oil (Muguerza *et al.,* 2003) produced softer sausages than the control ones. This decrease in the mechanical properties of the sausages due to the oil presence could be explained because the oil acts as a plasticizer; increasing the mobility of the meat matrix. It is well known that texture defects, as an excessive hardness, influences consumers' acceptability. Because of that, the reduction of the product hardness' due to the oil presence (i.e. sunflower oil) in non-acid lean fermented sausages might increase consumers' acceptability (Mora-Gallego *et al.,* 2011).

Table 3 shows the Pearson correlation coefficients for µCT parameters and hardness in non-acid pork lean fermented sausages. Hardness was positively correlated with POV-meat matrix, whereas it was negatively correlated with POV-fat and POV-holes. It can be observed that estimated fat content (POV-fat) and analytical fat content had the same tendency. These findings agree with several studies (Muguerza *et al*., 2001, 2003), which found that sausages with higher fat content were softer. Furthermore, the presence of holes decreases hardness since the meat matrix and the fat become more disconnected. OSVR-meat matrix was also negatively correlated with hardness, due to the fact that higher OSVR values were related with smaller sizes and more complex distribution of the sample constituents' (i.e. meat matrix). The higher the ST-meat matrix value, the higher was the force needed for the

Table 3

Significant Pearson correlation coefficients for µCT geometric parameters[x] and texture properties (hardness) in non-acid fermented sausages with low fat content samples (n = 64).

Parameter	Hardness	P-Value
POV		
POV-holes	-0.276	0.0273
POV-fat	-0.446	0.0002
POV-meat matrix	0.373	0.0024
Meat Matrix		
OSVR-meat matrix	0.422	0.0005
FI-meat matrix	0.063	0.6183
ST-meat matrix	0.454	0.0002
SS-meat matrix	-0.130	0.3058
DA-meat matrix	0.387	0.0016
NO-meat matrix	-0.359	0.0036
Final composition		
Fat content (%)	-0.884	0.0036
Water content (%)	0.948	0.0040

[x] µCT geometric parameters: POV, percent object volume (%); OSRV, object surface/volume ratio (mm^{-1}); FI, fragmentation index (mm^{-1}); DA, degree of anisotropy (no units); ST, structure thickness (mm); SS, structure separation index (mm); NO, number of objects (no units).

sample compression during the texture test. Higher DA-meat matrix results in more aligned connected and oriented meat matrix lattices meaning stronger structures. Negative correlation was found between hardness and NO-meat matrix, demonstrating that it is more difficult to compress a uniform sample than a sample made up of discrete objects.

4. Conclusions

µCT is not accurate enough to distinguish among the different constituents of a minced meat sample when the final product results on emulsions. µCT can only detect the visible fat and the fat accumulated in a liquid form inside the air holes and fissures of the meat matrix. The type of fat used in the formulation affects the meat matrix microstructure of non-acid pork lean fermented sausages. The melting point of fat determines the microstructural characteristics of meat matrix and the fat detection by µCT.

Instrumental hardness of non-acid lean fermented sausages decreases when a 5% of fat is included in the formulation. Nevertheless, DAGs might present less visible fat, which could be an advantage for consumers' preference.

Several µCT parameters (POV-meat matrix, POV-fat, POV-holes, OSVR-meat matrix, DA-meat matrix, ST-meat matrix, and NO-meat matrix) were correlated with instrumental texture (hardness).

Acknowledgements

This work was supported by the Government of Catalonia (2010 BE1 00151, Agència de Gestió d'Ajuts Universitaris i de Recerca) and the 6th EU framework Integrated Project Q-Porkchains (FOOD-CT-2007-036245). The information in this document reflects only the authors' views and the Community is not liable for any use that may be made of the information contained therein.

We thank Rikke Miklos and René Lametsch from the University of Copenhagen (Frederiksberg, Denmark), Xuebing Xu from the University of Aarhus (Aarhus, Denmark) and Danisco (Aarhus, Denmark) for providing the DAGs. We also thank Héctor Mora-Gallego from IRTA-XaRTA (Monells, Spain) for the technical assistance.

References

Abu Anas, E. M., Lee, S.Y., & Hasan, M. K. (2011). Classification of ring artifacts for their effective removal using type adaptive correction schemes. *Computers in Biology and Medicine*, 41 (6), 390–401.

Ansorena, D., & Astiasarán, I. (2004). The use of linseed oil improves nutritional quality of the lipid fraction of dry-fermented sausages. *Food Chemistry,* 87 (1), 69–74.

AOAC, 1990. Official method 950.46, moisture in meat, B. air drying. In: Helrich K. (Ed.), Official Methods of Analysis of the Association of Official Analytical Chemists, 15th ed., vol. II. Association of Official Analytical Chemists, Inc., Arlington, p. 931.

Babin, P., Della Valle, G., Dendievel, R., Lassoued, N., & Salvo, L. (2005). Mechanical properties of breadcrumbs from tomography based finite element simulations. *Journal of Materials Science*, 40 (22), 5867–5873.

Babin, P., Della Valle, G., Chiron, H., Cloetens, P., Hoszowska, J., Pernot, P., Réguerre, A.L., Salvo, L., & Dendievel, R. (2006). Fast x-ray tomography analysis of bubble growth and foam setting during breadmaking. *Journal of Cereal Science*, 43 (3), 393–397.

Bellido, G. G., Scanlon, M. G., Page, J. H., & Hallgrimsson, B. (2006). The bubble size distribution in wheat flour dough. *Food research International*, 39 (10), 1058–1066.

Bloukas, J.G., Paneras, E.D., & Fournitzis, G.C. (1997). Effect of replacing pork backfat with olive oil on processing and quality characteristics of fermented sausages. *Meat Science*, 45 (2), 133–144.

Bourne, M. C. (1978). Texture profile analysis. *Food Technology*, 32 (7), 62–66, 72.

British Nutrition Foundation. (1996). Diet and Heart Disease: A Round Table of Facts. Second Edition, M. Ashwell (ed).

Cáceres, E., García, M.L., & Selgas, M.D. (2008). Effect of pre-emulsified fish oil-as source of PUFA n-3 on microstructure and sensory properties of mortadella, a Spanish bologna-type sausage. *Meat Science*, 80 (2), 183–193.

Chaunier, L., Valle, G. D., & Lourdin, D. (2007). Relationships between texture, mechanical properties and structure of cornflakes. *Food Research International*, 40 (4), 493–503.

Claus, J. R., & Hunt, M. C. (1991). Low-fat, high added-water bologna formulated with texture-modifying ingredients. *Journal of Food Science*, 56 (3), 643–652.

Committee on Medical Aspects of Food Policy. (1984). Diet and Cardiovascular Disease. Report on Health and Social Subjects. Department of Health and Social Security. No. 28, HMSO, London.

Committee on Medical Aspects of Food Policy. (1994). Nutritional Aspects of Cardiovascular Disease. No. 46, HMSO, London.

Del Nobile M.A., Conte, A., Incoronato, A.L., Panza, O., Sevi, A., Marino, R. (2009). New strategies for reducing the pork back-fat content in typical Italian salami. *Meat Science*, 81 (1), 263–269.

Department of Health. (1994). Report on health and social subjects, no 46. Nutritional aspects of cardiovascular disease. London: HMSO.

Enser, M., Hallet, K., Hewitt, B., Fursey, G. A. J., & Wood, J. D. (1996). Fatty acid content and composition of English beef, lamb and pork at retail. *Meat Science*, 42 (4), 443–456.

Falcone, P. M., Baiano, A., Zanini, F., Mancini, L., Tromba, G., Montanari, F., & Del Nobile, M. A. (2004). A novel approach to the study of bread porous structure: phase-contrast x-ray microtomography. *Journal of Food Science*, 69 (5), 38–43.

Falcone, P. M., Baiano, A., Zanini, F., Mancini, L., Tromba, G., Dreossi, D., Montanari, F., Scuor, N., & Del Nobile, M.A. (2005). Three-dimensional quantitative analysis of bread crumb by x-ray microtomography. *Journal of Food Science*, 70 (3), 265–272.

Fernández-Ginés, J.M., Fernández-López, J., Sayas-Barberá, E., & Pérez-Alvarez, J.A. (2005). Meat products as functional foods: A review. *Journal of Food Science*, 70 (2), 37–43.

Frisullo, P., Laverse, J., Marino, R., & Del Nobile, MA. (2009). X-ray computer tomography to study processed meat micro-structure.

Journal of Food Engineering, 94 (3-4), 283–289.

García, M.L., Domínguez, R., Gálvez, M.D., Casas, C., Selgas, M.D. (2002). Utilization of cereal and fruit fibres in low fat dry fermented sausages. *Meat Science*, 60 (3), 227–236.

Giese, J. (1996). Fats, oils and fat replacers. *Food Technology*, 50 (4), 78–83.

Goldman LW. (2007a). Principles of CT: radiation dose and image quality. *Journal of Nuclear Medicine Technology,* 35 (4), 213–25.

Goldman LW. (2007b). Principles of CT and CT techology. *Journal of Nuclear Medicine Technology,* 35 (3), 115–128.

Haedelt, J., Pyle, D. L., Beckett, S.T., & Niranjan, K. (2005). Vacuum-induced bubble formation in liquid-tempered chocolate. *Journal of Food Science*, 70 (2), 159–164.

Hahn, M., Vogel, M., Pompesius-Kempa, M., & Delling, G. (1992). Trabecular bone pattern factor – A new parameter for simple quantification of bone microarchitecture. *Bone*, 13 (4), 327–330.

Higgs, J. D. (2000). The changing nature of red meat: 20 years of improving nutritional quality. *Trends in Food Science & Technology*, 11 (3), 85–95.

Hildebrand, T., & Ruegsegger, P. (1997). A new method for the model independent assessment of thickness in three dimensional images. *Journal of Microscopy,* 185 (1), 67–75.

ISO 1443, 1973. Determination of total fat content. International Organization for Standardization, Geneva.

Kayaardi, S., & Gök,V. (2003). Effect of the replacing beef fat with olive oil on quality characteristics of Turkish *soudjouk* (sucuk). *Meat Science*, 66 (1), 249–257.

Kerckhofs, G., Schrooten, J., Van Cleynenbreugel, T., Lomov, S.V., & Wevers, M. (2008). Validation of x-ray microfocus computed tomography as an imaging tool for porous structures. *Review of Scientific Instruments*, 79 (1), 013711–013719.

Koutsopoulos, D.A., Koutsimanis G.E., & Bloukas J.G. (2008). Effect of carrageenan level and packaging during ripening on processing and quality characteristics of low-fat fermented sausages produced with olive oil. *Meat Science*, 79 (1), 188–197.

Kuroki, S., Oshita, S., Sotome, I., Kawagoe, Y., & Seo, Y. (2004). Visualization of 3-D network of gas-filled intercellular spaces in cucumber fruit after harvest. *Postharvest biology and Technology*, 33 (3), 255–262.

Jiménez-Colmenero, F. (1996). Technologies for developing low-fat meat products. *Trends in Food Science & Technology*, 7 (2), 41–48.

Jiménez-Colmenero, F. (2000). Relevant factors in strategies for fat reduction in meat products. *Trends in Food Science & Technology*, 11 (2), 56–66.

Lammertyn, J., Dressalaers, T., Van Hecke, P., Jancsók, P., Wevers, M., & Nicolaï, B. M. (2002). MRI and x-ray CT study of spatial distribution of core breakdown in 'Conference' pears. *Magnetic Resonance Imaging*, 21 (7), 805–815.

Lammertyn, J., Dresselaers, T., Van Hecke, P., Jancsónk, P., Wevers, M., & Nicolaï, B. M. (2003). Analysis of the time course of core breakdown in 'Conference' pears by means of MRI and x-ray CT. *Postharvest biology and Technology*, 29 (1), 19–28.

Léonard, A., Blancher, S., Nimmol, C., & Devahastin, S. (2008). Effect of far-infrared radiation assisted drying on microstructure of banana slices: An illustrative use of x-ray microtomography in microstructural evaluation of a food product. *Journal of Food Engineering*, 85 (1), 154–162.

Lim, K. S., & Barigou, M. (2004). X-ray micro-computed tomography of cellular food products. *Food Research International*, 37 (10), 1001–1012.

Mendoza, E., García, M.L., Casas, C., & Selgas, M.D. (2001). Inulin as fat substitute in low fat, dry fermented sausages. *Meat Science*, 57 (4), 387–393.

Mendoza, F., Verboven, P., Mebatsion, H. M., Kerckhofs, G., Wevers, M., & Nicolaï, B. (2007). Three-dimensional pore space quantification of apple tissue using x-ray computed microtomography. *Planta*, 226 (3), 559–570.

Miles, R. S. (1996). Processing of low fat meat products. In 49th reciprocal meat conference proceedings, (pp. 17–22). American Meat Science Association, Chicago, IL.

Miklos, R., Xu, X., & Lametsch, R. (2011). Application of pork fat diacylglycerols in meat emulsions. *Meat Science*, 87 (3), 202–205.

Mozaffarian, D., Aro, A., & Willett, W.C. (2009). Health effects of trans-fatty acids: experimental and observational evidence. *European Journal of Clinical Nutrition*, 63 (2), 5–21.

Mora-Gallego, H., Serra, X., Guàrdia, M. D., Miklos, R., Lametsch, R., & Arnau, J. (2011). Effect of the type of fat on the sensory attributes and instrumental texture parameters of reduced-fat non-acid fermented sausages. ICoMST 2011, Ghent.

Muguerza, E., Gimeno, O., Ansorena, D., Bloukas, J.G., & Astiasarán, I. (2001). Effect of replacing pork backfat with pre-emulsified olive oil on lipid fraction and sensory quality of Chorizo de Pamplona – a traditional Spanish fermented sausage. *Meat Science*, 59 (3), 251–258.

Muguerza, E., Fistab, G., Ansorenaa, D., Astiasarana, I., & Bloukasb, J.G. (2002). Effect of fat level and partial replacement of pork backfat with olive oil on processing and quality characteristics of fermented sausages. *Meat Science*, 61 (4), 397–404.

Muguerza, E., Ansorena, D., & Astiasarán, I. (2003). Improvement of nutritional properties of Chorizo de Pamplona by replacement of pork backfat with soy oil. *Meat Science*, 65 (4), 1361–1367.

Muguerza, E., Ansorena, D., & Astiasarán, I. (2004). Functional dry fermented sausages manufactured with high levels of n-3 fatty acids: nutritional benefits and evaluation of the oxidation. *Journal of Food Science and Agriculture*, 84, 1061–1068.

Muguerza, E., Gimeno, O., Ansorena, D., &Astiasarán, I. (2004).New formulations for healthier dry fermented sausages: A review. *Trends in Food Science & Technology*, 15 (9), 452−457.

Olivares, A., Navarro, J.L., Salvador, A., & Flores, M. (2010). Sensory acceptability of slow fermented sausages based on fat content and ripening time. *Meat Science*, 86 (2), 251–257.

Osburn,W.N., & Keeton, J.T. (2004). Evaluation of low-fat sausage containing desinewed lamb and konjac gel. *Meat Science*, 68 (2), 221–233.

Pareyt, B., Talhaoui, F., Kerckhofs, G., Brijs, K., Goesaert, H., Wevers, M., & Delcour, J.A. (2009). The role of sugar and fat in sugar-snap cookies: Structural and textural properties. *Journal of Food Engineering*, 90 (3), 400–408.

Pelser, W. M., Linssen, J. P. H., Legger, A., & Houben, J. H. (2007). Lipid oxidation in n-3 fatty acid enriched Dutch style fermented sausages. *Meat Science*, 75, 1–11.

Sadi, F., Lee, S. Y., & Hasan, M. K. (2010). Removal of ring artifacts in computed tomographic imaging using iterative center weighted median filter. *Computers in Biology and Medicine*, 40 (1), 109–118.

Salazar, P., García, M. L., & Selgas, M. D. (2009). Short-chain fructooligosaccharides as potencial functional ingredient in dry fermented sausages with different fat levels. *International Journal of Food Science and Technology*, 44 (6), 1100−1107.

SAS, 2001. Statistical Analysis System for Windows. Release 8.01. SAS Institute Inc., Cary, NC, USA.

Serra, X., Ruiz-Ramírez, J., Arnau, J., & Gou, P. (2005). Texture parameters of dry-cured ham m. biceps femoris samples dried at different levels as a function of water activity and water content. *Meat Science*, 69 (2), 249–254.

Severini, C., De Pilli, T., & Baiano, A. (2003). Parcial substitution of pork backfat with extra-virgin olive oil in 'salami' products: effects on chemical, physical and sensorial quality. *Meat Science*, 64 (3), 323–331.

Sahoo, P. K., Soltani, S., Wong, A. K. C., & Chen, Y. C. (1988). A survey of thresholding techniques. *Computer Vision, Graphics and Image Processing,* 41 (2), 233–260.

Tabas, I. (2002). Cholesterol in health and disease. *Journal of Clinical Investigation*, 110 (5), 583–590.

Valencia, I., Ansorena, D., & Astiasarán, I. (2006a). Nutritional and sensory properties of dry fermented sausages enriched with n-3 PUFAs. *Meat Science*, 72, 727–733.

Valencia, I., Ansorena, D., & Astiasarán, I. (2006b). Stability of linseed oil and antioxidants containing dry fermented sausages: A study of the lipid fraction during different storage conditions. *Meat Science*, 73 (2), 269–277.

Van Dalen, G., Blonk, H., Van Aalst, H., & Hendriks, C. L. (2003). 3D imaging of foods using x-ray microthomography. G. I. T. *Imaging & Microscopy*, 3 (1), 18–21.

Virgili, R., Parolari, G., Schivazappa, C., Bordini, C. S., & Borri, M. (1995). Sensory and texture quality of dry-cured ham as affected by endogenous cathepsin B activity and muscle composition. *Journal of Food Science,* 60 (6), 1183–1186.

WHO. (2003). Diet, Nutrition and the Prevention of chronic diseases. WHO Technical report Series 916. Geneve.

Wirth, F. (1988). Technologies formaking fat-reducedmeat products. *Fleischwirtsch*, 68 (9), 1153−1156.

Wood, J. D., Richardson, R. I., Nute, G. R., Fisher, A. V., Campo, M. M., Kasapidou, E., Sherard, P. R., & Enser, M. (2003). Effect of fatty acids on meat quality: a review. *Meat Science*, 66 (1), 21–32.

5. GENERAL DISCUSSION

Although most of the results have been individually discussed in each of the papers enclosed in the previous section, a global discussion of the results is presented below.

In general, CT based prediction models developed in this work were proved to be useful for the estimation of salt content in dry-cured ham. These results are in agreement with previous studies where the usefulness of CT to predict salt content in dry-cured ham was reported (Vestergaard *et al.,* 2004, 2005; Håseth *et al.,* 2007, 2008, 2012). In addition, for the first time, CT was also found to be useful to predict water content and a_w. Annex I shows a summary of developed prediction models (Table 2, Table 3 and Table 4), some of them have not been published but they are included in the results section (Papers I, II, III and IV). Regarding the published papers, since the use of different tube voltages is known to be useful to obtain enhanced CT calibrations (Håseth *et al.,* 2008), all the possible voltage combinations were shown, but only optimal predictions are included in the tables present in Annex I, in order to simplify the information. Root Mean Square Error of Prediction or Calibration (RMSEC) obtained for the same parameter and muscle, or group of muscles can differ depending on the study because of the large variability in terms of composition (salt, water and fat contents) among the sets of samples used in each study. This is the reason why different RMSEC for the same parameter were obtained in the prediction models from different articles.

Prediction models developed using the combination of samples that came from different groups of muscles (SM, BF and ST) are valid for predicting the parameters of the entire ham, since the whole range of salt, water and fat contents is represented (Papers I, II, III and IV). RMSEC decreased as the number of muscles included for

developing the prediction models decreased, leading up to more accurate but local predictions, mainly when the ST muscle was not included (Papers I, II, and III). This fact is especially relevant in the case of the prediction in SM and BF muscles which are the most interesting to analyse. In general, RMSEC were also reduced when specific prediction models for different times of the elaboration process (initial and final stages) were used. In agreement with Håseth *et al.* (2008), RMSEC were higher in the prediction models developed for the final stages than those developed for the initial stages, due to the high dryness of the samples. Nevertheless, these models were only valid for predicting the parameters at specific stages of the process, making it necessary to also develop prediction models for the whole elaboration process, which allow the tracking of the same sample throughout the process (Paper III and Paper IV).

The use of a given prediction model will depend not only on the objective of the study, but also on the process stage. The choice of the most appropriate prediction models in each case will provide the most accurate information.

It has been found that intramuscular fat content (IMF) significantly affects the predictions (Vestergaard *et al.,* 2004; Håseth *et al.,* 2007, 2008). IMF produces a decrease of CT attenuation values which results in an underestimation of salt content prediction and an overestimation of water content and a_w predictions. In our studies, when fatty samples (i.e. ST samples) were removed from the prediction models (Papers I, II, and III) or when analytical IMF was included into the prediction models as a covariate (Paper II), the RMSEC decreased. Therefore, it was of maximum importance to achieve the estimation of IMF in a non-destructive way. Recent studies have described CT as a promising tool for the determination of IMF in raw hams by means of image analysis (Brun *et al.,* 2011); however, the estimation of IMF in dry-cured ham is not straightforward due to the presence of salt and the high dryness of the samples. In Paper III, a non-destructive estimation of IMF by image analysis of CT tomograms was successfully achieved. Nevertheless, IMF in dry-cured ham can only be correctly estimated in muscles with a homogeneous salt distribution at any time during the elaboration process. For the estimation of IMF in very salty areas or in areas which have a high gradient of salt (i.e. in the SM muscle during the post-salting stages) further studies are needed.

Incorporation of IMF estimate information into the prediction models significantly reduces RMSEC when estimating salt content, but more importantly when estimating water content and a_w. In the case of salt content, although the accuracy of the salt predictability was also improved by including IMF estimate into the models, this parameter was the least affected by the presence of IMF due to the higher attenuation values of salt ions in comparison to the attenuation values of IMF. In the case of water content and a_w predictions, errors of prediction were higher than in the case of salt content, since pixels containing dry lean and fat can produce attenuation values similar to those more humid and with a low fat content. RMSEC differences in a_w predictions were lower than in water content predictions and higher than in salt content predictions, because a_w depends on both water and salt contents.

Although the accuracy of the prediction models was lower than the reference analytical methods (around 10 times lower than the analytical standard deviation), the models can be considered useful for control purposes. Nevertheless, the information obtained needs to be properly managed in order to make the best use of it. Therefore, non-destructive CT analytical tools (distribution diagrams, line profiles and regions of interest (ROIs)) were developed, and their usefulness to monitor salt content, water content and a_w in dry-cured ham throughout the elaboration process was demonstrated (Paper IV). These findings are in agreement with initial studies where the potential usefulness of CT to study salt distribution in dry-cured ham (Vestergard *et al.* 2005; Håseth *et al.,* 2012) has been reported. In addition, the study of water content and a_w distributions can also be carried out. Information given by CT analytical tools is useful when the chemical composition of the sample is not homogeneous or when detailed information about composition in a specific region of the ham is needed. This type of information can only be acquired using CT or other non-destructive technologies such as Magnetic Resonance Imaging (MRI) (Antequera *et al.,* 2007), which can give a general view of the studied region, providing complementary information to chemical analysis. CT prediction models and CT analytical tools suitable for monitoring and optimizing manufacturing processes were applied in three case studies (Paper IV, Paper V and Paper VI).

In the first case study (Paper IV), CT based prediction models and CT analytical tools were used to monitor and compare two industrial salting procedures (pile salting and tumbler salting), in which standard (SS) and reduced (SR) salting levels were used. Differences between hams due to the characteristics of raw material, salting levels, and the industrial elaboration procedures can be analysed and quantified by using these CT applications. Estimated salt content, water content, and a_w values obtained in this study for each stage of the elaboration process and muscle, were in agreement with the values given by the literature (Grau *et al.,* 2008). In addition, CT analytical tools were found to be especially useful in the study of the dry-cured ham elaboration processes when salt content is reduced. Product safety and texture defects (such as softness and pastiness) relies on the correct salt content and a decrease of a_w, mainly in the inner parts of the ham (Leistner, 1986; Parolari *et al.,* 1988, 1994; Ruiz-Ramírez *et al.,* 2006; Virgili *et al.,* 1995). Therefore, determining when the minimal salt content and a_w values have been achieved in the inner part of the ham is of special interest in order to optimize salt reduced elaboration processes. In Paper IV, CT analytical tools were used to determine the appropriate length of the resting stage in SR hams, which was extended until achieving the minimal salt content and a_w values to ensure the safety of the product and avoid texture defects. Therefore, CT technology has been proved to be useful to be applied in dry-cured hams industry in order to improve quality and safety of the product.

In the second case study (Paper V), prediction models were also satisfactorily used to assess the effect of different pre-salting treatments (skin trimming and pressing) of hams during salting and drying processes in terms of salt content, water content, and a_w. Results showed that partial skinning or pressing increased both salt uptake and final weight loss, but did not reduce the variability in salt uptake within a batch. Trimmed hams (in V shape) exhibited higher salt content and lower water content than pressed hams in the inner areas of the hams after resting. Such detailed information on salt content, water content and a_w distribution can be only obtained using CT calibrated technology, which permit the monitoring of dynamic changes without interfering with the process or product studied (Frøystein *et al.,* 1989). Here,

information can be acquired pixel by pixel, which is not possible with analytical methods.

In the third case study, a salt diffusion model using CT analytical tools (specifically line profiles) and prediction models for salt and water contents was obtained for the SM muscle. The diffusion model was tested in hams subjected or not to a freezing/thawing treatment before the salting stage. Resulting diffusion model gives an estimation of salt diffusivity in the same range that values presented in literature (Fox, 1980; Palmia *et al.,* 1992; Vestegaard *et al.,* 2004; Gravier *et al.,* 2009; Håseth *et al.,* 2008; Costa-Corredor *et al.,* 2010). In this case study, differences in salt diffusivity due to the application or not of a freezing/thawing treatment can be observed. Results showed lower diffusivity in fresh hams than in hams that had been previously frozen and thawed before salting. These results are also in agreement with Sørheim and Berg (1987) and Frøystein *et al.* (1989), who reported that freezing/thawing accelerated the salt uptake and increased the weight loss of the hams after curing. These results pointed out the usefulness of CT prediction models in the control when new elaboration processes are proposed.

Microcomputed Tomography (µCT) is a variation of CT technology which allows higher resolution scanning (µm instead of mm), but with which only small samples can be analysed without being damaged. Several studies have tried to relate µCT and texture characteristics in different foodstuffs (Babin *et al.,* 2005; Chaunier *et al.,* 2007; Pareyt *et al.,* 2009). Nevertheless, no similar studies have been found in the scientific literature about meat products. Results presented in Paper VII showed that several µCT geometric parameters related to the meat matrix characteristics can be correlated with the instrumental texture (hardness) in non-acid pork lean fermented sausages. Therefore, µCT can be considered as a potential tool to analyse and understand texture changes in meat products. Nevertheless, this method is not accurate enough to distinguish properly fat and lean tissues in a minced meat dried product at small diameters (< 3 mm), such as non-acid pork lean fermented sausages, when the fat has been previously emulsionated. Although Frisullo *et al.* (2009) reported the usefulness of µCT to accurately distinguish between fat and lean tissues in coarsely minced meat

products (i.e. Italian salami), emulsified fat becomes invisible and cannot be quantified by µCT equipment. µCT can only detect the visible fat and the fat accumulated in a liquid form inside the air holes and fissures of the meat matrix usually present in these types of products. µCT geometric parameters obtained for the meat matrix showed that the melting point of the type of fat used in the formulation (pork backfat, sunflower oil, and DAGs) affects the meat matrix microstructure and texture and also the possibility of detection using µCT.

Nevertheless, the high cost and limited portability of CT and µCT devices, restricts its use in meat industries either to off-line process control or to research purposes. For this reason, the development of a more economical and simple X-ray technology (i.e. an industrial CT equipment) could be of special interest. Current efforts are focused in the implementation of industrial CT equipment for product classification, of both raw material and dry-cured ham. On the one hand, in raw hams the determination of total fat content (inter and intramuscular fat and subcutaneous fat) as well as its distribution within the product could be useful in order to adjust the proper salting conditions for each fat range. On the other hand, information regarding the final salt and fat contents in the whole ham could be also of great interest for the final product characterization, permitting dry-cured ham classification and labelling depending on its characteristics. This fact would guaranty to the consumers a constant quality of the product, increasing the competiveness of companies. The use of CT technology could also be extended to other food products including fish, meat, fruits or vegetables, in which a density variation detectable by X-rays is present, especially in High Value-Added (HVA) products or when food elaboration processes are long.h

µCT technology has also great potential in meat research (Frisullo *et al.,* 2009, 2010; Paper VII) and it could be applied to study dry-cured ham. Current studies are focused on the evaluation of microstructure differences between dry-cured ham muscles using µCT and its correlation with instrumental texture. µCT research is also currently focused on the study of possible changes in the texture properties of dry-cured ham due to the application of specific treatments, such as High Hydrostatic Pressure (HHP).

6. CONCLUSIONS

I. The precision of the developed prediction models is accurate enough to consider CT as a useful non-destructive tool for monitoring salt content, water content and a_w during the whole dry-cured ham elaboration process.

II. The predictions are negatively affected by high drying level and high intramuscular fat content (IMF). Specific models for different areas of interest within the ham and for different elaboration times significantly reduce the disturbances that low water content and IMF produce in the predictions.

III. The non-destructive estimation of IMF can be achieved by image analysis of CT tomograms only in the regions of the ham with a more homogeneous salt distribution during the entire dry-cured ham elaboration process. The image analysis employed is not accurate enough to properly distinguish IMF present in muscles with a high gradient of salt during the post-salting stages (i.e. SM muscle).

IV. The incorporation of IMF estimate into the CT based models improves the prediction of salt content, water content and a_w predictions.

V. Although the precision of CT based prediction models is lower than the reference analytical methods, it can be considered enough for control purposes.

VI. The developed CT analytical tools (distribution diagrams, line profiles, and ROIs) are useful to study local salt content, water contents, and a_w but also to study the distribution of these parameters in dry-cured ham during the elaboration process.

VII. The obtained information using prediction models in combination with the CT analytical tools might be used for monitoring and comparing industrial manufacturing processes (i.e. pre-salting or salting procedures), which could help to the optimization of elaboration processes.

VIII. Salt diffusion in the *Semimembranosus* (SM) muscle during the salting process can be determined by using CT based prediction models and a simple diffusion model.

IX. The melting point of the type of fat determines the microstructural characteristics of the meat matrix and the fat detection in non-acid pork lean fermented sausages by using µCT.

X. µCT is not accurate enough to distinguish between lean and fat constituents of a finely minced meat dried sample when the final product results in emulsions. µCT can only detect the visible fat and the fat accumulated in a liquid form inside the air holes and fissures of the meat matrix.

XI. Several µCT parameters (POV-meat matrix, POV-fat, POV-holes, OSVR-meat matrix, DA-meat matrix, ST-meat matrix, and NO-meat matrix) are correlated with instrumental texture (hardness).

7. REFERENCES

Abrahamsen, R.K., Byre, O., Steinsholt, K., & Strand, A.H. (2006). Jarlsbergosten historie og utvikling: Jarlsberg cheese history and development (1st edition). BZGraf SA, Poland. *ISBN-10: 82-529-3056-5*, *ISBN-13: 978-82-529-3056-6*.

Allen, P. (2003). WP3 Summary. EUPIGCLASS - Final Workshop, 6-7 October. Roskilde, Denmark.

http://www.eupigclass.net/Work3/04_Paul_WP%203Summary-filer/frame.htm

Antequera, T., Caro, A., Rodríguez, P.G., & Pérez, T. (2007).Monitoring the ripening process of Iberian ham by computer vision on magnetic resonance imaging. *Meat Science*, 76 (3), 561-567.

Arnau, J., Guerrero, L., & Sárraga, C. (1998). The effect of green ham pH and NaCl concentration on cathepsin activities and sensory characteristics of dry-cured ham. *Journal of the Science of Food and Agriculture*, 77 (3), 387-392.

Arnau, J., Hugas, M., & Monfort, J.M. (1987). *Jamón curado: Aspectos técnicos* (1st edition). Barcelona: Institut de Recerca i Tecnologia Agroalimentàries. *ISBN: 84-404-1575-3*.

Arnau, J., Serra, X., Comaposada, J., Gou, P., & Garriga, M. (2007). Technologies to shorten the drying period of dry-cured meat products. *Meat Science*, 77 (1), 81-89.

Babin, P., Della Valle, G., Chiron, H., Cloetens, P., Hoszowska, J., Pernot, P., Réguerre, A.L., Salvo, L., & Dendievel, R. (2006). Fast x-ray tomography analysis of bubble growth and foam setting during breadmaking. *Journal of Cereal Science*, 43 (3), 393-397.

Babin, P., Della Valle, G., Dendievel, R., Lassoued, N., & Salvo, L. (2005). Mechanical properties of bread crumbs from tomography based Finite Element simulations. *Journal of Materials Science*, 40 (22), 5867-5873.

Barcelon, E.G., Tojo, S., & Watanabe, K. (1999). X-ray computed tomography for internal quality evaluation of peaches. *Journal of Agricultural Engineering Research*, 73 (4), 323-330.

Beauvallet, C., & Renou, J-P. (1992). Applications of NMR spectroscopy in meat research. *Trends in Food Science & Technology*, 3 (8-9), 241-246.

Bellido, G.G., Scanlon, M.G., Page, J.H., & Hallgrimsson, B. (2006). The bubble size distribution in wheat flour dough. *Food Research International*, 39 (10), 1058-1066.

Berg, E.P., Forrest, J.C., & Fisher, J.E. (1994). Electromagnetic scanning of pork carcasses in an on-line industrial configuration. *Journal of Animal Science*, 72 (10), 2642-2652.

Binkley, N., & Adle, R.A. (2010). Dual-Energy X-ray Absorptiometry (DXA) in Men (Chapter 43, pp 525-540). In *Osteoporosis in Men* (2nd edition). *The Effects of Gender on Skeletal Health* (1st edition). Orwoll, E.S., Bilezikian, J.P., & Vanderschueren, D., (Eds.). *ISBN: 978-0-12-374602-3*.

Branscheid, W., & Dobrowolski, A. (1996). Zur Genauigkeit der Video-Image-Analyse: Erfassung des Teilstückwertes und der Fleischhelligkeit von Schweineschlachtkörpern. *Fleischwirtschaft*, 76 (12), 1228-1238.

Brienne, J.P, Denoyelle, C., Baussart, H., & Daudin, J.D. (2001). Assessment of meat fat content using dual energy X-ray absorption. *Meat Science*, 57 (3), 235-244.

Brun, A., Gispert, M., Valero, A., & Font i Furnols, M. (2011). Determinación del porcentaje de grasa intramuscular en lomo de cerdo mediante métodos químicos y métodos no invasivos. *EUROCARNE*, 199, 70–77.

Cartz, L. (1995). Nondestructive Testing: Radiography, Ultrasonics, Liquid Penetrant, Magnetic Particle, Eddy Current (1st edition) (pp 15-77). ASM International. *ISBN: 0-87170-517-4*.

Cava, R., Estevez, M., Ruiz, J., & Morcuende, D., (2003). Physicochemical characteristics of three muscles from free-range reared Iberian pigs slaughtered at 90 kg live weight. *Meat Science*, 63 (4), 533-541.

Chaunier, L., Della Valle, G, & Lourdin, D. (2007). Relationships between texture, mechanical properties and structure of cornflakes. *Food Research International*, 40 (4), 493-503.

Commission Regulation (EC) No 1249/2008 of 10 December 2008 laying down detailed rules on the implementation of the Community scales for the classification of beef, pig and sheep carcasses and the reporting of prices thereof.

Costa-Corredor, A., Muñoz, I., Arnau, J., & Gou, P. (2010). Ion uptakes and diffusivities in pork meat brine-salted with NaCl and K-lactate. *LWT - Food Science and Technology*, 43 (8), 1226-1233.

Daza, A., Mateos, A., Ovejero, I., & López Bote, C.J. (2006). Prediction of body composition of Iberian pigs by means bioelectrical impedance. *Meat Science*, 72 (1), 43-46.

Du, C.J., & Sun, D.W. (2004). Recent developments in the applications of image processing techniques for food quality evaluation. *Follow Trends in Food Science & Technology*, 15 (5), 230-249.

Falcone, P.M., Baiano, A., Zanini, F., Mancini, L., Tromba, G., Montanari, F., & Del Nobile, M.A. (2004). A novel approach to the study of bread porous structure: phase-contrast x-ray microtomography. *Journal of Food Science*, 69 (1), 38-43.

Falcone, P.M., Baiano, A., Zanini, F., Mancini, L., Tromba, G., Dreossi, D., Montanari, F., Scuor, N., & Del Nobile, M.A. (2005). Three-dimensional quantitative analysis of bread crumb by x-ray microtomography. *Journal of Food Science*, 70 (3), 265-272.

Fantazzini, P., Bortolotti, V., Garavaglia, C., Gombia, M., Riccardi, S., Schembri, P., Virgili, R., & Bordini, C.S. (2005). Magnetic resonance imaging and relaxation analysis to predict noninvasively and nondestructively salt-to-moisture ratios in dry-cured meat. *Magnetic Resonance Imaging*, 23 (2), 359-361.

Fantazzini, P., Gombia, M., Schembri, P., Simoncini, N., & Virgili R. (2009). Use of Magnetic Resonance Imaging for monitoring Parma dry-cured ham processing. *Meat Science*, 82 (2), 219-227.

Flores, J. (1997). Mediterranean vs northern European meat products. Processing technologies and main differences. *Food Chemistry*, 59 (4), 505-510.

Folkestad, A., Wold, J.P., Rørvik, K-A., Tschudi, J., Haugholt, K.H., Kolstad, K., & Mørkøre, T. (2008). Rapid and non-invasive measurements of fat and pigment concentrations in live and slaughtered Atlantic salmon (*Salmo salar* L.). *Aquaculture*, 280 (1-4), 129-135.

Font i Furnols, M., & Gispert, M. (2009). Comparison of different devices for predicting the lean meat percentage of pig carcasses. *Meat Science*, 83 (3), 443-446.

Font i Furnols, M., Teran, F., & Gispert, M. (2009). Estimation of lean meat content in pig carcasses using x-ray computed tomography images and PLS regression. *Chemometrics and Intelligent Laboratory Systems*, 98 (1), 31-37.

Fontana, C., Cocconcelli, P., & Vignolo, G. (2005). Monitoring the bacterial population dynamics during the fermentation of artisanal Argentinean sausages. *International Journal of Food Microbiology*, 103 (2), 131-142.

Fox, J.B., (1980). Diffusion of chloride, nitrite and nitrate in beef and pork. *Journal of Food Science*, 45 (6), 1740-1744.

Frisullo, P., Laverse, J., Marino, R., & Del Nobile, M.A. (2009). X-ray computer tomography to study processed meat microstructure. *Journal of Food Engineering*, 94 (3-4), 283-289.

Frisullo, P., Marino, R., Laverse, J., Albenzio, M., & Del Nobile, M.A. (2010). Assessment of intramuscular fat level and distribution in beef muscles using X-ray microcomputed tomography. *Meat Science*, 85 (2), 250-255.

Frøystein, T., Sørheim, O., Berg, S.A., & Dalen, K. (1989). Salt distribution in cured hams, studied by computer X-ray tomography. *Fleishwirtschaft*, 69 (2), 220-222.

Fulladosa, E., Serra, X., Gou, P., Arnau, J., Virgili, R., & Rossi, A. (2011). Non invasive technologies for assessment of fat content (pp 15-16). Q-PorkChain Newstetter, December, No 9 (9th Edition).

http://www.q-porkchains.org/news/newsletters/no_9/non_invasive.aspx

García, C., Berdagué, J.L., Antequera, T., López-Bote, C., Córdoba, J.J., & Ventanas, J. (1991). Volatile components of dry-cured ham Iberian ham. *Food Chemistry*, 41 (1), 23-32.

García-Garrido, J., Quiles-Zafra, R., Tapiador, J., & Luque de Castro, M. (2000). Activity of cathepsin B, D, H and L in Spanish dry-cured ham of normal and defective texture. *Meat Science*, 56 (1), 1-6.

Giese, J. (1996). Fats, oils and fat replacers. *Food Technology*, 50 (4), 78-84.

Goldman, L.W. (2007a). Principles of CT: radiation dose and image quality. *Journal of Nuclear Medicine Technology*, 35 (4), 213-25.

Goldman, L.W. (2007b). Principles of CT and CT technology. *Journal of Nuclear Medicine Technology*, 35 (3), 115-128.

Gonzalez, R.C., & Woods, R.E. (2001). Digital Image Processing (2nd edition). Prentice Hall Inc. Upper Saddle River, New Jersey. *ISBN: 0201180758*.

Graiver, N., Pinotti, A., Califano, A., & Zaritzky, N. (2009). Mathematical modeling of the uptake of curing salts in pork meat. *Journal of Food Engineering*, 95 (4), 533-540.

Grau, R., Albarracín, W., Toldrá, F., Antequera, T., & Barat, J.M. (2008). Study of salting and post-salting stages of fresh and thawed Iberian hams. *Meat Science*, 79 (4), 677-682.

Guerrero, L., Gou, P., & Arnau, J. (1999). The influence of meat pH on mechanical and sensory textural properties of dry-cured ham. *Meat Science*, 52 (3), 267-273.

Guerrero, L., Guàrdia, M.D., Xicola, J., Verbeke, W., Vanhonacker, F., Zakowska-Biemans, S., Sajdakowska, M., Sulmont-Rossé, C., Issanchou, S., Contel, M.L., Scalvedi, M., Granli, B.S., & Hersleth, M. (2009). Consumer-driven definition of traditional food products and innovation in traditional foods. A qualitative cross-cultural study. *Appetite*, 52 (2), 345-354.

Haedelt, J., Pyle, D.L., Beckett, S.T., & Niranjan, K. (2005). Vacuum-induced bubble formation in liquid-tempered chocolate. *Journal of Food Science*, 70 (2), 159-164.

Haff, R.P., & Toyofuku, N. (2008). X-ray detection of defects and contaminants in the food industry. *Sensing and Instrumentation for Food Quality and Safety*, 2 (4), 262-273.

Håseth, T., Egelandsdal, B., Bjerke, F., & Sørheim, O. (2007). Computed tomography for quantitative determination of sodium chloride in ground pork and dry-cured hams. *Journal of Food Science*, 72 (8), 420-427.

Håseth, T., Høy, M., Egelandsdal, B., & Sørheim, O. (2009). Nondestructive analysis of salt, water, and protein in dried salted cod using computed tomography. *Journal of Food Science*, 74 (3), 147-153.

Håseth, T., Høy, M., Kongsro, J., Kohler, A., Sørheim, O., & Egelandsdal, B. (2008). Determination of sodium chloride in pork meat by computed tomography at different voltages. *Journal of Food Science*, 73 (7), 333-339.

Håseth, T., Sørheim, O., Høy, M., & Egelandsdal, B. (2012). Use of computed tomography to study raw ham properties and predict salt content and distribution during dry-cured ham production. *Meat Science*, 90 (3), 858-864.

Honikel, K.O. (2008). The use and control of nitrate and nitrite for the processing of meat products. *Meat Science*, 78 (1-2), 68-76.

Hunter, T.E., Suster, D., Dunshea, F.R., Cummins, L.J., Egan, A.R., & Leury, B.J. (2011). Dual energy X-ray absorptiometry (DXA) can be used to predict live animal and whole carcass composition of sheep. *Small Ruminant Research*, 100 (2), 143-152.

Jia, J., Schinckel, A.P., Forrest, J.C., Chen, W., & Wagner J.R. (2010). Prediction of lean and fat composition in swine carcasses from ham area measurements with image analysis. *Meat Science*, 85 (2), 240-244.

Jiménez-Colmenero, F. (1996). Technologies for developing low-fat meat products. *Trends in Food Science & Technology*, 7 (2), 41-48.

Jiménez-Colmenero, F. (2000). Relevant factors in strategies for fat reduction in meat products. *Trends in Food Science & Technology*, 11 (2), 56-66.

Jimenez-Colmenero, F., Ventanas, J., & Toldrà, F. (2010). Nutritional composition of dry-cured hams and its role in a healthy diet. *Meat Science*, 84 (4), 585-593.

Kalender, W.A. (2005). Computed tomography: fundamentals, system technology, image quality, applications (2nd edition). Erlangen, Germany. *ISBN: 3-89578-081-2*.

Kerckhofs, G., Schrooten, J., Van Cleynenbreugel, T., Lomov, S.V., & Wevers, M. (2008). Validation of x-ray microfocus computed tomography as an imaging tool for porous structures. *Review of Scientific Instruments*, 79 (1), 013711-013719.

Kohrt, W.M. (1997). Dual-Energy X-Ray Absorptiometry: Research Issues and Equipment (Chapter 6, pp 151-168). In *Emerging technologies for nutrition research* (1st edition). Committee on Military Nutrition Research, Institute of Medicine (U.S.) (Eds.). National Academic Press. Washington, DC. *ISBN: 0-309-05797-3*.

Kolstad, K., Mørkøre, T., & Thomassen, M.S. (2008). Quantification of dry matter % and liquid leakage in Atlantic cod (*Gadus morhua*) using computerised X-ray tomography (CT). *Aquaculture*, 275 (1–4), 209-216.

Kolstad, K., Vegusdal, A., Baeverfjord, G., & Einen, O. (2004). Quantification of fat deposits and fat distribution in Atlantic halibut (*Hippoglossus hippoglossus* L.) using computerized x-ray tomography (CT). *Aquaculture*, 229 (1-4), 255-264.

Kraggerud, H., Wold, J.P., Høy, M., & Abrahamsen, K. (2009). X-ray images for the control of eye formation in cheese. *International Journal of Diary Technology*, 62 (2) 147-153.

Kröger, C., Bartle, C.M., West, J.G., Purchas, R.W., & Devine, C.E. (2006). Meat tenderness evaluation using dual energy X-ray absorptiometry (DEXA). *Computers and Electronics in Agriculture*, 54 (2), 93-100.

Kukori, S., Oshita, S., Sotome, I., Kawagoe, Y., & Seo, Y. (2004). Visualization of 3-D network of gas-filled intercellular spaces in cucumber fruit after harvest. *Postharvest Biology and Technology*, 33 (3), 255-262.

Lammertyn, J., Dressalaers, T., Van Hecke, P., Jancsók, P., Wevers, M., & Nicolaï, B.M. (2002). MRI and x-ray CT study of spatial distribution of core breakdown in 'Conference' pears. *Magnetic Resonance Imaging*, 21 (7), 805-815.

Lammertyn, J., Dresselaers, T., Van Hecke, P., Jancsónk, P., Wevers, M., & Nicolaï, B.M. (2003). Analysis of the time course of core breakdown in 'Conference' pears by means of MRI and X-ray CT. *Postharvest Biology and Technology*, 29 (1), 19-28.

Lebert, I., Leroy, S., Giammarinaro, P., Lebert, A., Chacomac, J.P., Bover-Cid, S., Vidal-Carou, M.C., & Talon, R. (2007). Diversity of microorganisms in the environment and dry fermented sausages of French traditional small units. *Meat Science*, 76 (1), 112-122.

Leistner, L., (1986). Allgemeines über Rohschinken. *Fleishwirtschaft*, 66 (4), 496-510.

Leistner, L. (1985). Empfehlungen für sichere Produkte (pp 219-244). In *Mikrobiologie und Qualität für Rohwurst und Rohschinken*. Kulmbach: Institut für Mikrobiologie, Toxikologie und Histologie der Bundesanstalt für Fleischforschung.

Léonard, A., Blancher, S., Nimmol, C., & Devahastin, S. (2008). Effect of far-infrared radiation assisted drying on microstructure of banana slices: An illustrative use of X-ray microtomography in microstructural evaluation of a food product. *Journal of Food Engineering*, 85 (1), 154-162.

Lim, K.S., & Barigou, M. (2004). X-ray micro-computed tomography of cellular food products. *Food Research International*, 37 (10), 1001-1012.

Luiting, P., Kolstad, K., Enting, H., & Vangen, O., (1995). Pig breed comparison for body composition at maintenance: analysis of computerized tomography data by mixture distributions. *Livestock Production Science*, 43 (3), 225-234.

Maire, E., Buffière, J.Y., Salvo, L., Blandin, J.J., Ludwig, W., & Létang, J.M. (2001). On the Application of X-ray Microtomography in the Field of Materials Science. *Advanced Engineering Materials*, 3 (8), 539-546.

Marcoux, M., Bernier, J.F., & Pomar, C. (2003). Estimation of Canadian and European lean yields and composition of pig carcasses by dual-energy X-ray absorptiometry. *Meat Science*, 63 (3), 359-365.

Mendoza, F., Verboven, P., Mebatsion, H.M., Kerckhofs, G., Wevers, M., & Nicolaï, B. (2007). Three-dimensional pore space quantification of apple tissue using X-ray computed microtomography. *Planta*, 226 (3), 559-570.

Mercier, J., Pomar, C., Thériault, M., Goulet, F., Marcoux, M., & Castonguay, F. (2006). The use of dual-energy X-ray absorptiometry to estimate the dissected composition of lamb carcasses. *Meat Science*, 73 (2), 249-257.

Miles, R.S. (1996). Processing of low fat meat products. *Proceedings of the 49th Reciprocal Meat Conference* (pp 17-22). American Meat Science Association, Chicago, IL.

Mitchell, A.D., Conway, J.M., & Pott, W.J.E. (1996). Body composition analysis of pigs by dual-energy x-ray absorptiometry. *Journal of Animal Science*, 74 (11), 2663-2671.

Mitchell, A.D., Scholz, A.M., Pursel, V.G., & Evock-Clover, C.M. (1998). Composition analysis of pork carcasses by dual-energy x-ray absorptiometry. *Journal of Animal Science*, 76 (8), 2104-2114.

Mizutani, R., & Suzuki, S. (2012). X-ray microtomography in biology. *Micron*, 43 (2-3), 104-115.

Mizutani, R., Takeuchi, A., Hara, T., Uesugi, K., & Suzuki, Y. (2007). Computed tomography imaging of the neuronal structure of *Drosophila* brain. *Journal of Synchrotron Radiation*, 14 (3), 282–287.

NAOS Strategy (Strategy for Nutrition, Physical Activity and the Prevention of Obesity). (2005).

http://www.naos.aesan.msps.es/naos/ficheros/estrategia/NAOS_Strategy.pdf

Niñoles, L., Mulet, A., Ventanas, S., & Benedito, J. (2011). Ultrasonic characterisation of *B. femoris* from Iberian pigs of different genetics and feeding systems. *Meat Science*, 89 (2), 174-180.

Official Journal of the European Communities (C 371, 1.12.1998). Publication of an application for registration pursuant to the second subparagraph of Article 8 (1) of Regulation (EEC) no. 2082/92 on certificates of specific character.

Palmia, F., Mazoyer, C., Diafaria, C., Baldini, P., & Poretta D. (1992). Salt and water distribution in typical Italian hams. *Revista Española de Ciencia y Tecnología de Alimentos*, 32 (1), 71–83.

Pareyt, B., Talhaoui, F., Kerckhofs, G., Brijs, K., Goesaert, H., Wevers, M., & Delcour, J.A. (2009). The role of sugar and fat in sugar-snap cookies: Structural and textural properties. *Journal of Food Engineering*, 90 (3), 400-408.

Parolari, G., Rivaldi, P., Leonelli, C., Bellatti, M., & Bovis, N. (1988). Colore e consistenza del prosciutto crudo in rapporto alla materia prima e alla técnica di stagionatura. *Industria Conserve*, 63 (1), 45-49.

Parolari, G., Virgili, R., & Schivazappa, C. (1994). Relationship between cathepsin B activity and compositional parameters in dry-cured hams of normal and defective texture. *Meat Science*, 38 (1), 117-122.

Pearce, K.L., Ferguson, M., Gardner, G., Smith, N., Greef, J., & Pethick, D.W. (2009). Dual X-ray absorptiometry accurately predicts carcass composition from live sheep and chemical composition of live and dead sheep. *Meat Science*, 81 (1), 285-293.

Pérez-Palacios, T., Antequera, T., Durán, M.L., Caro, A., Rodríguez, P.G., & Palacios, R.. (2011). MRI-based analysis of feeding background effect on fresh Iberian ham. *Food Chemistry*, 126 (3), 1366-1372.

Picouet, P., Teran, F., Gispert, M., & Font i Furnols, M. (2010). Lean content prediction in pig carcasses, loin and ham by computerized tomography (CT) using a density model. *Meat Science*, 86 (3), 616-622.

Pomar, C., & Rivest, J. (1996). Évaluation d'une méthode à balayage aux rayons-x pour prédire la composition corporelle des porcs vivants. In *Journées de recherche en zootechnie*, C.P.A.Q., 30-31 May.

Ruiz, J., García, C., Muriel, E., Andrés, A.I., & Ventanas, J. (2002). Influence of sensory characteristics on the acceptability of dry-cured ham. *Meat Science*, 61 (4), 347-354.

Ruiz-Cabrera, M.A., Gou, P., Foucat, L., Renou, J.P., & Daudin, J.D. (2004). Water transfer analysis in pork meat supported by NMR imaging. *Meat Science*, 67 (1), 169-178.

Ruiz-Ramírez, J., Arnau, J., Serra, X., & Gou, P. (2006). Effect of pH_{24}, NaCl content and proteolysis index on the relationship between water and texture parameters in *biceps femoris* and *semimembranosus* muscles in dry-cured ham. *Meat Science*, 72 (2), 185-194.

Rye, M. (1991). Prediction of carcass composition in Atlantic salmon by computerized-tomography. *Aquaculture*, 99 (1-2), 35-48.

Seeram, E. (2009). Computed tomography: physical principles, clinical applications, and quality control (3rd edition). Philadelphia, P.A.: W.B. Saunders Co. *ISBN: 9781416028956*.

Segtnan, V., Høy, M., Sørheim, O., Kohler, A., Lundby, F., Wold, J.P., & Ofstad, R. (2009). Noncontact salt and fat distributional analysis in salted and smoked salmon fillets using x-ray computed tomography and NIR interactance imaging. *Journal of Agricultural and Food Chemistry*, 57 (5), 1705-1710.

Serra, X., & Fulladosa, E. (2011). Online total fat prediction in green hams (pp 8). Q-PorkChain Newstetter, March, No 8 (8th edition).

http://www.q-porkchains.org/news/~/media/Qpork/docs/pdf/newsletter/QPorkChains_Newsletter_8_march2011.ashx

Skjervold, H., Grønseth, K., Vangen, O., & Evensen, A. (1981). In vivo estimation of body composition by computerized tomography. *Zeitschrift für Tierzüchtung und Züchtungsbiologie*, 98 (1-4), 77-79.

Sørheim, O., & Berg, S.A. (1987a). Computed X-ray tomography (CT) as a non-destructive method to study salt distribution in meat (pp 196-200). In *Rapid analysis in food processing and food control*. Baltes, W., Baardseth, P., Czedik-Eysenberg, P., Davidek, Davies, J., Dirinck, A., Genty, P., Jensen, C., Linko, S. A., Mattson, R., Mercier, P., Pfannhauser, C., Pungor, W., E., & Skovgaard, N., (Eds). MATFORSK: Ås, Norway.

Sørheim, O., & Berg, S.A (1987b). Dry cured hams produced from frozen/thawed raw materials. *Proceedings of the 33rd International Congress of Meat Science and Technology* (pp 327-329), Helsinki.

Speakman, J.R., Booles, D., & Butterwick, R. (2001). Validation of dual energy X-ray absorptiometry (DXA) by comparison with chemical analysis of dogs and cats. *International Journal of Obesity*, 25 (3), 439-447.

Straadt, I.K., Aaslyngb, M.D., & Bertram, H.C.. (2012). Assessment of meat quality by NMR – an investigation of pork products originating from different breeds. *Magnetic Resonance in Chemistry*, 49 (1), 71-78.

Strand, A.H. (1985). Skanning av Jarlsbergost på datatomograf. *Meieriteknikk,* 39 (1), 2-7.

Swantek, P.M., Crenshaw, J.D., Marchello, M.J., & Lukaski, H.C. (1992). Bioelectrical impedance: a nondestructive method to determine fat-free mass of live swine and pork carcasses. *Journal of Animal Science*, 70 (1), 169-177.

Toldi, G., Molnár, A., Németh, T., & Kukovics, S. (2007). Slaughter value evaluation of large weight Ile de France and Hungarian Merino lambs by CT and traditional slaughter cutting (pp 201-204). In *Evaluation of carcass and meat quality in cattle and sheep*. EAAP Publication, vol. 123. Wageningen Academic Publishers, The Netherlands. *ISBN: 978-90-8686-022-7*.

Toldrá, F. (2002). Manufacturing of dry-cured ham. In *Dry-cured meat products* (Chapter 3, pp 27-62). Trumbull: Food and Nutrition Press, Inc. Connecticut, USA. *ISBN 0-917678-54-0*.

Toldrá, F., & Flores, M. (1998). The role of muscle proteases and lipases in flavor development during the processing of dry-cured ham. *Critical Reviews in Food Science and Nutrition,* 38 (4), 331-352.

Toldrá, F., Flores, M., & Sanz, Y. (1997). Dry-cured ham flavour: enzymatic generation and process influence. *Food Chemistry*, 59 (4), 523-530.

Trichopoulou, A., Soukara, S., & Vasilopoulou, E. (2007). Traditional foods: a science and society perspective. *Trends in Food Science & Technology*, 18 (8), 420-427.

Van Dalen, G., Blonk, H., Van Aalst, H., & Hendriks, C.L. (2003). 3D imaging of foods using x-ray microtomography. *G.I.T. Imaging & Microscopy*, 3 (1), 18-21.

Van de Kamp, T., Vagovič, P., Baumbach, T., Riedel, & A. (2011). A biological screw in a Beetle's leg. *Science*, 333 (6038), 52.

Verdelis, K., Lukashova, L., Atti, E., Mayer-Kuckuk, P., Peterson, M.G.E., Tetradis, S., Boskey, A.L., & van der Meulen, M.C.H. (2011). MicroCT morphometry analysis of mouse cancellous bone: Intra- and inter-system reproducibility, *Bone*, 49 (3), 580-587.

Vestergaard, C., Erbou, S. G., Thauland, T., Adler-Nissen, J., & Berg, P. (2005). Salt distribution in dry-cured ham measured by computed tomography and image analysis. *Meat Science*, 69 (1), 9-15.

Vestergaard, C., Risum, J., & Adler-Nissen, J. (2004). Quantification of salt concentrations in cured pork by computed tomography. *Meat Science*, *68* (1), 107-113.

Vinegar, H.J., & Wellington, S.L. (1987). Tomographic imaging of three-phase flow experiments. *Review of Scientific Instruments*, 58 (1), 96-107.

Virgili, R., Parolari, G., Schivazappa, C., Bordini, C.S., & Borri, M. (1995). Sensory and texture quality of dry-cured ham as affected by endogenous cathepsin B activity and muscle composition. *Journal of Food Science*, 60 (6), 1183-1186.

World Health Organization (WHO). (2004). Global Strategy on Diet, Physical Activity and Health. *ISBN: 92-4-159222-2*.

http://www.who.int/dietphysicalactivity/strategy/eb11344/strategy_english_web.pdf

Wilson, D.E. (1992). Application of ultrasound for genetic improvement. *Journal of Animal Science*, 70 (3), 973-983.

Wirth, F. (1988). Technologies for making fat-reduced meat products. *Fleishwirtschaft*, 68 (9), 1153-1156.

Wood, J.D., Richardson, R.I., Nute, G.R., Fisher, A.V., Campo, M.M., Kasapidou, E., Sherard, P.R., & Enser, M. (2003). Effect of fatty acids on meat quality: a review. *Meat Science*, 66 (1), 21-32.

ANNEX I: *Prediction Models*

Table 2

Sumary of prediction models developed during this study for salt content.

Prediction models	RMSEC	Paper	Developed from (muscles)	Timing
Salt (%) = - 2.16 + 0.0411·HU_{80}	0.290	Paper I	**SM, BF**	Initial stages
Salt (%) = 0.91 + 0.2222·HU_{80} - 0.2631·HU_{120} + 0.0389·HU_{140}	0.343	Paper II	**SM, BF, ST**	Final stages
Salt (%) = - 0.08 + 0.2045·HU_{80} - 0.2361·HU_{120} + 0.0381·HU_{140}	0.279		**SM, BF**	
Salt (%) = - 0.06 + 0.2148·HU_{80} - 0.2513·HU_{120} + 0.0420·HU_{140}	0.272		**SM**	
Salt (%) = 1.07 + 0.2368·HU_{80} - 0.2458·HU_{120}	0.263		**BF**	
Salt (%) = 3.41 + 0.3106·HU_{80} - 0.3461·HU_{120}	0.222		**ST**	
Salt (%) = - 0.268 + 0.1421·HU_{80} - 0.1307·HU_{120}	0.370	Paper I	**SM, BF, ST**	Entire elaboration process
Salt (%) = 0.17 + 0.1926·HU_{80} - 0.1889·HU_{120}	0.396	Paper IV	**SM, BF**	
Salt (%) = 1.88 + 0.2297·HU_{80} - 0.1856·HU_{120} - 0.0607·HU_{140}	0.266	Paper III	**BF, ST**	
Salt (%) = 1.26 + 0.2379·HU_{80} - 0.2499·HU_{120} + 0.0625·IMF	0.191			
Salt (%) = 1.13 + 0.2113·HU_{80} - 0.2174·HU_{120}	0.199		**BF**	
Salt (%) = 1.45 + 0.2437·HU_{80} - 0.2577·HU_{120} + 0.0487·IMF	0.188			
Salt (%) = 1.42 + 0.2074·HU_{80} - 0.1793·HU_{120} - 0.0355·HU_{140}	0.254		**ST**	
Salt (%) = 1.10 + 0.2314·HU_{80} - 0.2413·HU_{120} + 0.0627·IMF	0.201			

HU_{80}, HU_{120} and HU_{140}: CT value expressed in HU obtained at 80, 120 and 140 kV, respectively.
BF: *Biceps femoris*, SM: *Semimembranosus*, and ST: *Semitendinosus* muscles.

Table 3

Sumary of prediction models developed during this study for water content.

Prediction models	RMSEC	Paper	Developed from (muscles)	Timing
Water (%) = 84.5 + 0.244·HU_{80} - 0.425·HU_{120}	1.46	Paper I	**SM, BF**	Initial stages
Water (%) = 80.2 + 0.425·HU_{80} - 0.616·HU_{120}	3.53	Paper II	**SM, BF, ST**	Final stages
Water (%) = 92.5 + 0.642·HU_{80} - 0.936·HU_{120}	1.88		**SM, BF**	
Water (%) = 101.8 + 0.825·HU_{80} - 1.196·HU_{120}	1.64		**SM**	
Water (%) = 84.0 + 0.267·HU_{80} - 0.446·HU_{120}	1.60		**BF**	
Water (%) = 67.3 - 0.042·HU_{80}	3.24		**ST**	
Water (%) = 93.4 + 1.033·HU_{80} - 1.410·HU_{120}	3.95	Paper I	**SM, BF, ST**	Entire elaboration process
Water (%) = 90.0 + 0.575·HU_{80} - 0.844·HU_{120}	1.76	Paper IV	**SM, BF**	
Water (%) = 86.0 + 0.8580·HU_{80} - 2.4040·HU_{120} + 1.3259·HU_{140}	4.58	Paper III	**BF, ST**	
Water (%) = 96.0 + 0.5870·HU_{80} - 1.2437·HU_{120} + 0.3933·HU_{140} - 1.2630·IMF	2.24			
Water (%) = 102.4 + 1.1617·HU_{80} - 1.6016·HU_{120}	2.78		**BF**	
Water (%) = 89.4 - 0.1543·HU_{120} - 1.2710·IMF	2.30			
Water (%) = 90.6 + 1.2345·HU_{80} - 2.6677·HU_{120} + 1.0881·HU_{140}	3.90		**ST**	
Water (%) = 95.4 + 0.6617·HU_{80} - 1.4291·HU_{120} + 0.5051·HU_{140} - 1.2802·IMF	2.12			

HU_{80}, HU_{120} and HU_{140}: CT value expressed in HU obtained at 80, 120 and 140 kV, respectively.
BF: *Biceps femoris*, SM: *Semimembranosus*, and ST: *Semitendinosus* muscles.

Table 4

Sumary of prediction models developed during this study for a_w.

Prediction models	RMSEC	Paper	Developed from (muscles)	Timing
$a_w = 0.9882 - 0.00158 \cdot HU_{80} + 0.00161 \cdot HU_{140}$	0.0048	Proceedings Reims 2010	**SM, BF, ST**	Initial stages
$a_w = 1.0207 - 0.00145 \cdot HU_{80} + 0.00164 \cdot HU_{120} - 0.00064 \cdot HU_{140}$	0.0100	Paper II	**SM, BF, ST**	Final stages
$a_w = 1.0521 - 0.00091 \cdot HU_{80} + 0.00091 \cdot HU_{120} - 0.00071 \cdot HU_{140}$	0.0074		**SM, BF**	
$a_w = 1.0263 - 0.00135 \cdot HU_{80} + 0.00093 \cdot HU_{120}$	0.0051		**SM**	
$a_w = 1.0424 - 0.00065 \cdot HU_{80}$	0.0053		**BF**	
$a_w = 0.9803 - 0.00251 \cdot HU_{80} + 0.00253 \cdot HU_{120}$	0.0087		**ST**	
$a_w = 1.0387 - 0.00037 \cdot HU_{80} - 0.00027 \cdot HU_{120}$	0.0080	Paper IV	**SM, BF**	Entire elaboration process
$a_w = 1.0606 + 0.00158 \cdot HU_{80} - 0.00509 \cdot HU_{120} + 0.00254 \cdot HU_{140}$	0.0100	Paper III	**BF, ST**	
$a_w = 1.0859 + 0.00121 \cdot HU_{80} - 0.00237 \cdot HU_{120} - 0.00271 \cdot IMF$	0.0059			
$a_w = 1.0936 + 0.00239 \cdot HU_{80} - 0.00382 \cdot HU_{120}$	0.0062		**BF**	
$a_w = 1.0809 + 0.00109 \cdot HU_{80} - 0.00221 \cdot HU_{120} - 0.00195 \cdot IMF$	0.0055			
$a_w = 1.0828 + 0.00277 \cdot HU_{80} - 0.00630 \cdot HU_{120} + 0.00215 \cdot HU_{140}$	0.0074		**ST**	
$a_w = 1.0879 + 0.00187 \cdot HU_{80} - 0.00418 \cdot HU_{120} + 0.00106 \cdot HU_{140} - 0.00189 \cdot IMF$	0.0058			

HU_{80}, HU_{120} and HU_{140}: CT value expressed in HU obtained at 80, 120 and 140 kV, respectively.
BF: *Biceps femoris*, SM: *Semimembranosus*, and ST: *Semitendinosus* muscles.

ANNEX II: *Book Chapter*

Fulladosa, E., Garcia-Gil, N., **Santos-Garcés, E.**, Font i Furnols, M., Muñoz, I., & Gou, P. (2011). Computed Tomography in Food Science. In *Focus on Food Engineering* (Chapter 5, pp 157-186). Shreck, R.J. (Ed). Nova Science Publishers, Inc. *ISBN: 978-1-61209-598-1*.

In: Focus on Food Engineering
Editor: Robert J. Shreck
ISBN: 978-1-61209-598-1

Chapter 5

COMPUTED TOMOGRAPHY IN FOOD SCIENCE

Elena Fulladosa, Núria Garcia-Gil, Eva Santos-Garcés, Maria Font i Furnols, Israel Muñoz and Pere Gou
IRTA. Finca Camps i Armet, E-17121 Monells,
Girona, Spain

ABSTRACT

Computed tomography (CT) is one of the emerging technologies of interest to food science as it permits a non-destructive characterization of food products and their control throughout processing. This work describes the history and physical basis of this technology as well as the working principles of CT. It focuses on the latest research findings related to the application of this technology to different food products; especially dry-cured ham production as well as other issues like pig carcass classification. A revision of other X-ray technologies applied to food science is also included. In dry-cured ham production, CT helps the study of the factors which affect the salting/curing processes. These processes can be monitored because salt can easily be detected due to the differences in densities of meat and salt. Using experimental models, salt and water contents can be non-destructively determined at any moment during the process thus enabling the establishment of safety and quantity criteria in order to avoid either sensory defects or the microbiological hazards common in dry-cured ham. For carcass classification purposes, CT can be used to obtain the lean content of carcasses which is of interest to the food industry as it defines the commercial value of the pig. The estimation of the lean content is usually calculated from the physical measurements of subcutaneous fat depths and muscle thicknesses in specific locations. Devices for this task need to be calibrated and therefore, the dissection is the reference method most commonly used, but this method is difficult and time consuming. CT is an excellent tool for this task as it easily distinguishes the differences between lean, fat and bone.

I have been a good competitor;

I have accepted a challenge...

and I have not surrendered.